DOT/FAA/AR-99/87

Office of Aviation Research
Washington, D.C. 20591

Vertical Drop Test of a Shorts 3-30 Airplane

Allan Abramowitz
Philip A. Ingraham
Robert McGuire

November 1999

Final Report

This document is available to the U.S. public through the National Technical Information Service (NTIS), Springfield, Virginia 22161.

U.S. Department of Transportation
Federal Aviation Administration

NOTICE

Technical Report Documentation Page

1. Report No. DOT/FAA/AR-99/87	2. Government Accession No.	3. Recipient's Catalog No.
4. Title and Subtitle VERTICAL DROP TEST OF A SHORTS 3-30 AIRPLANE		5. Report Date November 1999
		6. Performing Organization Code
7. Author(s) Allan Abramowitz, Philip A. Ingraham, and Robert McGuire		8. Performing Organization Report No.
9. Performing Organization Name and Address Federal Aviation Administration, Airframe Structures Section, AAR-431, William J. Hughes Technical Center, Atlantic City International Airport, NJ 08405		10. Work Unit No. (TRAIS)
		11. Contract or Grant No.
12. Sponsoring Agency Name and Address U.S. Department of Transportation, Federal Aviation Administration, Office of Aviation Research, Washington, DC 20591		13. Type of Report and Period Covered Final Report
		14. Sponsoring Agency Code ANM-100
15. Supplementary Notes The FAA William J. Hughes Technical Center Project Manager was Gary Frings.		

16. Abstract

A Short Brothers PLC, Model SD 3-30, airplane was subjected to a vertical impact drop test at the Federal Aviation Administration (FAA) William J. Hughes Technical Center, Atlantic City International Airport, New Jersey. The objective of the test was to determine the impact response of the fuselage, seat tracks, seats, and anthropomorphic test dummies on a high-wing, commuter type airplane. The test was conducted to simulate the vertical velocity component of a severe, but survivable, crash impact. A final impact velocity of 30 feet per second was therefore selected. The airplane was configured in a typical maximum gross weight flight condition, including seats, simulated occupants, fuel, and cargo.

The Shorts 3-30 is a twin turboprop, 30-passenger regional transport airplane. The total test weight of the airplane was 21,210 pounds. The internal seating arrangement consisted of pilot and copilot seats, eight rows of standard passenger seats, and two nonstandard seats mounted in the aisle. Twenty-one of the 28 seats were occupied by mannequins; the remaining seven seats were occupied by instrumented anthropomorphic test dummies.

The Shorts 3-30 fuel system is unique insofar as the two fuel tanks are located on top of the fuselage as opposed to the more conventional location in the wings. During the drop test, a massive amount of simulated fuel spilled into the passenger compartment.

The stiff structure of the airplane allowed for only small amounts of airframe crushing. As a result, the fuselage experienced high G_{max} levels of approximately 90 g's with an impact pulse duration of 15 ms. The stiff structure also prevented fuselage crushing which allowed the airplane to maintain a protective shell.

The seat tracks remained attached to the fuselage. However, 23 of the 26 passenger seats experienced structural failure. The crew seats were undamaged. The occupants experienced G_{peak} levels in the range of 31-67 g's with a pulse duration of 21-59 ms as measured in the pelvic region. This may be considered a severe impact which would have resulted in moderate to severe injuries to the occupants.

17. Key Words Airplane, Airplane crash test, Crashworthiness, Commuter airplane, Regional transport airplane, Vertical impact, Drop test, Crash impact		18. Distribution Statement This document is available to the public through the National Technical Information Service (NTIS) Springfield, Virginia 22161.	
19. Security Classif. (of this report) Unclassified	20. Security Classif. (of this page) Unclassified	21. No. of Pages 121	22. Price

Form DOT F1700.7 (8-72) Reproduction of completed page authorized

ACKNOWLEDGMENTS

The authors would like to thank Mr. Stephen Soltis, the Federal Aviation Administration's National Resource Specialist for crash dynamics and Dr. Tong Vu, Electronics Engineer, Crashworthiness Group, for their technical direction during this test.

In addition, they would also like to thank Mr. Anthony Dang, Mr. Michael Van Pelt, and Mr. Robert Scarlett, airframe and powerplant technicians, for their invaluable assistance.

Finally, they would like to thank Mr. Ludovic Leroy, of the Ecole Nationale de l'Aviation Civile, Toulouse, France, for his help in the compilation and editing of this technical report.

TABLE OF CONTENTS

LIST OF ILLUSTRATIONS

LIST OF TABLES

EXECUTIVE SUMMARY

A Short Brothers PLC, Model SD 3-30, airplane was subjected to a vertical impact drop test at the Federal Aviation Administration (FAA) William J. Hughes Technical Center, Atlantic City International Airport, New Jersey. The objective of the test was to determine the impact response of the fuselage, seat tracks, seats, and anthropomorphic test dummies on a high-wing, commuter type airplane. The test was conducted to simulate the vertical velocity component of a severe, but survivable, crash impact. A final impact velocity of 30 feet per second was therefore selected. The airplane was configured in a typical maximum gross weight flight condition, including seats, simulated occupants, fuel, and cargo. The data collected in this test will supplement the existing certification basis for improved seat and restraint systems for commuter category airplanes as defined in Title 14 of the Code of Federal Regulations (CFR) Part 23 (19,000 pounds gross weight limit).

The Shorts 3-30 is a twin turboprop, 30-passenger regional transport airplane. It is 58 feet long and has a wing span of 75 feet. The total test weight of the airplane was 21,210 pounds. The internal seating arrangement consisted of pilot and copilot seats, eight rows of standard passenger seats, and two nonstandard seats mounted in the aisle. Twenty-one of the 28 seats were occupied by mannequins; the remaining seven seats were occupied by instrumented anthropomorphic test dummies.

The Shorts 3-30 fuel system is unique insofar as the two fuel tanks are located on top of the fuselage as opposed to the more conventional location in the wings. A more detailed analysis of the potential for fuel spillage was therefore done due to the increased possibility of injury to the passengers with this fuel system configuration. During the drop test, a massive amount of simulated fuel spilled into the passenger compartment.

The stiff structure of the airplane allowed for only small amounts of airframe crushing. As a result, the fuselage experienced high G_{max} levels of approximately 90 g's with an impact pulse duration of 15 ms. The stiff structure also prevented fuselage crushing which allowed the airplane to maintain a protective shell.

The seat tracks remained attached to the fuselage. However, 23 of the 26 passenger seats experienced structural failure. The crew seats were undamaged. The occupants experienced G_{peak} levels in the range of 31-67 g's with a pulse duration of 21-59 ms as measured in the pelvic region. This may be considered a severe impact which would have resulted in moderate to severe injuries to the occupants.

All exits remained operable after the impact. Nine of 23 external windows and 13 of 23 internal windows shattered.

The overhead fuel tanks broke loose from their mountings and large quantities of simulated fuel spilled onto the occupants.

INTRODUCTION

This report presents the results of a vertical impact test conducted at the Federal Aviation Administration (FAA) William J. Hughes Technical Center, Atlantic City International Airport, New Jersey. The objective of this test was to determine the impact response of the fuselage, seat tracks, seats, and anthropomorphic test dummies on a high-wing airplane. This test was conducted to simulate the vertical velocity component of a severe, but survivable, crash impact. This test entailed dropping a Short Brothers PLC, Model SD 3-30, a 30-passenger regional transport airplane, from a height of 14 feet, which would result in an impact velocity of 30 feet per second. The airplane was configured to simulate a typical flight condition, including seats, simulated occupants, simulated fuel, and cargo. The data collected in this test will supplement the existing basis for improved seat and restraint systems for commuter category airplanes as defined in title 14 of the Code of Federal Regulations (CFR) part 23. The Shorts 3-30 airplane weighs more than 12,500 pounds and therefore is certified to Federal Aviation Regulation (FAR) Part 25 although it has been primarily operated as regional transport in a commuter role.

BACKGROUND

This vertical impact test is one of a series of fuselage section and full-scale airplane tests conducted in support of the FAA's ongoing Airplane Safety Research Plan [1]. The FAA has proposed seat dynamic performance standards for 14 CFR Part 23 commuter category airplanes. Those standards were established empirically using the results of prior airplane crash impact test programs. In the development of those standards it was noted that the full-scale airplane impact test database did not include airplanes representative in size of commuter category airplanes. To provide data for those size airplanes, the FAA initiated a full-scale vertical impact test program of 14 CFR Part 23 commuter category airplanes [2, 3]. The tests were structured to assess the impact response characteristics of airframe structures and seats and the potential for occupant impact injury.

DESCRIPTION OF TEST FACILITY AND TEST ARTICLE

TEST FACILITY.

The drop test facility, shown in figure 1, is comprised of two 57-foot vertical steel towers connected at the top by a horizontal platform. An electrically powered winch, mounted on the platform, is used to raise or lower the airplane and is controlled from the base of one of the tower legs. Attached to the winch is a reeved hoisting cable which is used to raise the airplane. A sheave block assembly hanging from the free end of the reeved cable is attached to a solenoid operated release hook. The airplane is connected to the release hook by a cable/turnbuckle assembly with hooks bolted to the fuselage section at four locations. Located below the winch cable assembly and between the tower legs is a 15- by 36-foot wooden platform which rests upon steel I-beams and is supported by 12 load cells.

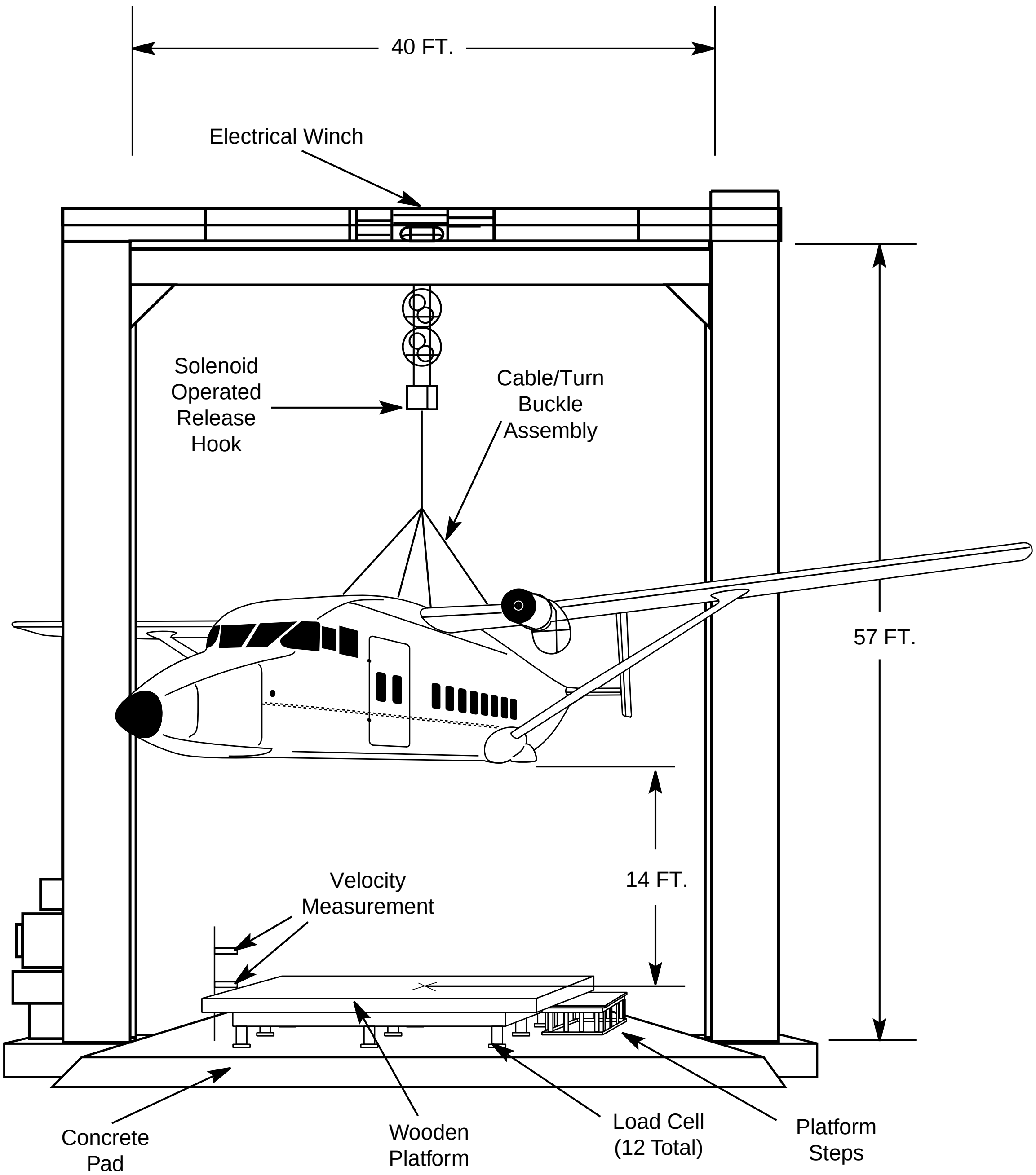

FIGURE 1. DYNAMIC DROP TEST FACILITY

TEST ARTICLE.

The airplane tested was a Shorts 3-30, figure 2, which is a high-wing, twin-turboprop, 30-passenger regional transport airplane. The airplane is 58 feet long, with a wing span of 75 feet. Prior to the test, modifications were made to the airplane as follows:

- The engines were simulated using partially filled concrete barrels designed and constructed to replicate the weight and the center of gravity (CG) of the real engines.

- The landing gear was removed.

- The lower portion of the landing gear fairing on the stub wing of the airplane was removed.

- All fuel ports on the tanks were capped before the test with the exception of the cell 3 to 4 interconnect pipe.

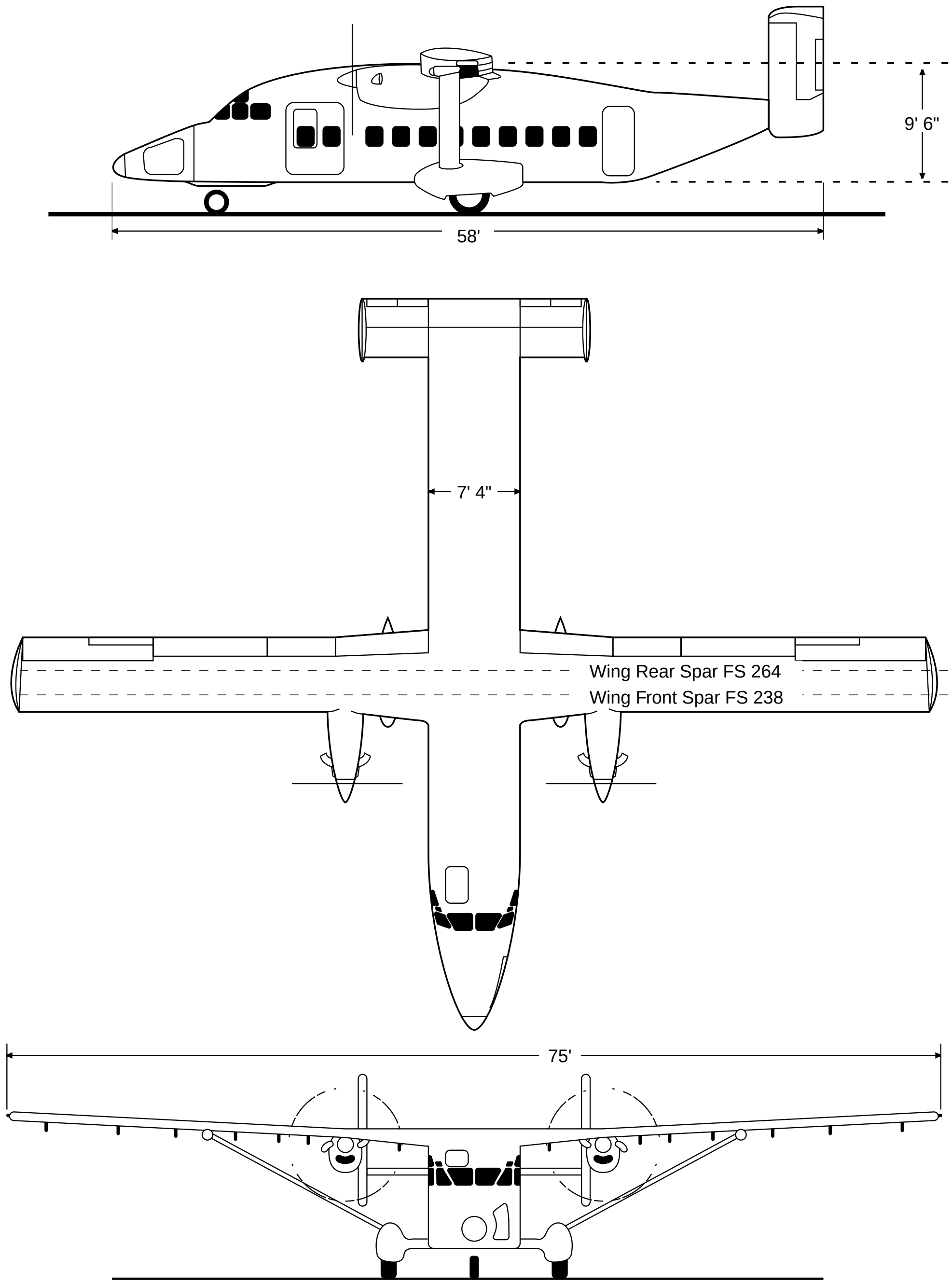

FIGURE 2. SHORTS 3-30

The internal seating arrangement consisted of a pilot and copilot seat as well as ten rows of passenger seats. The seating arrangement was modified by installing two nonstandard seats in the aisle as they would not fit in the standard seat tracks. The nonstandard seats included one FAA Civil Aeromedical Institute (CAMI) experimental energy-absorbing seat and one Beechcraft King Air seat. Twenty-six standard Shorts 3-30 seats were also on board. Twenty-one of the 28 seats were occupied by a mannequin. Seven of the seats were occupied by instrumented 50th percentile Hybrid II anthropomorphic test dummies (ATD). Table 1 gives the descriptions of the seats and ATD locations by fuselage station (FS). All seats to the left of the cabin aisle (pilot side) were single seats and to the right of the cabin aisle (copilot side) were double seats. All the dummies were strapped firmly into the seats with lap belt restraint systems. The CAMI seat ATD was also secured using a shoulder harness.

TABLE 1. SEAT AND ATD LOCATIONS

Location	Occupants	Description	ATD Location
FS 55	2	Flight Deck Seat	Copilot Seat - ATD #1
FS 110	3	Shorts Seat	Center Seat - ATD #2
FS 145	3	Shorts Seat	
FS 173	3	Shorts Seat	Right Seat - ATD #3
FS 190	1	FAA CAMI Seat	Aisle - ATD #4
FS 224	3	Shorts Seat	
FS 262	3	Shorts Seat	Center Seat - ATD #5
FS 292	3	Shorts Seat	
FS 315	1	Beechcraft King Air Seat	Aisle - ATD #6
FS 357	3	Shorts Seat	Left Seat - ATD #7
FS 385	3	Shorts Seat	

Note: ATD = Anthropomorphic Test Dummy

For the purpose of seat identification, seats on the far left are called left seats; seats in the aisle will be referred to as aisle seats. The seats on the copilot side are double seats and the left side of the double seat will be referred to as the center seat and the right side of the double seat will be called the right seat. Figure 3 shows the seat and ATD locations.

Fuselage location identifications are measured in three directions, longitudinal (X), lateral (Y), and vertical (Z). The origin for location reference is in the nose of the airplane laterally centered, at the floor seat track level, which is consistent with the airplane reference system. All measurements are taken from this point and are recorded in inches. Positive measurements are taken from this point aft (X), toward the copilot side (Y), and toward the ceiling of the fuselage (Z).

The Shorts 3-30 fuel system configuration is unique insofar as the two fuel tanks are located on top of the fuselage (figure 4) as opposed to the more conventional location in the wings. A more detailed analysis of the fuel system was done due to its unique location with respect to the passenger cabin.

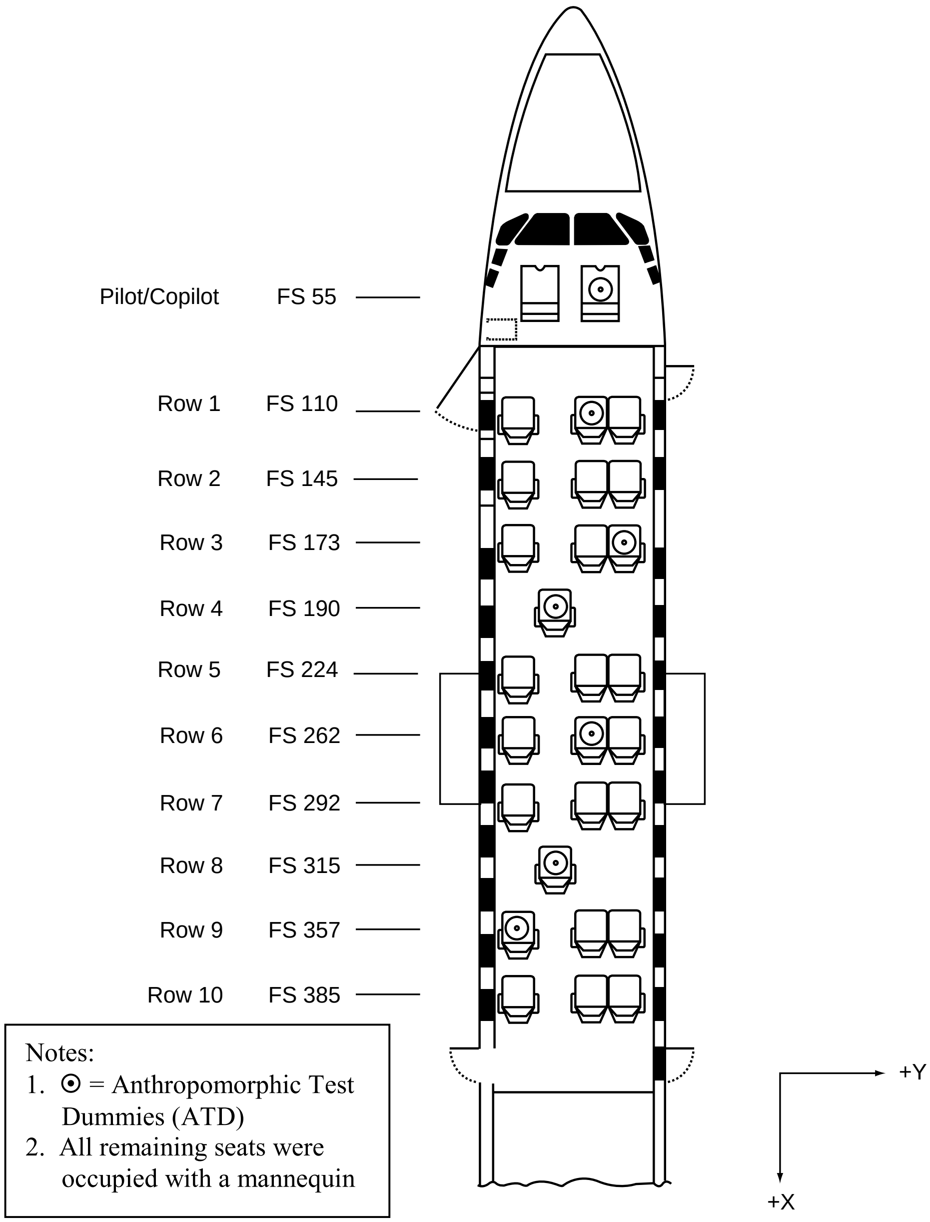

FIGURE 3. SHORTS 3-30 AIRPLANE SEATS AND ATD LOCATIONS

Each tank holds 288 gallons of fuel and was comprised of two fuel cells. For this test the tanks were filled to approximately ¾ capacity with water to represent a full load of fuel (fuel is approximately ¾ the weight of water).

Even though cells 1, 2, and 3 are located together and cell 4 is separate (figure 4), cells 1 and 2 comprised tank 1 and cells 3 and 4 comprised tank 2.

For this test, all 24 fuel lines emanating from the tanks were capped. The cell 3 to 4 interconnect pipe remained in place.

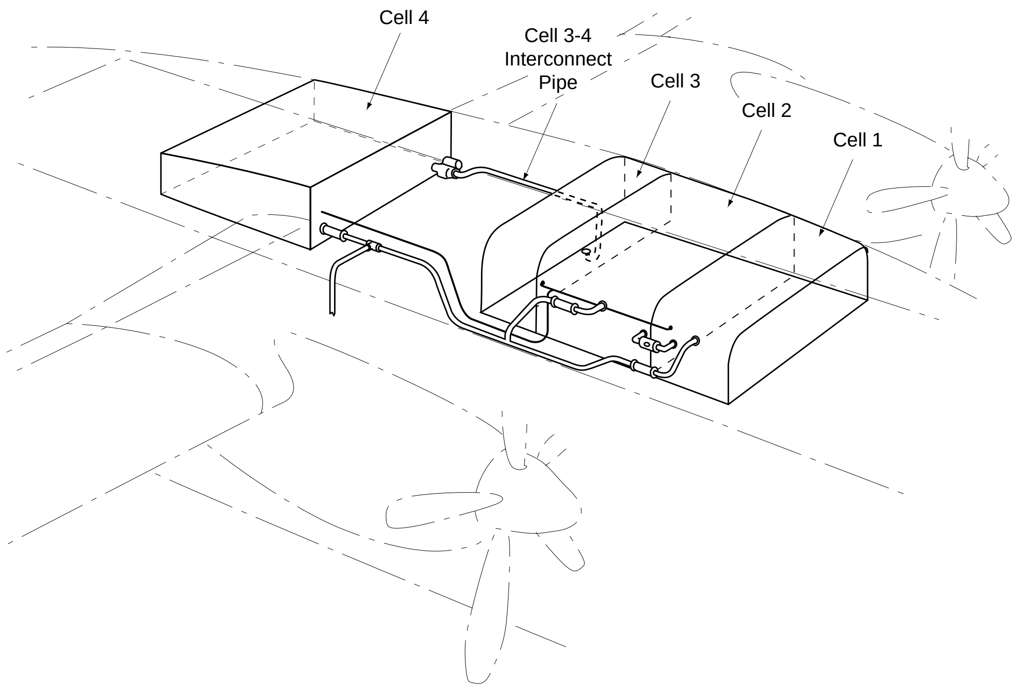

FIGURE 4. SHORTS 3-30 FUEL SYSTEM

The total weight of the airplane was 21,210 pounds. This weight represents the maximum gross takeoff weight of the airplane (22,352 pounds) minus the portions of the airplane that were removed and/or modified (1142 pounds). A list of all weights and moments about the airplane datum are presented in table 2. For this test, the airplane datum were deemed to be at FS 0 which is located in the nose of the airplane. The CG was calculated to be at FS 240.

TEST INITIATION

Prior to the test, the four supporting cable/turnbuckle assemblies were adjusted to level the fuselage forward to aft and left to right. The airplane was then raised to the desired height of 14 feet. Four guide ropes, manned by members of the drop test team, steadied the airplane while it hung above the platform. When the airplane was steady and level, the automatic timing sequence was started. The high-speed film cameras and video cameras were activated, the data acquisition systems were started, and two seconds later the airplane was released. Wind speed prior to and during the test was less than 5 mph.

INSTRUMENTATION

FUSELAGE.

The fuselage instrumentation (table 3) for this test included 42 Endevco model 7231C-750 accelerometers. The accelerometers were located on the side wall frame sections, on the side wall seat tracks, on the floor seat tracks, and on the ceiling wing box spar area. The locations selected were deemed to be the most suitable in order to characterize the fuselage response and its affect on the occupants.

TABLE 2. TEST ARTICLE WEIGHTS AND MOMENTS

Item	Weight (lb)	Fuselage Station (inch)	Moment (lb-inch)
Luggage	412	-27	-11124
Pilot/Copilot	340	55	18700
Seats/Dummies	555	110	61050
Seats/Dummies	550	145	79750
Seats/Dummies	555	173	96015
CAMI/Dummy	325	190	61750
Seats/Dummies	550	224	123200
Seats/Dummies	555	262	145410
Seats/Dummies	550	292	160600
Beech/Dummy	313	315	98595
Seats/Dummies	555	357	198135
Seats/Dummies	550	385	211750
Luggage	602	472	284144
Fuselage	10480	244	2557120
Fuel	3875	235	910625
Cameras/Ballast	443	238	105434
TOTAL	21210		5101154

Notes: 1. FS 190 and FS 315 seats were mounted on ½-inch steel plates
2. Fuselage includes simulated engines, wings, and struts

TABLE 3. DATA ACQUISITION SYSTEMS CONFIGURATIONS AND SENSOR LOCATIONS

NEFF 490							
Channel	Description	Sensor Mfg-Model	Range +/-	Units	Fuselage Location X	Y	Z
101	Left Engine Accelerometer X Direction	Endevco 7231C-750	342	g’s	154	-103	84
102	Left Engine Accelerometer Y Direction	Endevco 7231C-750	398	g’s	154	-103	84
103	Left Engine Accelerometer Z Direction	Endevco 7231C-750	458	g’s	154	-103	84
104	Left Outside Spar Accelerometer Z Direction	Endevco 7231C-750	360	g’s	251	-56	78
105	Platform Load Cell #5A	Sensotec 41	50000	lb			
106	Platform Load Cell #6A	Sensotec 41	50000	lb			
107	Platform Load Cell #7A	Sensotec 41	50000	lb			
108	Platform Load Cell #8A	Sensotec 41	50000	lb			
109	Left Strut Accelerometer X Direction	Endevco 7231C-750	508	g’s	251	-246	90
110	Left Strut Accelerometer Y Direction	Endevco 7231C-750	558	g’s	251	-246	90
111	Left Strut Accelerometer Z Direction	Endevco 7231C-750	536	g’s	251	-246	90
112	Left Outside Spar String Potentiometer	Celesco PT 101-20	10.5	inch	251	-56	78/0
113	Platform Load Cell #1A	Sensotec 41	50000	lb			
114	Platform Load Cell #2A	Sensotec 41	50000	lb			
115	Platform Load Cell #3A	Sensotec 41	50000	lb			
201	Platform Accelerometer #1 Z Direction	Endevco 2262A-200	200	g’s			
202	Platform Accelerometer #2 Z Direction	Endevco 2262A-200	200	g’s			

TABLE 3. DATA ACQUISITION SYSTEMS CONFIGURATIONS AND SENSOR LOCATIONS (Continued)

NEFF 490							
Channel	Description	Sensor Mfg-Model	Range +/-	Units	Fuselage Location X	Y	Z
203	Platform Accelerometer #3 Z Direction	Endevco 2262A-200	200	g's			
204	Platform Accelerometer #4 Z Direction	Endevco 2262A-200	200	g's			
205	Platform Accelerometer #5 Z Direction	Endevco 2262A-200	200	g's			
206	Platform Accelerometer #6 Z Direction	Endevco 2262A-200	200	g's			
207	Forward Velocity Measurement	Not Applicable	1000	ft/sec			
208	Aft Velocity Measurement	Not Applicable	1000	ft/sec			
209	FS55 ATD #1 Load Cell	R. Denton 1708	5000	lb	55	15	33
210	FS55 ATD #1 Accelerometer Z Direction 100 g	Endevco 7265A-100	100	g's	55	15	33
211	FS55 ATD #1 Accelerometer Z Direction 750 g	Endevco 7231C-750	144	g's	55	15	33
212	FS110 ATD #2 Load Cell	R. Denton 1708	5000	lb	110	10	20
213	Platform Load Cell # 9A	Sensotec 41	50000	lb			
214	Platform Load Cell #10A	Sensotec 41	50000	lb			
215	Platform Load Cell #11A	Sensotec 41	50000	lb			
216	FS89 LSW Accelerometer Z Direction	Endevco 7231C-750	418	g's	89	-43	32
217	FS89 LST Accelerometer Z Direction	Endevco 7231C-750	303	g's	89	-37	10
218	FS89 LFT Accelerometer Z Direction	Endevco 7231C-750	367	g's	89	-20	0
219	FS89 RFT Accelerometer Z Direction	Endevco 7231C-750	399	g's	89	9	0
220	FS110 ATD #2 Accelerometer Z Direction 100 g	Endevco 7265A-100	100	g's	110	10	20
221	FS110 ATD #2 Accelerometer Z Direction 750 g	Endevco 7231C-750	144	g's	110	10	20
222	FS89 RST Accelerometer Z Direction	Endevco 7231C-750	487	g's	89	37	10
223	FS89 RSW Accelerometer Z Direction	Endevco 7231C-750	460	g's	89	43	35
224	FS161 LSW Accelerometer Z Direction	Endevco 7231C-750	534	g's	161	-43	40
225	FS161 LST Accelerometer Z Direction	Endevco 7231C-750	404	g's	161	-37	10
226	FS161 LFT Accelerometer Z Direction	Endevco 7231C-750	400	g's	161	-20	0
227	FS161 RFT Accelerometer Z Direction	Endevco 7231C-750	290	g's	161	9	0
228	FS173 ATD #3 Load Cell	R. Denton 1708	5000	lb	173	28	20
229	FS173 ATD #3 Accelerometer Z Direction 750 g	Endevco 7231C-750	185	g's	173	28	20
230	FS161 RST Accelerometer Z Direction	Endevco 7231C-750	382	g's	161	37	10
231	FS161 RSW Accelerometer Z Direction	Endevco 7231C-750	469	g's	161	43	36
301	FS190 ATD #4 Load Cell	R. Denton 1708	5000	lb	190	6	15
302	FS190 ATD #4 Accelerometer Z Direction 100 g	Endevco 7265A-100	100	g's	190	6	15
303	FS190 ATD #4 Accelerometer Z Direction 750 g	Endevco 7231C-750	117	g's	190	6	15
304	Platform Load Cell #4A	R. Denton 1708	50000	lb			
305	FS238 LFS Accelerometer Z Direction	Endevco 7231C-750	555	g's	238	-15	82
306	FS238 RFS Accelerometer Z Direction	Endevco 7231C-750	377	g's	238	-13	82
307	FS238 LFS String Potentiometer	Celesco PT101-020	10.5	inch	238	-20	80/0
308	FS238 RFS String Potentiometer	Celesco PT101-020	10.5	inch	238	9	80/0
309	FS264 LRS Accelerometer Z Direction	Endevco 7231C-750	379	g's	264	-13	82

TABLE 3. DATA ACQUISITION SYSTEMS CONFIGURATIONS AND SENSOR LOCATIONS (Continued)

NEFF 490							
		Sensor	Range		Fuselage Location		
Channel	Description	Mfg-Model	+/-	Units	X	Y	Z
310	FS264 RRS Accelerometer Z Direction	Endevco 7231C-750	570	g's	264	-23	82
311	FS264 LRS String Potentiometer	Celesco PT101-020	10.5	inch	264	-20	80/0
312	Platform Load Cell #12A	Sensotec 41	50000	lb			
313	FS340 RFT Accelerometer Z Direction	Endevco 7231C-750	399	g's	340	9	0
314	FS340 RST Accelerometer Z Direction	Endevco 7231C-750	384	g's	340	37	10
315	FS340 RSW Accelerometer Z Direction	Endevco 7231C-750	375	g's	340	43	36
401	Right Engine Accelerometer X Direction	Endevco 7231C-750	589	g's	154	103	84
402	Right Engine Accelerometer Y Direction	Endevco 7231C-750	390	g's	154	103	84
403	Right Engine Accelerometer Z Direction	Endevco 7231C-750	560	g's	154	103	84
404	Right Outside Spar Accelerometer Z Direction	Endevco 7231C-750	418	g's	251	56	78
405	FS264 LSW Accelerometer Y Direction	Endevco 7231C-750	442	g's	264	-43	35
406	FS264 LSW Accelerometer Z Direction	Endevco 7231C-750	527	g's	264	-43	35
407	FS264 LST Accelerometer Z Direction	Endevco 7231C-750	399	g's	264	-37	10
408	FS264 LFT Accelerometer X Direction	Endevco 7231C-750	403	g's	264	-20	0
409	FS264 LFT Accelerometer Z Direction	Endevco 7231C-750	400	g's	264	-20	0
410	FS264 RFT Accelerometer X Direction	Endevco 7231C-750	364	g's	264	9	0
411	FS264 RFT Accelerometer Z Direction	Endevco 7231C-750	429	g's	264	9	0
412	FS262 ATD #5 Load Cell	R. Denton 1708	5000	lb	262	10	20
413	FS315 ATD #6 Load Cell	R. Denton 1708	5000	lb	315	6	17
414	FS315 ATD #6 Accelerometer Z Direction 100 g	Endevco 7265A-100	100	g's	315	6	17
415	FS315 ATD #6 Accelerometer Z Direction 750 g	Endevco 7231C-750	189	g's	315	6	17
416	FS262 ATD #5 Accelerometer Z Direction 750 g	Endevco 7231C-750	101	g's	262	10	20
417	FS264 RST Z Direction	Endevco 7231C-750	412	g's	264	37	10
418	FS264 RSW Y Direction	Endevco 7231C-750	536	g's	264	43	35
419	FS264 RSW Z Direction	Endevco 7231C-750	578	g's	264	43	35
420	FS340 LSW Accelerometer Z Direction	Endevco 7231C-750	411	g's	340	-43	36
421	FS340 LST Accelerometer Z Direction	Endevco 7231C-750	416	g's	340	-37	10
422	FS340 LFT Accelerometer Z Direction	Endevco 7231C-750	395	g's	340	-20	0
423	FS264 RRS String Potentiometer	Celesco PT101-020	10.5	inch	264	9	80/0
424	FS357 ATD #7 Load Cell	R. Denton 1708	5000	lb	357	-27	20
425	FS357 ATD #7 Accelerometer Z Direction 100 g	Endevco 7265A-100	100	g's	357	-27	20
426	FS357 ATD #7 Accelerometer Z Direction 750 g	Endevco 7231C-750	186	g's	357	-27	20
428	Right Strut Accelerometer X Direction	Endevco 7231C-750	318	g's	251	246	90
429	Right Strut Accelerometer Y Direction	Endevco 7231C-750	533	g's	251	246	90
430	Right Strut Accelerometer Z Direction	Endevco 7231C-750	418	g's	251	246	90
431	Right Outside Spar String Potentiometer	Celesco PT101-020	10.5	inch	251	56	78/0

TABLE 3. DATA ACQUISITION SYSTEMS CONFIGURATIONS AND SENSOR LOCATIONS (Continued)

DAS-48S							
		Sensor	Range		Fuselage Location		
Channel	Description	Mfg/Model	+/-	Units	X	Y	Z
1	Platform Load Cell #1B	Sensotec 41	50000	lb			
2	Platform Load Cell #2B	Sensotec 41	50000	lb			
3	Platform Load Cell #3B	Sensotec 41	50000	lb			
4	Platform Load Cell #4B	Sensotec 41	50000	lb			
5	Platform Load Cell #5B	Sensotec 41	50000	lb			
6	Platform Load Cell #6B	Sensotec 41	50000	lb			
7	Platform Load Cell #7B	Sensotec 41	50000	lb			
8	Platform Load Cell #8B	Sensotec 41	50000	lb			
9	Platform Load Cell #9B	Sensotec 41	50000	lb			
10	Platform Load Cell #10B	Sensotec 41	50000	lb			
11	Platform Load Cell #11B	Sensotec 41	50000	lb			
12	Platform Load Cell #12B	Sensotec 41	50000	lb			
13	FS173 ATD #3 Accelerometer Z Direction 100 g	Endevco 7265A-100	100	g’s	173	28	20
14	FS187 LST Accelerometer Z Direction	Endevco 7231C-750	300	g’s	187	-37	10
15	FS187 LFT Accelerometer Z Direction	Endevco 7231C-750	300	g’s	187	-20	0
16	FS187 RFT Accelerometer Z Direction	Endevco 7231C-750	300	g’s	187	9	0
17	FS187 RST Accelerometer Z Direction	Endevco 7231C-750	300	g’s	187	37	10
18	FS238 LST Accelerometer Z Direction	Endevco 7231C-750	300	g’s	238	-37	10
19	FS238 LFT Accelerometer Z Direction	Endevco 7231C-750	300	g’s	238	-20	0
20	FS238 RFT Accelerometer Z Direction	Endevco 7231C-750	300	g’s	238	9	0
21	FS238 RST Accelerometer Z Direction	Endevco 7231C-750	300	g’s	238	37	10
22	FS238 RFS Accelerometer Z Direction	Endevco 7231C-750	300	g’s	238	33	82
23	FS264 RRS Accelerometer Z Direction	Endevco 7231C-750	300	g’s	264	33	82
24	FS262 ATD #5 Accelerometer Z Direction 100 g	Endevco 7265A-100	100	g’s	262	10	20
25	Forward Platform String Potentiometer	Celesco PT101-020	10.5	inch			
26	Center Platform String Potentiometer	Celesco PT101-020	10.5	inch			

Note: All sensor excitation voltage was 10 volts.
All sensors were calibrated prior the test.
LSW = LEFT SIDE WALL, LST = LEFT SIDE TRACK, LFT = LEFT FLOOR TRACK
LFS = LEFT FRONT SPAR, LRS = LEFT REAR SPAR
Right side follows the same logic as the left.

Four Celesco model PT101-020 string potentiometers were located at the wing box area inside the fuselage to determine the deformation of the interior cabin height. String potentiometers stretch from the ceiling spar to the floor seat track and were located at FS 238 and FS 264. There were two string potentiometers at each of these locations, one above the right side floor seat track and one above the left side floor seat track.

TEST DUMMIES.

There were seven 50th percentile Hybrid II anthropomorphic test dummies on board. All of the ATDs were instrumented with load cells (Denton model 1708) to measure the spinal column axial loading at the lumbar area and accelerometers (Endevco model 7231C-750 and 7265A-100) to measure the g forces in the pelvic region. The ATDs were located at FS 55, 110, 173, 190, 262, 315, and 357 as noted in table 1 and shown in figure 3.

PLATFORM.

The impact platform rested on 12 Sensotec model 41 (dual-bridge A, B) load cells, numbered 1 to 12, each with a load capacity of 50,000 pounds, figure 5. A hydraulic jack was located above each load cell, and each jack was plumbed to a central hydraulic system. Prior to the drop test, the platform was raised off the ground, leveled, and isolated from the hydraulic system by closing a shutoff valve located at each of the respective jacks. Just prior to the drop test the platform tare weight was electronically zeroed by the computer system. The platform load cells measured the reactive forces generated during the impact of the airplane and were used to measure the impact loads and determine their distribution.

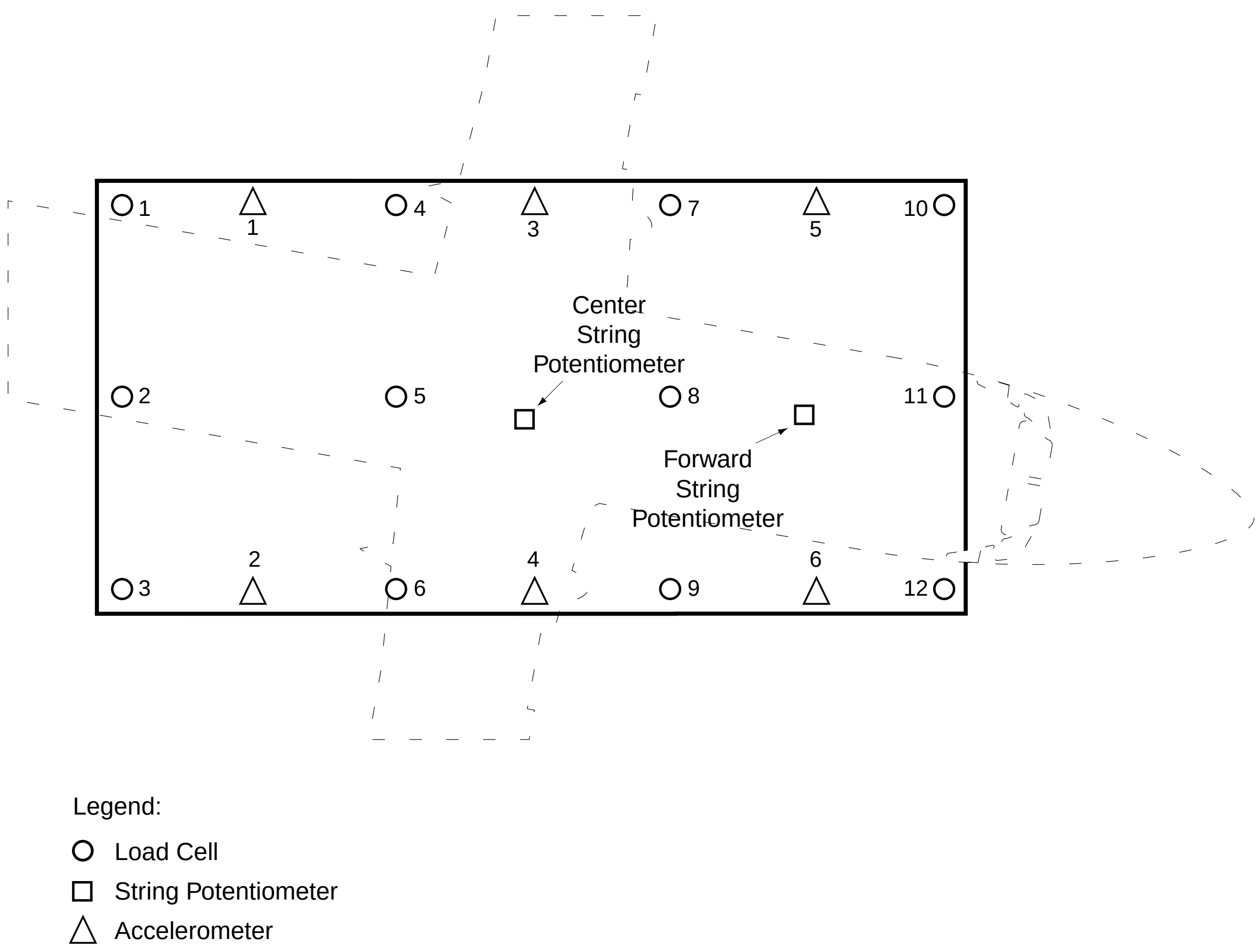

FIGURE 5. PLATFORM INSTRUMENTATION

Six Endevco model 2262A-200 accelerometers, numbered 1 to 6, were mounted on the bottom of the platform to characterize the platform response to the impact, figure 5. Platform response is measured because of the potential influence it may have on fuselage accelerometer readings.

Two Celesco model PT101-020 string potentiometers were attached to the forward and center section of the platform to measure platform displacement, figure 5.

ENGINES, WINGS, AND OUTSIDE SPAR AREAS.

The simulated engines were instrumented with three single-axis Endevco model 7231C-750 accelerometers configured to measure accelerations in the X, Y, and Z directions. The accelerometers were mounted to a single bracket located on the forward frontal area of the simulated engine, figure 6.

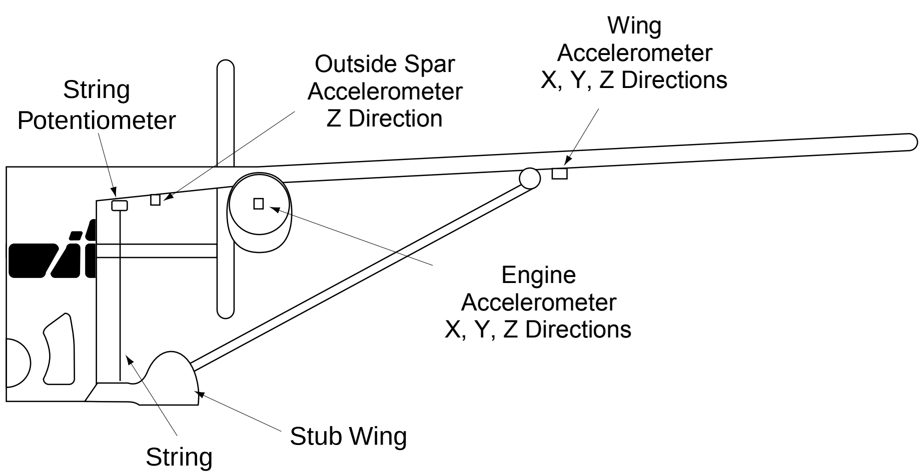

FIGURE 6. WING AND ENGINE INSTRUMENTATION

The wings were similarly instrumented with three single-axis Endevco model 7231C-750 accelerometers to measure the accelerations in the X, Y, and Z directions. These were located under the wing near the strut/wing intersection, figure 6.

An Endevco model 7231C-750 accelerometer and a Celesco model PT101-020 string potentiometer were installed at both the left and right outside spar area to determine the g force loading and displacement at that area, figure 6.

HIGH-SPEED FILM AND VIDEO CAMERAS.

Eight high-speed film cameras were used to record the test. Four of these cameras were onboard the airplane to record the internal impact reactions. The remaining four cameras were located around the exterior of the airplane. One external high-speed camera was used to determine the impact velocity, while the others were used to record various views of the impact.

Video cameras were also used to record the test. One video camera was located onboard the airplane to view the interior of the airplane during the test. Eight video cameras were located around the exterior of the airplane in order to capture a variety of views of the test. A diagram of camera locations can be seen in figure 7.

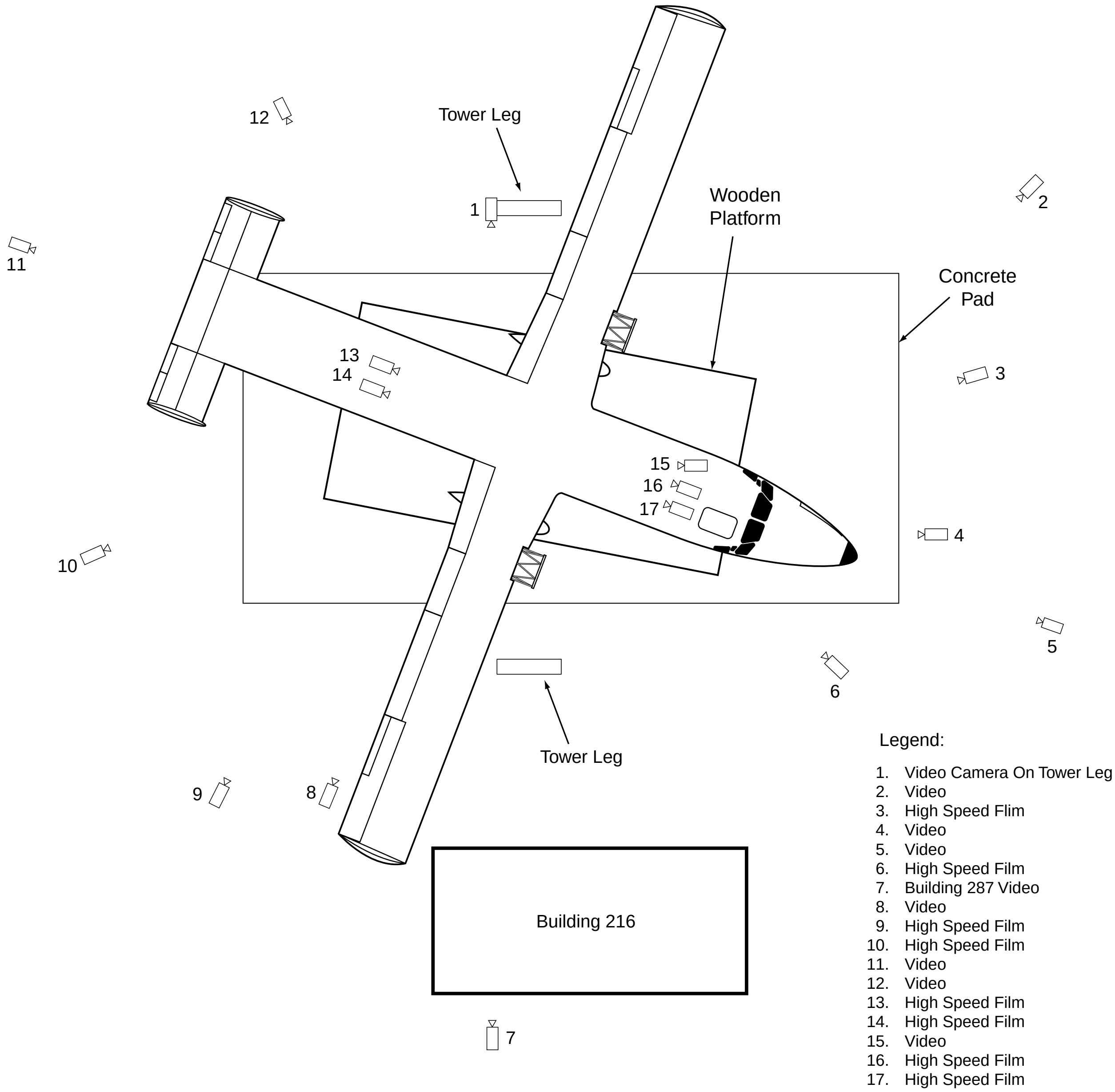

FIGURE 7. CAMERA LOCATIONS

DATA ACQUISITION

DATA ACQUISITION SYSTEMS.

Two data acquisition systems were used a Neff 490 and an EME DAS-48S. A complete listing of all sensor locations for both systems is given in table 3.

NEFF 490. The NEFF 490 is a high-speed data acquisition system with the capability to sample and record data at sampling rates of up to 100 kHz. The system consists of 92 channels. Each channel includes a 12-bit analog-to-digital (A/D) converter with an accuracy of 0.1% of programmable full-scale, a 6-pole Bessel low-pass filter with four programmable cutoff frequencies which cover a range from 100 Hz to 2 kHz, and a differential input amplifier with 12 programmable gain steps. Full-scale range inputs are selectable from ±5 mVdc to ±10.24 Vdc.

For this test, the system was set to sample and record the 92 channels of data simultaneously at 10,000 samples per second per channel. All data channels were prefiltered at a cutoff frequency of 1 kHz and the collected data was temporarily stored in "onboard 256 k word DRAM memory" during the test. Test data were then transferred to an IBM compatible computer by an IEEE-488 interface for further analysis. The full-scale range for each channel was selected to be consistent with the expected output of the transducer.

EME DAS-48S. The EME DAS-48S is a high-speed, small, flexible, ruggedized portable data acquisition system. The system can acquire analog and digital data at rates of up to 20 kHz per channel. The system consists of 48 analog channels and 24 digital channels of data; all channels are simultaneously sampled. The system has a 12-bit A/D converter, and a 6-pole Butterworth anti-alias filter whose corner frequency can be programmed from 10 Hz to 20 kHz. Analog input is fed to a differential input amplifier with variable gain of 1 to 1000; the maximum input voltage is ±2.5 volts.

For the test, the system was set to sample and record 26 channels of data simultaneously at 10,000 samples per second per channel. All data channels were prefiltered at a cutoff frequency of 1 kHz and collected data was temporarily stored in the 16 megawords of memory onboard during the test. Test data were then transferred to an IBM compatible computer by an RS-232/422 interface for further analysis. The gain value for each channel was selected to be consistent with the expected output of the transducer.

Before the test the bridge output voltage for each channel’s sensor was zero-balanced to compensate for any variation in the zero state of the sensor. The channels were then calibrated. All phases of balancing the bridge output voltage, calibrating the channels, measuring sensitivity and determining conversion coefficients for calculating engineering units were controlled by the data acquisition system software based upon operator inputs.

The two acquisition systems were externally triggered by a Bowen 10-channel electronic sequencer, which also controlled all the test processes. “Block Recording” mode was selected for the NEFF 490 system and “Immediate” mode was selected for the EME system. A back up relay was installed to detect hook release and trigger the data acquisition systems in the event of inadvertent hook release or sequencer failure.

WORK STATION.

A Micron Millennia XRU-400 IBM compatible computer was used to configure and run the NEFF 490 system software and to download data from the NEFF 490 DRAM memory. A DEC PC XL SERVER 560 IBM compatible computer was used to configure and run the

EME DAS-48S software and to download the data from the DAS-48S resident memory. The data were then transferred to the Micron system and analyzed.

DATA ANALYSIS

DATA REDUCTION.

As stated, all sensor data was first filtered with a 1 kHz analog filter and then recorded at a sampling rate of 10,000 samples per second. All accelerometers and load cell sensors were then further filtered with a SAE J211class 60 digital filter [4]. All data were filtered and analyzed using DSP Development Corporation's DADiSP data analysis software.

The data were recorded for 22 seconds, starting 2 seconds prior to hook release. For the purposes of this test Time Zero was defined as 1 millisecond prior to the first observed indication of significant impact on any of the recorded channels.

TIME TO IMPACT.

The expected free fall time of the airplane, 0.933 second, was calculated using the equation

$$t = \sqrt{2h/g} \tag{1}$$

where t is time, h is the drop test distance (14 ft), and g is the acceleration due to gravity (32.2 ft/sec^2). This is close to the observed free fall time (t = 0.915 sec) which was determined from the high-speed films of the front view and quarter view cameras, which were equipped with IRIG B timing devices

TEST VELOCITY.

The impact velocity was determined by the kinematic equation

$$v_f = \sqrt{2gh} \tag{2}$$

where v_f is the final velocity, g is the acceleration due to gravity (32.2 ft/sec^2), and h is the drop test distance (14 ft). Using this equation, the theoretical impact velocity is 30 ft/sec. This velocity was compared to the observed and measured velocities.

The observed impact velocity was calculated using the kinematic linear motion equation

$$v_f - v_0 = gt \tag{3}$$

where v_f is the final velocity, v_o is the initial velocity (0 ft/sec), g is the acceleration due to gravity (32.2 ft/sec^2), and t is the observed free fall time (0.915 sec). The resulting observed velocity was 29.5 ft/sec.

The measured velocity was calculated by determining the average velocity of the airplane through the aft velocity measuring system (figure 8). The measured average velocity (28.1 ft/sec) was calculated using the equation

$$v = \frac{\Delta d}{\Delta t} \tag{4}$$

where v is the velocity, Δd = 1 ft, and Δt equals the elapsed time (0.0356 sec). The forward velocity measuring system malfunctioned.

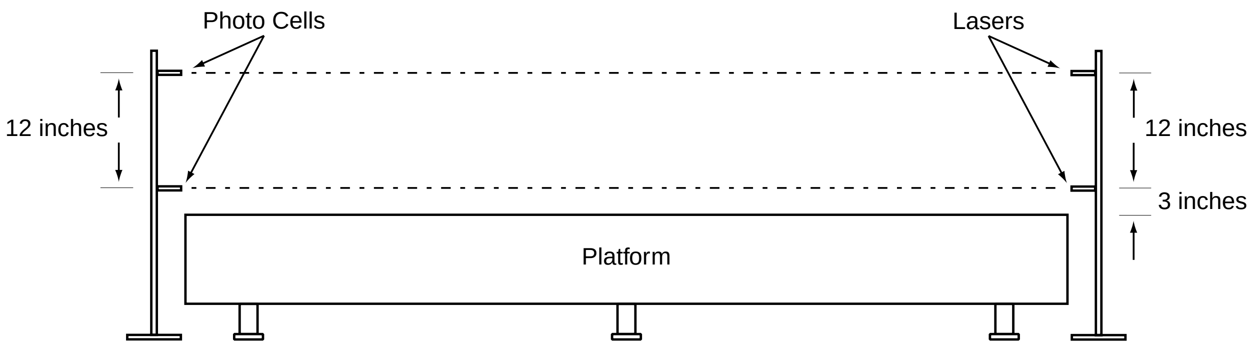

FIGURE 8. VELOCITY SYSTEM CONFIGURATION

Table 4 shows the drop test velocity obtained using the above different methodologies.

TABLE 4. DROP TEST VELOCITY

Methodology	Velocity (ft/sec)
Theoretical	30
Observed	30
Measured	28

AIRFRAME ACCELERATION AND STRING POTENTIOMETER DATA.

The airframe acceleration data are presented in six groups: side-wall accelerations, side-wall seat track accelerations, floor track accelerations, engine accelerations, wing accelerations, and spar accelerations. The G_{peak} values were read directly from the filtered data. Filtered acceleration data are shown in the appendix. The G_{max} normalized values were computed using equation (5), which assumes an idealized triangular pulse

$$G_{max} = \frac{2\Delta V}{\Delta t} \tag{5}$$

where Δt is the difference between the start and stop times of the integration interval, and ΔV is the velocity change determined by integrating the acceleration data during Δt.

The data in the appendix indicates that the airplane experienced a secondary pulse at some fuselage stations during the impact. To determine the G_{max} level of the impact, only the primary pulse is used and the secondary pulse is considered inconsequential. However, the secondary pulse could cause erroneous values in calculating G_{max}. To compensate for the secondary pulse in the G_{max} calculation, the total velocity change was computed by combining the primary and secondary pulse as shown in figure 9. Figure 9 is a simplified presentation of a primary and secondary pulse. To compensate for the secondary pulse in the G_{max} calculation, the total velocity change was computed by adding from time t_1 to time t_2 to include areas A and B but not C.

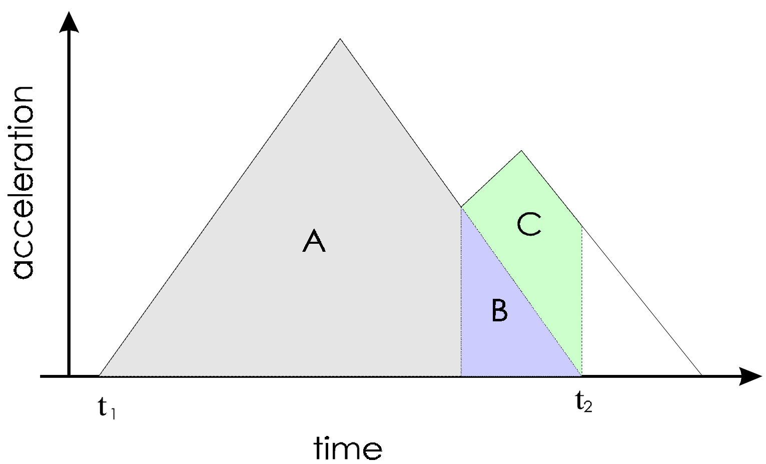

FIGURE 9. TYPICAL PRIMARY AND SECONDARY IMPACT PULSE

The G_{max} normalized acceleration data of the side wall, side wall seat track, and floor seat track and the impact pulse duration are presented in figure 10. Tables 5, 6, and 7 show the corresponding G_{peak} value, G_{max} value, and pulse duration. Engine, wing, and spar data are shown in tables 8, 9, and 10 respectively.

The airplane string potentiometer data are shown in the appendix. The mounting area for the right outside spar string potentiometer suffered severe distortion and effected the data.

PLATFORM.

The platform load cell data are presented in the appendix. Seven of the twelve load cells exceeded their rated load ratings. The platform load data was collected with the expectations that it would provide information in helping to characterize the platform reaction to the impact.

The platform acceleration data are presented in the appendix. Analysis indicated there was no significant platform response superimposed on the airframe data.

Platform string potentiometer data are shown in the appendix. The data indicates that the platform displaced approximately ±0.5 inches during impact and rebound at both locations.

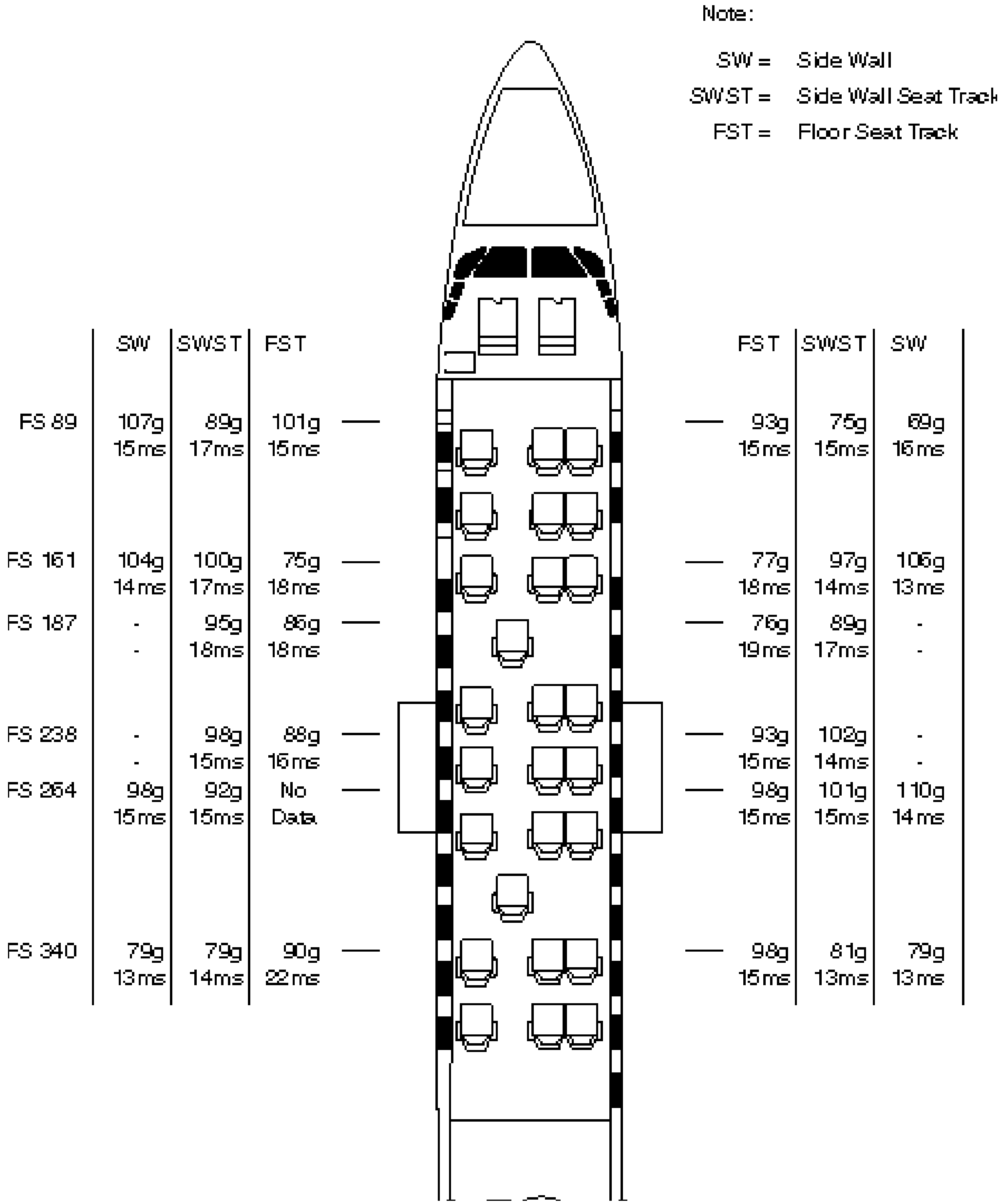

FIGURE 10. FUSELAGE SIDE WALL, SIDE WALL SEAT TRACK, AND FLOOR SEAT TRACK G_{max} ACCELERATIONS AND PULSE DURATIONS

TABLE 5. SIDE WALL ACCELERATIONS

Fuselage Station	Direction	G_{peak} (g)	G_{max} (g)	Pulse Duration (msec)
FS 89 L	Z	103	107	15
FS 89 R	Z	60	69	16
FS 161 L	Z	101	104	14
FS 161 R	Z	95	106	13
FS 264 L	Y	48	47	7
FS 264 L	Z	95	98	15
FS 264 R	Y	42	46	6
FS 264 R	Z	107	110	14
FS 340 L	Z	69	79	13
FS 340 R	Z	77	79	13

Note: L = Pilot/Left side, R = Copilot/Right side

TABLE 6. SIDE WALL SEAT TRACK ACCELERATIONS

Fuselage Station	Direction	G_{peak} (g)	G_{max} (g)	Pulse Duration (msec)
FS 89 L	Z	90	89	17
FS 89 R	Z	64	75	15
FS 161 L	Z	96	100	17
FS 161 R	Z	92	97	14
FS 187 L	Z	93	95	18
FS 187 R	Z	94	89	17
FS 238 L	Z	92	98	15
FS 238 R	Z	105	102	15
FS 264 L	Z	89	92	15
FS 264 R	Z	102	101	15
FS 340 L	Z	74	79	14
FS 340 R	Z	75	81	13

Note: L = Pilot/Left side, R = Copilot/Right side

TABLE 7. FLOOR SEAT TRACK ACCELERATIONS

Fuselage Station	Direction	G_{peak} (*g*)	G_{max} (g)	Pulse Duration (msec)
FS 89 L	Z	97	101	15
FS 89 R	Z	83	93	15
FS 161 L	Z	72	75	18
FS 161 R	Z	72	77	18
FS 187 L	Z	85	86	18
FS 187 R	Z	67	76	19
FS 238 L	Z	84	88	16
FS 238 R	Z	94	93	15
FS 264 L	X	7	11	7
FS 264 L	Z	No data	No data	No data
FS 264 R	X	12	13	8
FS 264 R	Z	104	98	15
FS 340 L	Z	86	90	22
FS 340 R	Z	103	98	15

Note: L = Pilot/Left side, R = Copilot/Right side

TABLE 8. ENGINE ACCELERATIONS

Engine Location	Direction	G_{Peak} (g)
L	X	20
L	Y	5
L	Z	21
R	X	14
R	Y	27
R	Z	25

Note: L = Pilot/Left side, R = Copilot/Right side

TABLE 9. WING ACCELERATIONS

Wing	Direction	G_{peak} (g)
L	X	35
L	Y	59
L	Z	52
R	X	28
R	Y	41
R	Z	75

Note: L = Pilot/Left side, R = Copilot/Right side

TABLE 10. SPAR ACCELERATIONS

Spar Station	Direction	G_{peak} (g)	G_{max} (g)	Pulse Duration (msec)
FS 251 L Outside	Z	100	71	13
FS 251 R Outside	Z	110	73	15
FS 238 LFS	Z	116	98	16
FS 238 RFS	Z	154	103	13
FS 238 RFS-Far Right	Z	108	80	15
FS 264 LRS	Z	120	96	14
FS 264 RRS	Z	136	96	14
FS 264 RRS-Far Right	Z	113	79	14

Note: L = Pilot/Left side, R = Copilot/Right side.
LFS = Left Front Spar, RFS = Right Front Spar
LRS = Left Rear Spar, RRS = Right Rear Spar

ANTHROPOMORPHIC TEST DUMMIES.

Seven ATDs were used to measure loads and accelerations in their respective lumbar and pelvic areas for various types of passenger seats during this test. The ATD data are presented in table 11 and the appendix.

TABLE 11. ANTHROPOMORPHIC TEST DUMMY DATA

Fuselage Station	Lumbar Load (lb)	Accelerometer Model	Accelerometer Data G_{peak} (g)	Accelerometer Data Pulse Duration (msec)
55	2440	7265 A-100	58	33
55		7231 C-750	60	34
110	1605	7265 A-100	35	21
110		7231 C-750	35	22
173	2055	7265 A-100	35	59
173		7231 C-750	36	58
190	2271	7265 A-100	53	37
190		7231 C-750	52	37
262	1489	7265 A-100	31	34
262		7231 C-750	38	36
315	1309	7265 A-100	63	27
315		7231 C-750	67	26
357	2000	7265 A-100	56	47
357		7231 C-750	55	44

Note: This test was not a seat certification test. The data in this table should not be related to certification seat test standards.

The pelvic accelerations seen by the ATDs would have resulted in moderate to severe injuries as defined in reference 5.

RESULTS AND DISCUSSION

FUSELAGE STRUCTURE.

EXTERNAL. The lower section of the Shorts 3-30 fuselage experienced minimal external crushing during the drop test. The lower section, for this purpose, is the area from the fuselage bottom, referred to as water line 0 (WL 0), to approximately 28 inches above the fuselage bottom (WL 28). The maximum external deformation in this area was approximately 1.3 inches and occurred in the forward section of the fuselage on the copilot's side. Deformation was as little as 0.5 inch in the rear of the airplane and no external deformation was noticed over the wheel wells. Small crush distances were a result of the box shape fuselage, which is extremely rigid and can carry large loads in compression. Table 12 gives crush distances, as well as pre- and posttest measurements, at various fuselage stations.

TABLE 12. LOWER FUSELAGE EXTERNAL CRUSH MEASUREMENTS

Location	Pretest (inch)	Posttest (inch)	Crush (inch)
FS 89 L	27.8	26.9	0.9
FS 161 L	27.9	26.9	1.0
FS 264 L (over wheel well)	14.4	14.4	0.0
FS 340 L	28.3	27.3	1.0
FS 89 R	27.8	26.5	1.3
FS 161 R	27.9	26.6	1.3
FS 264 R (over wheel well)	14.4	14.4	0.0
FS 340 R	28.3	27.8	0.5

Note: L = Pilot/Left side, R = Copilot/Right side

High-speed film analysis showed that the fuselage deformation was minimal during the impact (dynamic deformation) as well as after the test (static deformation). This means the fuselage did not crush and then rebound after the impact. This additional crushing, or lack there of, is important to note because it would allow for additional energy absorption.

The external upper section of the fuselage, WL 72 and above, sustained significant deformation during the test. On the left side, major deformation and buckling was seen from FS 89 to FS 212 and also from FS 289 to FS 340. The right side also experienced major buckling between FS 89 and FS 187 as well as some less significant buckling from FS 264 to FS 340.

All of the deformation seen in the upper section of the fuselage was caused by the loads imparted by the fuel tanks. This crushing is not as significant, in term of energy absorption, as is the lower section crush because crushing in the upper section does not reduce the loads seen by the occupants. Upper fuselage damage is more crucial with regard to maintaining a survivable volume. This issue will be discussed further in the following sections.

There were a number of large cracks in the fuselage skin after impact. The left side experienced a crack at FS 289 from the top of the fuselage down to the rivet line at WL 59. The crack then continued forward along the rivet line to FS 277. It then continued downward at FS 277 to the window and then on the bottom of the window down to the rivet line at WL 29. The crack then ran aft along the rivet line to FS 289. At FS 289 the crack continued downward to a point approximately 18 inches above the fuselage bottom at WL 18. The crack described above is shown schematically in figure 11.

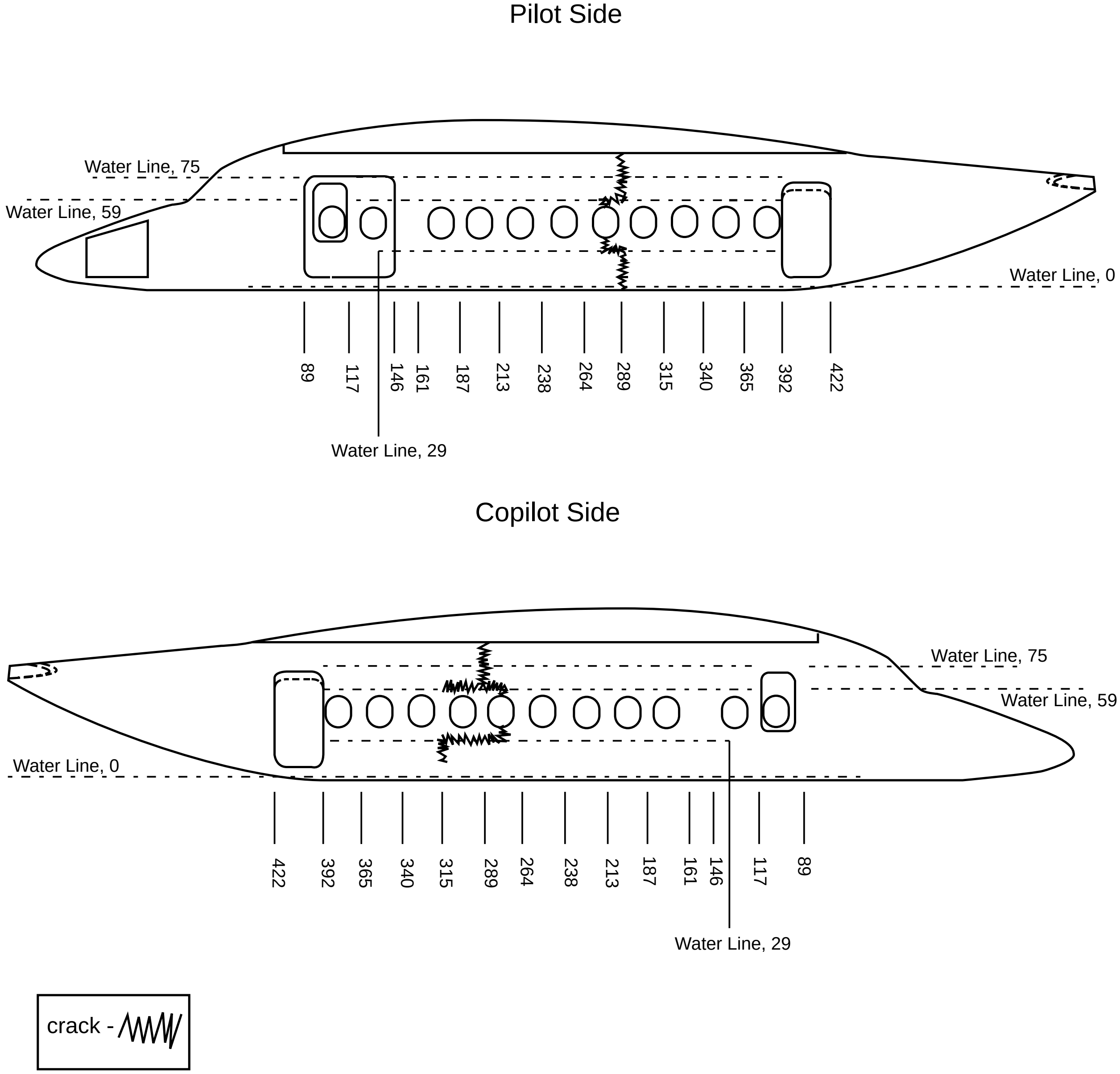

FIGURE 11. FUSELAGE CRACK

The right side experienced a similar crack, which also is shown in figure 11. The copilot-side crack began at the top of the fuselage at FS 289. The crack ran down FS 289 to the rivet line at WL 59. At WL 59 it continued both aft and forward along the rivet line to FS 315 and FS 277, respectively. The crack then moves down along FS 277 from the WL 59 rivet line to the top of the window at FS 277 and continues at FS 277 on the bottom of the window down to the rivet line at WL 29. The crack then continues aft along the rivet line at WL 29 from FS 277 back to FS 315. It then continues down FS 315 and ends approximately 12 inches above the bottom of the fuselage at WL 12.

The underside of the fuselage experienced no significant damage. Only minor buckling in a few small areas was noted.

All exits and emergency exits functioned properly after the impact.

Nine of the 23 external passenger windows shattered during the impact due to fuselage buckling.

INTERNAL. The fuselage of the airplane maintained a survivable volume after the impact. This means that there was sufficient room for the passengers to survive the impact (i.e., without being crushed), and there was sufficient room for safe passenger egress.

Measurements were taken pre- and posttest under the floor boards to record any internal crushing of the lower portion of the fuselage. Due to the stiffness in the structure and the small space under the floorboards (approximately 8 inches) only minimal crushing was recorded. The average crush under the floorboards was approximately 0.1 inches. Table 13 gives crush distances, as well as pre- and posttest measurements, at various fuselage stations under the floorboards.

TABLE 13. UNDERFLOOR CRUSH MEASUREMENTS

Location	Pretest (inch)	Posttest (inch)	Crush (inch)
FS 89 L	8.19	8.13	0.06
FS 161 L	8.19	8.13	0.06
FS 238 L	8.31	8.25	0.06
FS 264 L	8.31	8.25	0.06
FS 340 L	8.19	8.06	0.13
FS 391 L	7.75	7.69	0.06
FS 89 R	8.19	8.13	0.06
FS 161 R	8.19	8.13	0.06
FS 238 R	8.44	8.38	0.06
FS 264 R	8.19	8.06	0.13
FS 340 R	8.19	8.06	0.13
FS 391 R	7.75	7.69	0.06

L = Pilot/Left side, R = Copilot/Right side

The ceiling of the fuselage protruded into the cabin space at the location of the overhead fuel tanks. The ceiling deformation ranged from 0 to 1.5 feet. The deformation was due mainly to the load the fuel tanks exerted on the fuselage ceiling. Crushing was seen on the pilot side between FS 89 and FS 238 and from FS 264 to FS 365. On the copilot side crushing was seen between FS 117 and FS 238 as well as from FS 264 and FS 340. The fuel tanks will be discussed in the next section.

Some floor panels experienced cracking and deformation due to the loads exerted by the legs of the anthropomorphic test dummies.

As mentioned earlier, the side walls experienced a severe crack on both the pilot and copilot side. No additional significant cracking or buckling was noticed.

Thirteen of the 23 internal passenger windows shattered during the impact due to fuselage buckling.

FUEL TANKS.

Both fuel tanks protruded into the cabin area. The forward ceiling below cells 1, 2, and 3, protruded approximately 1.5 feet into the cabin. The total simulated fuel weight in these cells was 2195 pounds. The rear ceiling, below cell 4 was protruded approximately 1 foot into the cabin; the simulated fuel in cell 4 weighed 1680 pounds. External views of this are shown in figures 12 and 13.

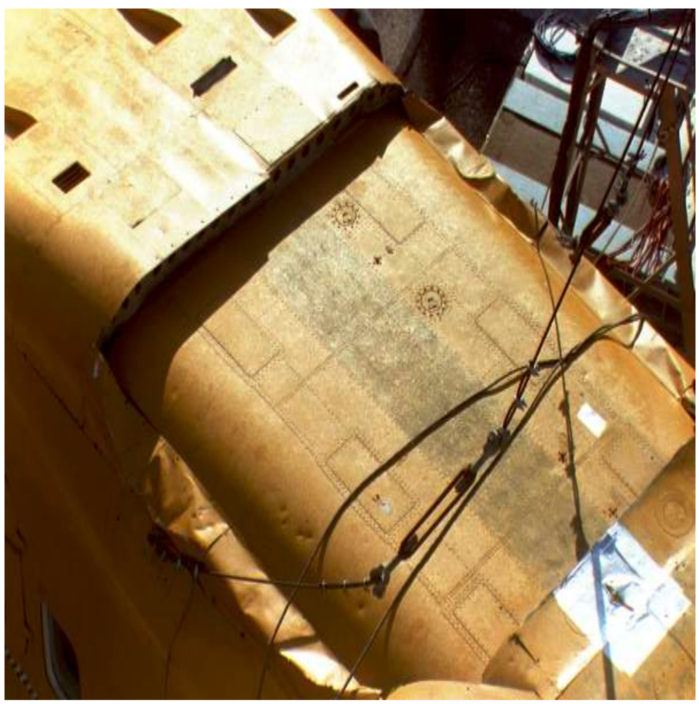

FIGURE 12. FUEL CELLS 1, 2, AND 3 COLLAPSED INTO FUSELAGE

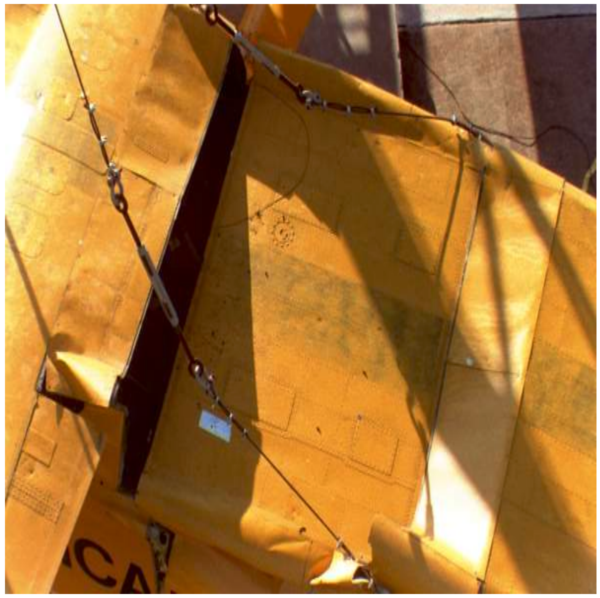

FIGURE 13. FUEL CELL 4 COLLAPSED INTO FUSELAGE

Figure 14 shows the Shorts 3-30 fuel system schematic with damaged areas noted.

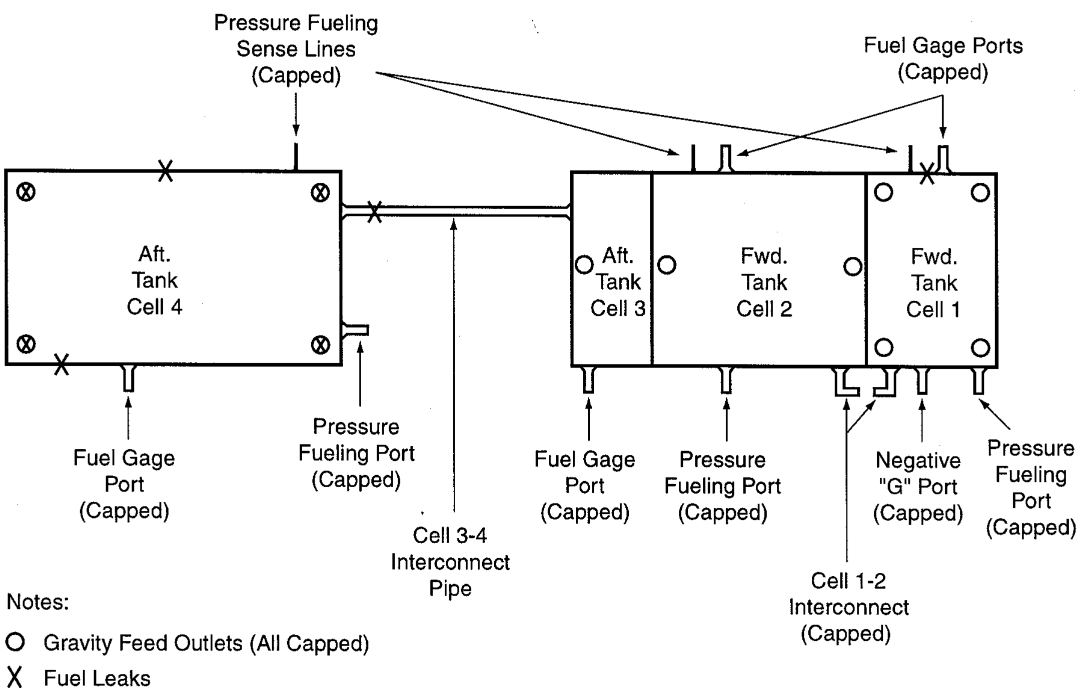

FIGURE 14. SHORTS 3-30 FUEL SYSTEM SCHEMATIC SHOWING LEAK LOCATIONS

After the test, numerous rips and tears were observed in the fuel tanks. Cell 1 experienced a crack on the pilot side of the tank, figure 15. Cell 2 experienced no leaks. Cell 3 had a massive leak through the 2-inch cell 3 to 4 interconnect pipe, figure 16. Cell 4 experienced seven leaks.

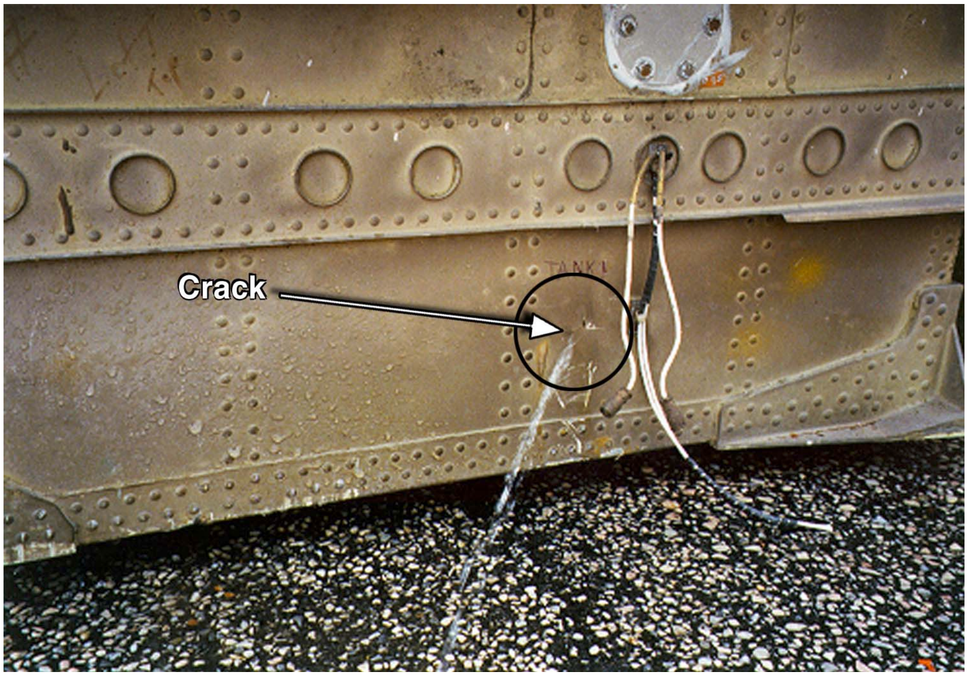

FIGURE 15. CRACK IN CELL 1 PILOT SIDE

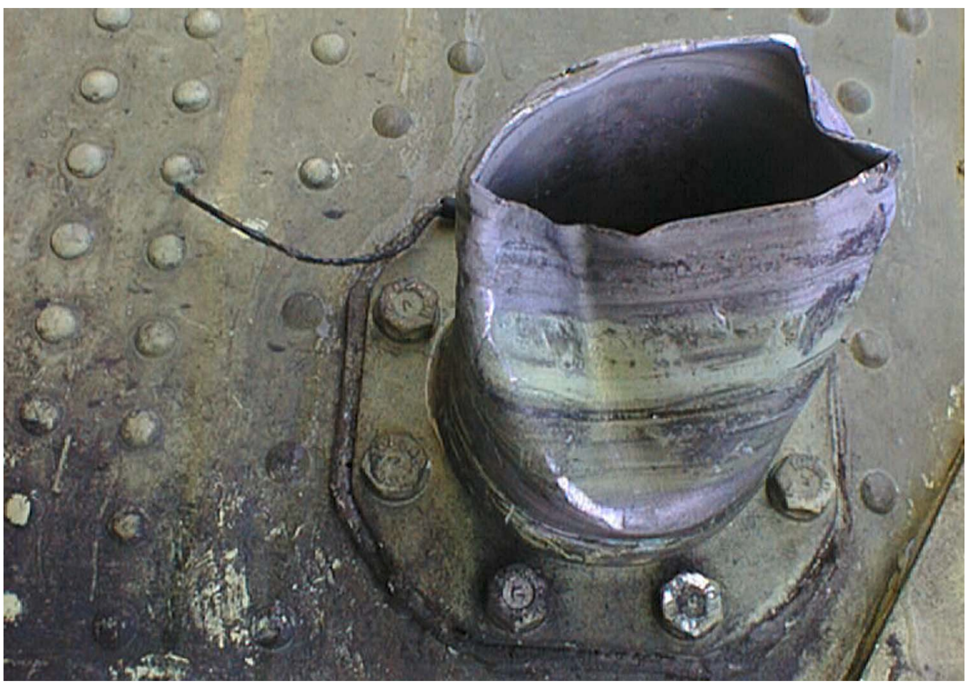

FIGURE 16. CELL 4 INTERCONNECT FITTING DAMAGE

The impact caused major cracks in both the pilot and copilot sides of the tank, figures 17 and 18, respectively. The four gravity feed outlets were crushed. Figure 19 shows typical gravity feed outlet damage. Simulated fuel also leaked from the cell 3 to 4 interconnect pipe.

FIGURE 17. CRACK IN CELL 4 PILOT SIDE

FIGURE 18. CRACK IN CELL 4 COPILOT SIDE

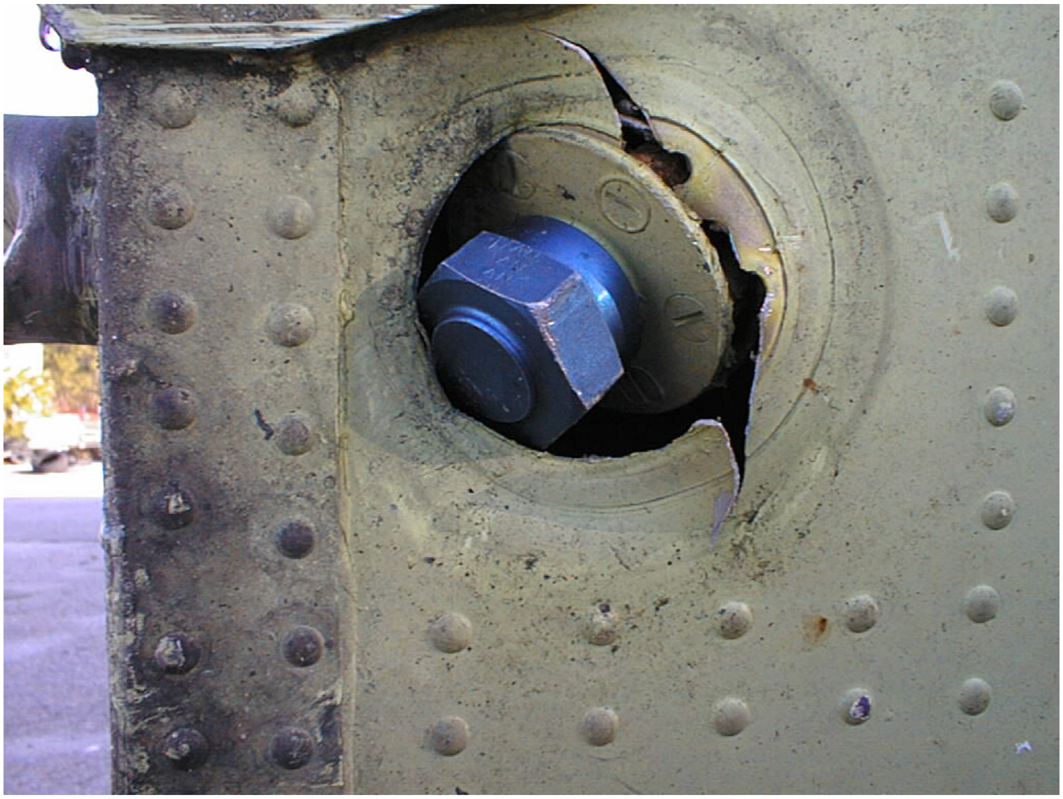

FIGURE 19. CRUSHED GRAVITY FEED OUTLET IN CELL 4

WINGS, STRUTS, AND EMPENAGE.

Both wings experienced major structural damage during the test. The pilot-side wing displaced downward causing a compressive failure of the wing strut. The downward deflection of the wing was so severe that the wing tip was below the bottom of the fuselage. The final position of the fuselage was elevated on a platform which allowed the movement past the bottom of the fuselage. In an actual crash the wing tips would have come in contact with the ground. In addition, the simulated engine on the pilot side broke away from its mounting.

The copilot-side wing also deflected downward and experienced a similar failure of the wing strut. Again the wing tip deflected below the fuselage bottom. However, the simulated engine on this side remained attached to the engine mount.

The empennage remained attached to the fuselage and experienced no noticeable damage or buckling.

SEATS.

Most of the seats had a strap added around the seat pan, figure 20. These seats are noted in table 14 by an asterisk after the row number. The purpose of the strap was to prevent the seat pan aft support pin from potentially shearing off during the test. Shearing of the seat pan would be undesirable because it would prevent an accurate reading of the lumbar load experienced by the occupants. Seats in which the seat pan did experience this type of failure are noted in table 14 by the term "sheared" in the seat pan column.

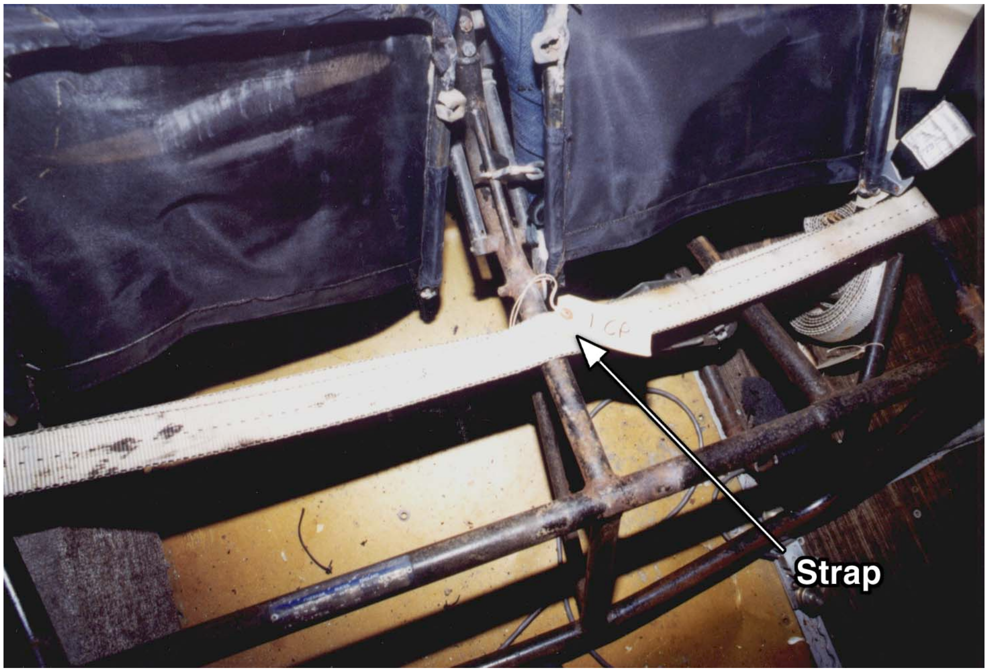

FIGURE 20. TYPICAL SEAT STRAP INSTALLATION

TABLE 14. SEAT DAMAGE

	Pilot Side (Left/Aisle)			Copilot Side (Center/Right)				
				Seat Legs	Seat Back		Seat Pan	
Row	Seat Legs	Seat Back	Seat Pan		Center	Right	Center	Right
Pilot/ Copilot	Intact	Upright	Intact	Intact	N/A	Upright	N/A	Intact
1 *	Intact	Upright	Intact	Intact	Upright	Upright	Intact	Sheared
2 *	Broken	Upright	Intact	Broken	Upright	Upright	Intact	Intact
3 *	Broken	Upright	Intact	Broken	Upright	Upright	Intact	Intact
4	Intact	Upright	Stroke 1″	N/A	N/A	N/A	N/A	N/A
5 *	Broken	Upright	Intact	Broken	Upright	Upright	Intact	Sheared
6	Intact	Upright	Sheared	Broken	Upright	Upright	Intact	Intact
7 *	Intact	Upright	Sheared	Broken	Upright	Upright	Intact	Intact
8	Intact	Upright	Ripped	N/A	N/A	N/A	N/A	N/A
9 *	Intact	Upright	Intact	Broken	Upright	Upright	Intact	Intact
10 *	Intact	Reclined	Intact	Broken	Reclined	Reclined	Intact	Intact

Note: * means that a strap was added around seat pan to add support.

The seat legs experienced a variety of failures. Some legs were bent, while others were completely broken, and still others had no noticeable damage. In addition, some seat legs remained in the seat track while others were pulled out of the seat track. Table 14 shows that any seat experiencing significant damage to the seat legs is indicated by a “broken” entry in the seat leg column. If the seat was damaged, a picture of the damage can be seen in the photographic documentation section.

Seat back damage (i.e., excessive reclining) was minimal, mainly because the seat backs were supported by the legs of the occupants in the seats behind them. The seats in the last row, row 10, saw significant deformation as there was nothing behind them to stop their movement.

The stroking mechanism in the CAMI seat (row 4) failed to function properly. The lack of stroking resulted in higher than expected pelvic loads.

The pilot and copilot seats experienced no damage.

PHOTOGRAPHIC DOCUMENTATION.

The photographs in this report were taken prior to and after the test. All photographs were taken with a 35-mm camera.

Figures 21 and 22 show the test facility and exterior of the airplane prior to and after the test.

Figures 23 – 30 show external damage to the fuselage, wings, and struts.

Figures 31 and 32 show overall internal pictures after the impact.

Figures 33 – 35 show internal ceiling and floor damage.

Figures 36 – 56 show the posttest views of the seats that were damaged during the test. These include the CAMI seat, Beechcraft seat, and the standard Shorts seats.

Figures 57 – 67 show the posttest views of the ATD.

FIGURE 21. OVERALL PRETEST

FIGURE 22. OVERALL POSTTEST

FIGURE 23. REAR QUARTER VIEW POSTTEST

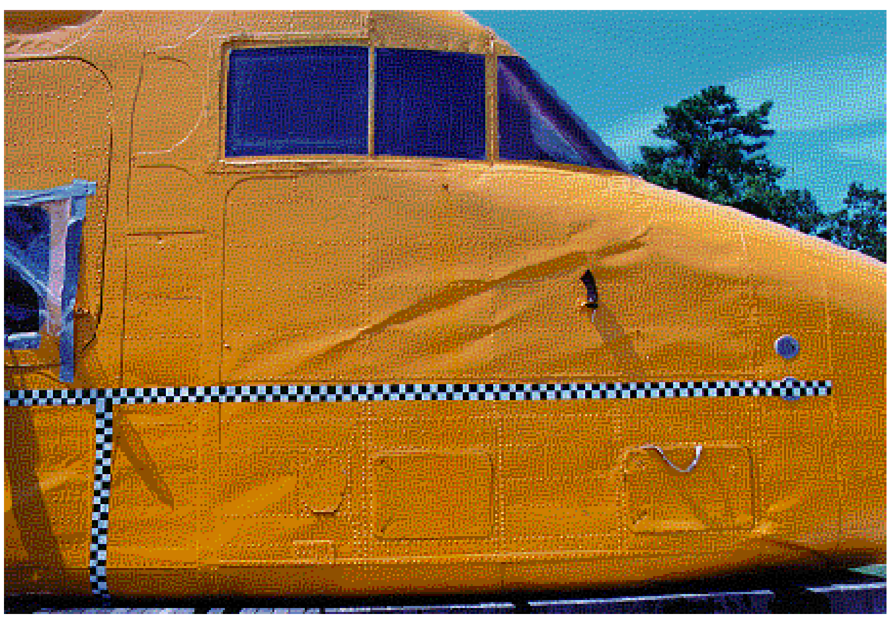

FIGURE 24. SKIN BUCKLING COPILOT-SIDE POSTTEST

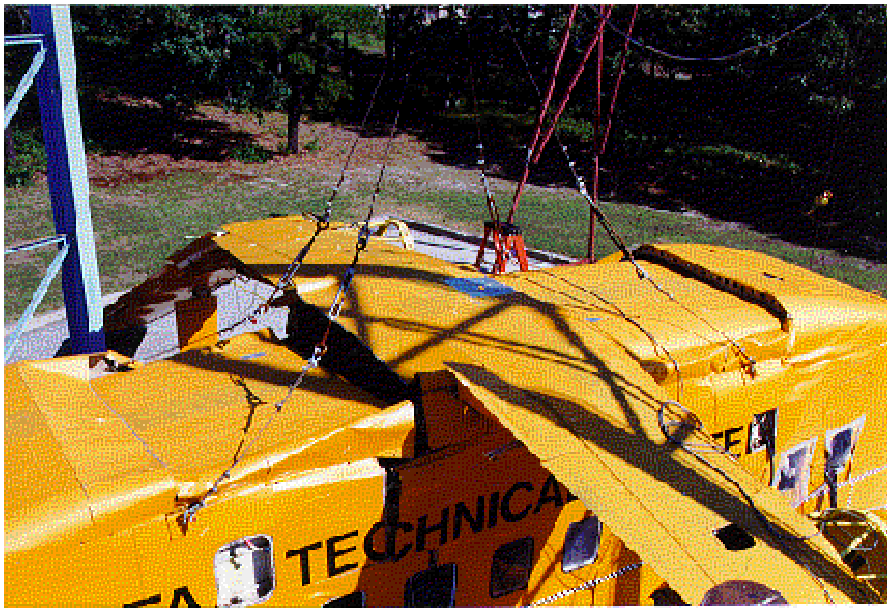

FIGURE 25. EXTERIOR FUEL TANK DEFORMATION POSTTEST

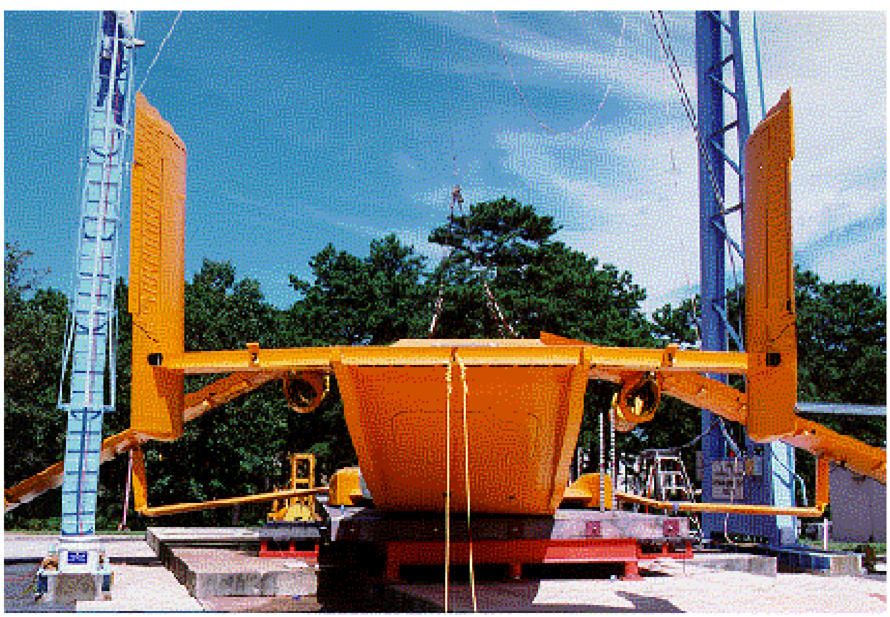

FIGURE 26. REAR VIEW POSTTEST

FIGURE 27. PILOT-SIDE FUSELAGE CRACK POSTTEST

FIGURE 28. COPILOT-SIDE FUSELAGE CRACK POSTTEST

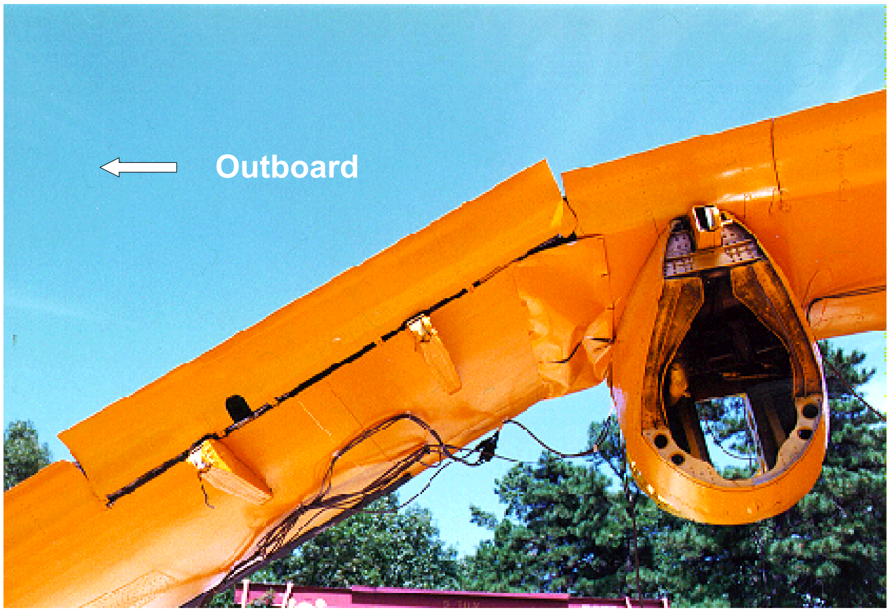

FIGURE 29. PILOT-SIDE WING DEFORMATION POSTTEST

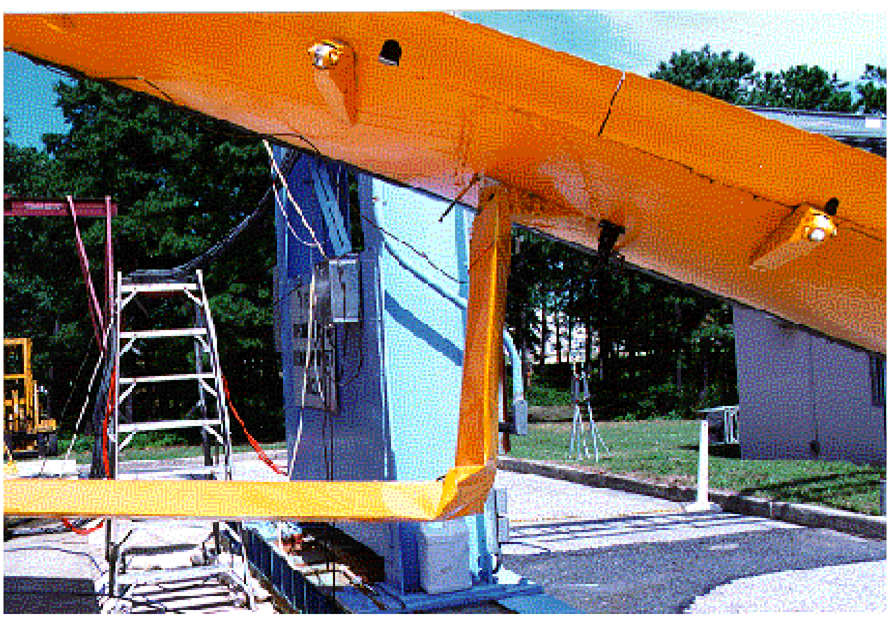

FIGURE 30. COPILOT-SIDE STRUT DEFORMATION POSTTEST

FIGURE 31. OVERALL INTERIOR POSTTEST AFT VIEW

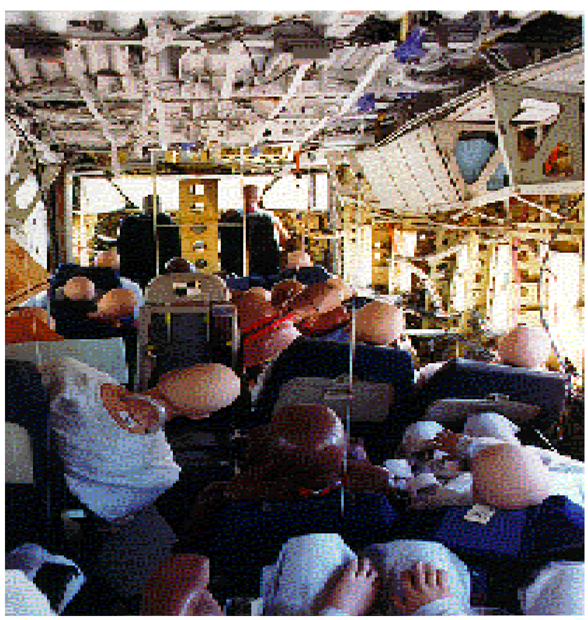

FIGURE 32. OVERALL INTERIOR POSTTEST FORWARD VIEW

FIGURE 33. CEILING DEFORMATION POSTTEST PILOT SIDE

FIGURE 34. CEILING DEFORMATION POSTTEST COPILOT SIDE

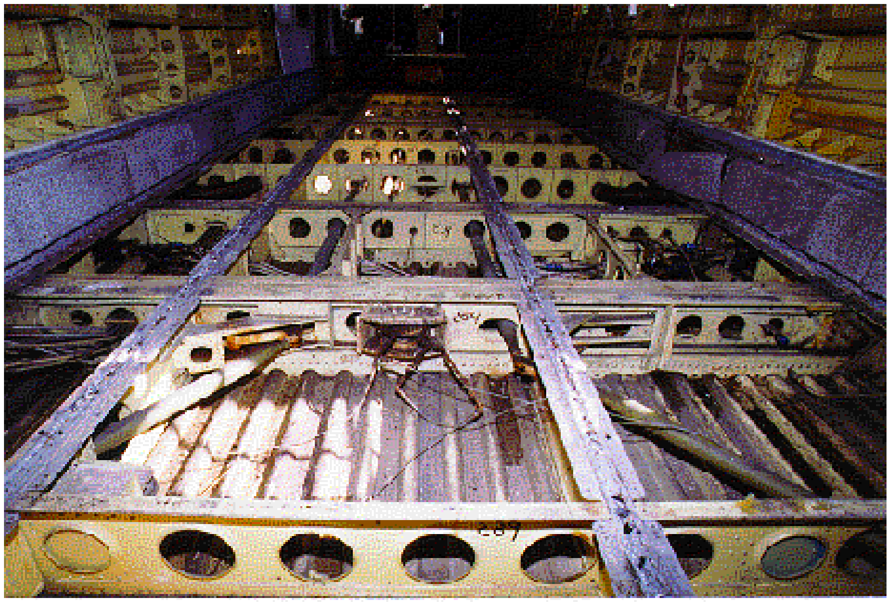

FIGURE 35. SEAT TRACK AND UNDERFLOOR POSTTEST

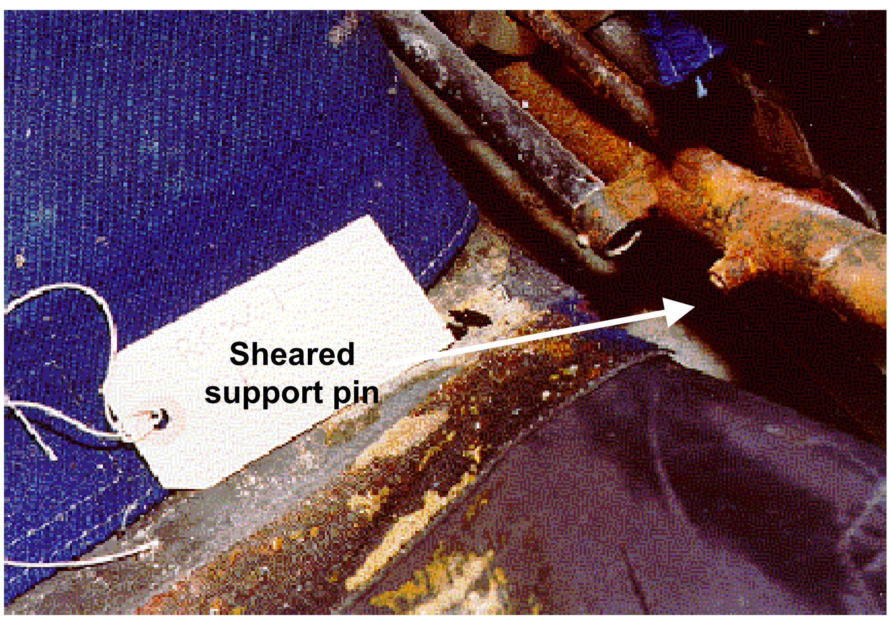

FIGURE 36. ROW 1 COPILOT-SIDE SEAT PAN

FIGURE 37. ROW 2 PILOT-SIDE SEAT LEG

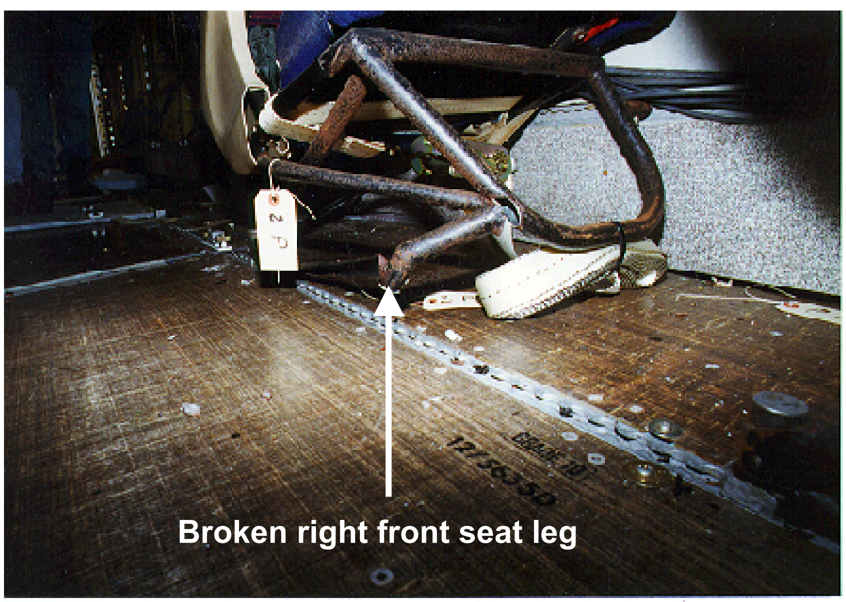

FIGURE 38. ROW 2 PILOT-SIDE SEAT LEG CLOSEUP

FIGURE 39. ROW 2 COPILOT-SIDE SEAT LEG

FIGURE 40. ROW 3 PILOT-SIDE SEAT LEG

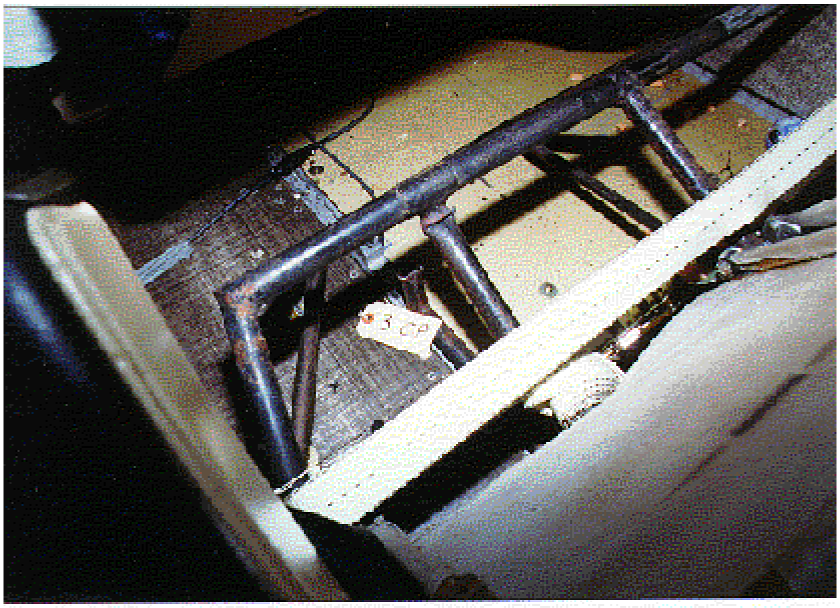

FIGURE 41. ROW 3 COPILOT-SIDE SEAT LEG

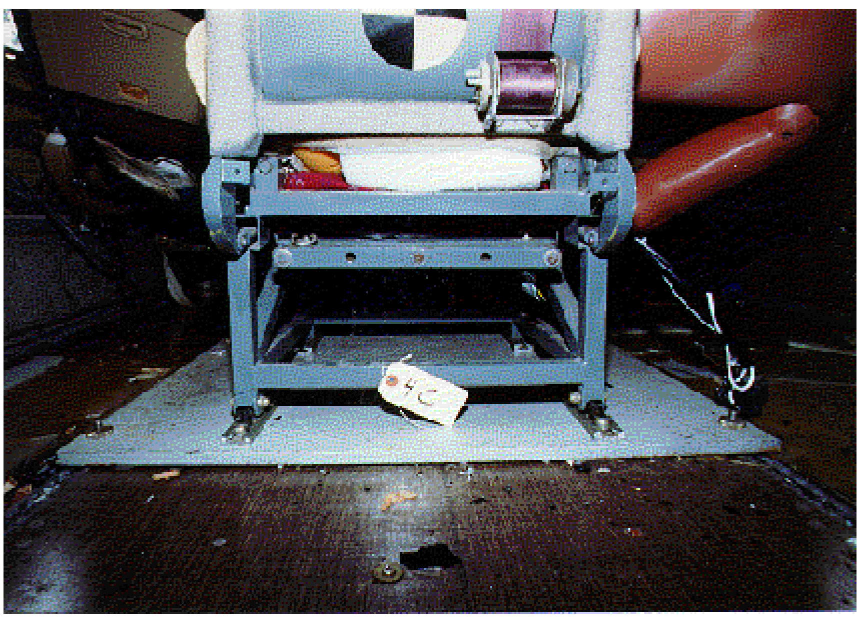

FIGURE 42. ROW 4 CAMI SEAT REAR VIEW

FIGURE 43. ROW 5 PILOT-SIDE SEAT LEG

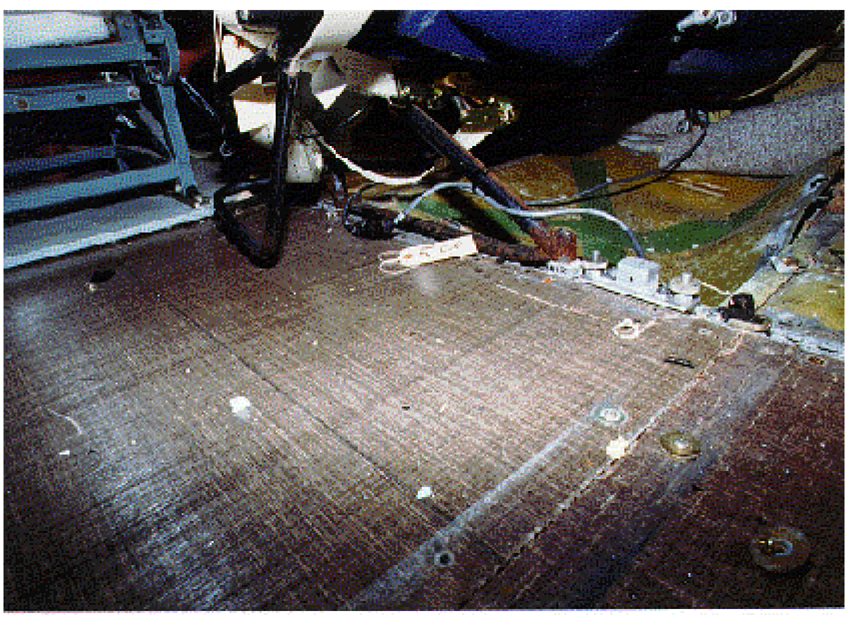

FIGURE 44. ROW 5 COPILOT-SIDE SEAT LEG

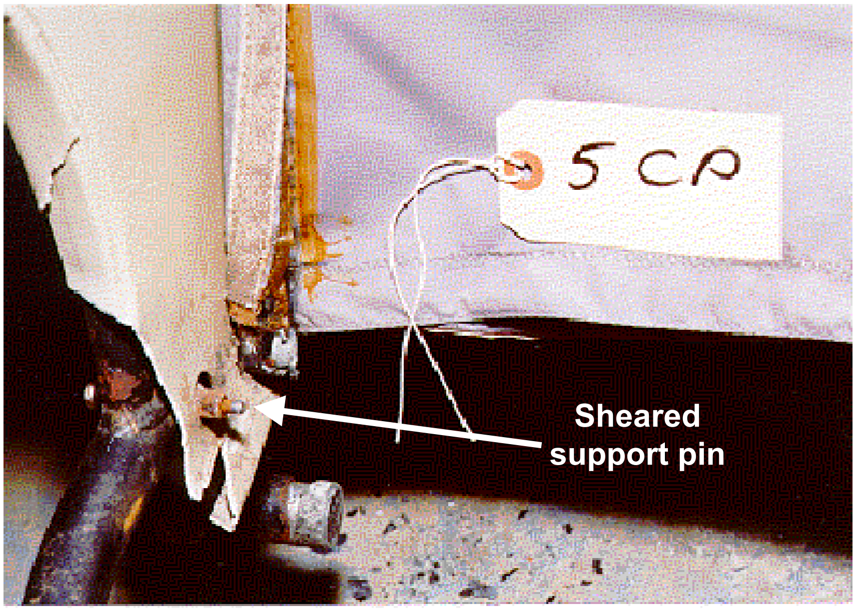

FIGURE 45. ROW 5 COPILOT-SIDE SEAT PAN

FIGURE 46. ROW 6 PILOT-SIDE SEAT LEG

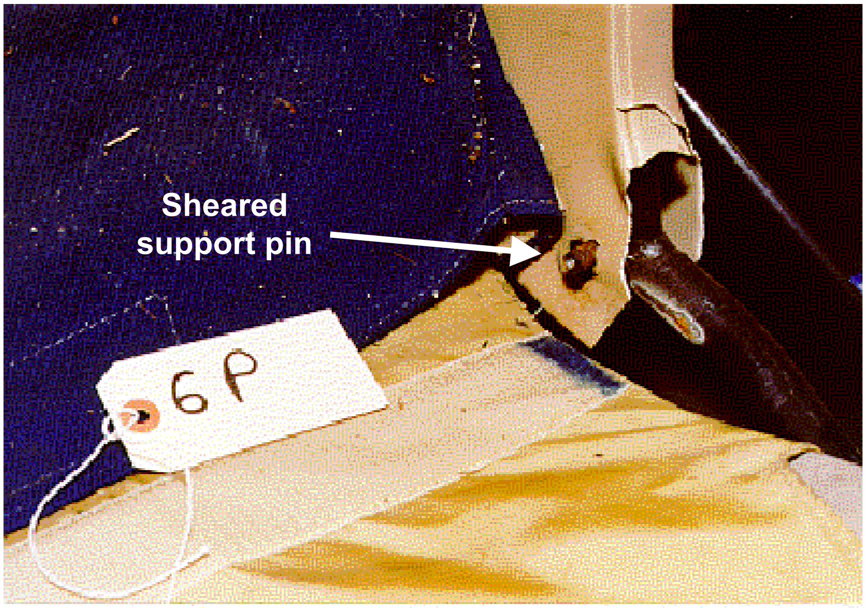

FIGURE 47. ROW 6 PILOT-SIDE SEAT PAN

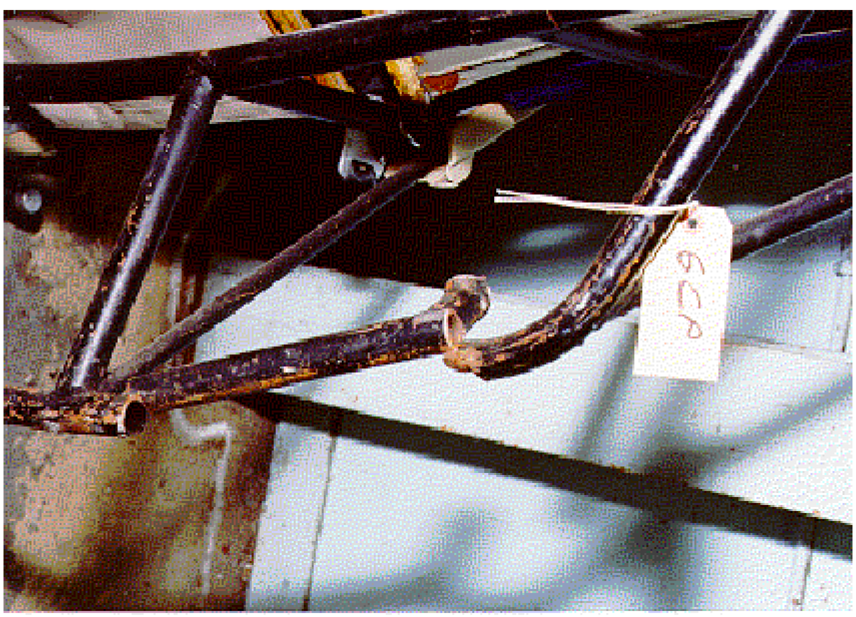

FIGURE 48. ROW 6 COPILOT-SIDE SEAT LEG

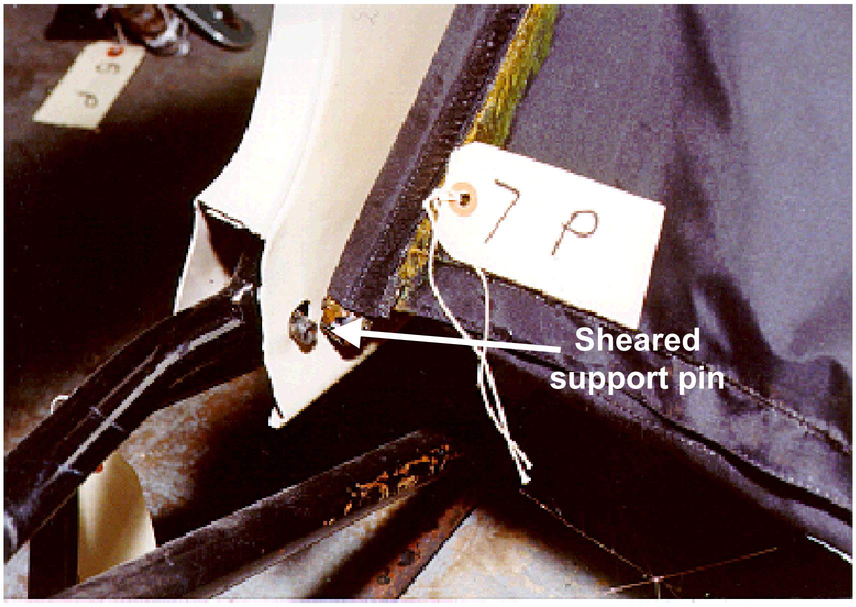

FIGURE 49. ROW 7 PILOT-SIDE SEAT PAN

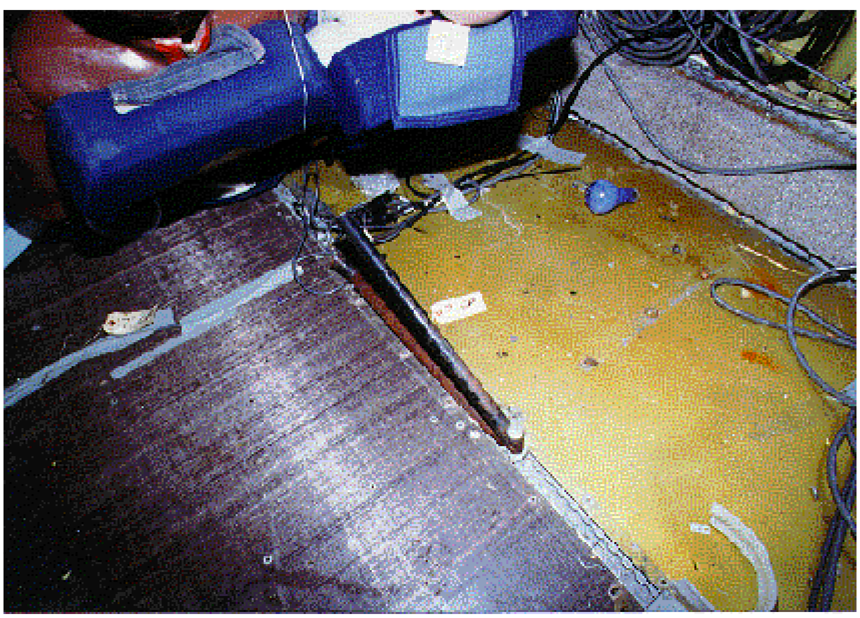

FIGURE 50. ROW 7 COPILOT-SIDE SEAT LEG

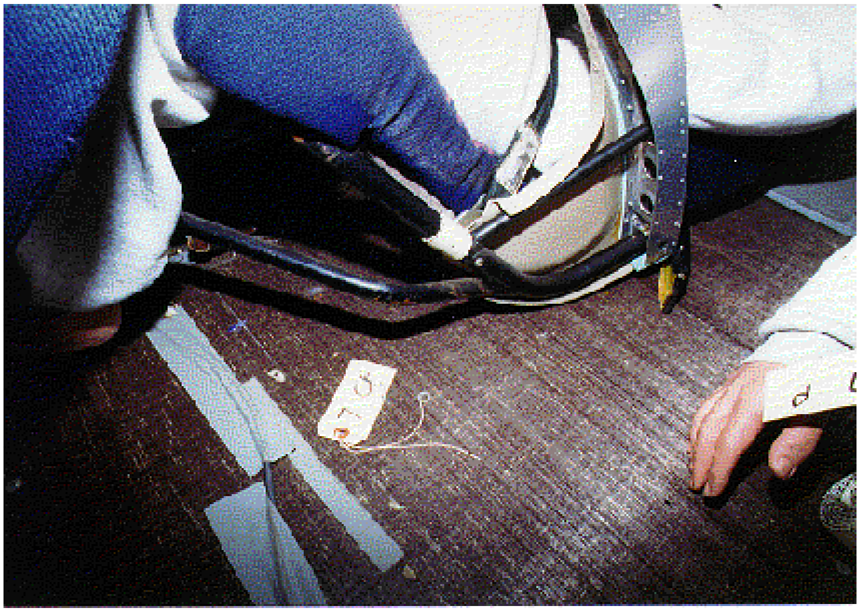

FIGURE 51. ROW 7 COPILOT-SIDE SEAT LEG CLOSEUP

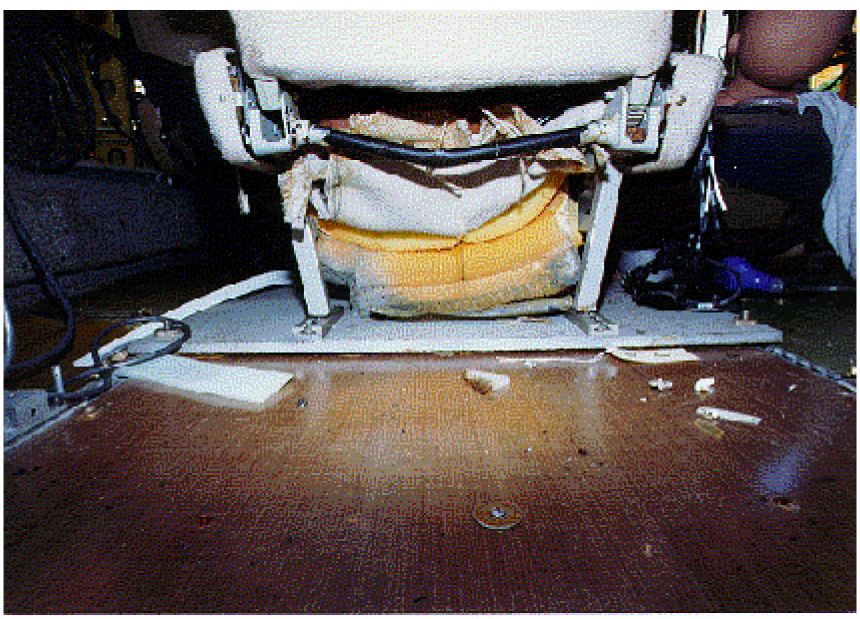

FIGURE 52. ROW 8 BEECHCRAFT SEAT REAR VIEW

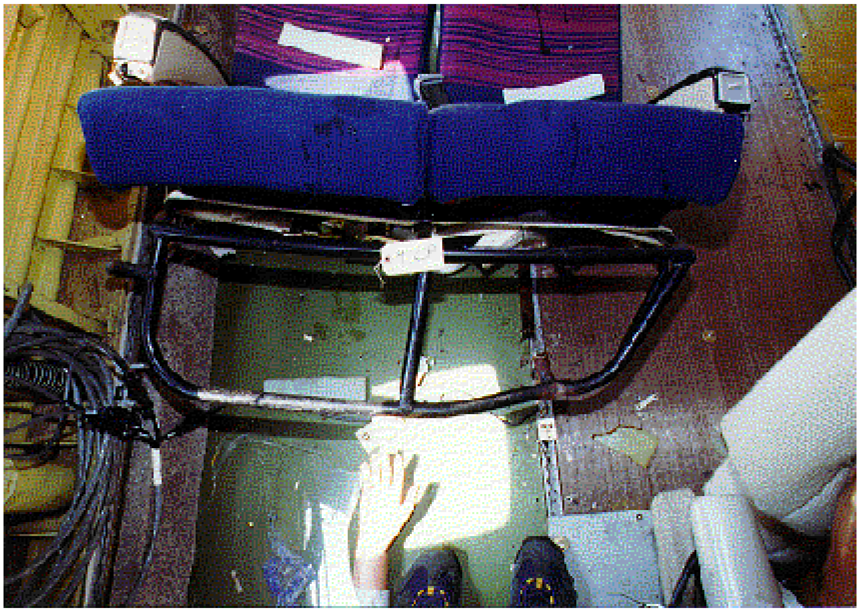

FIGURE 53. ROW 9 COPILOT-SIDE SEAT LEG

FIGURE 54. ROW 10 PILOT-SIDE SEAT BACK

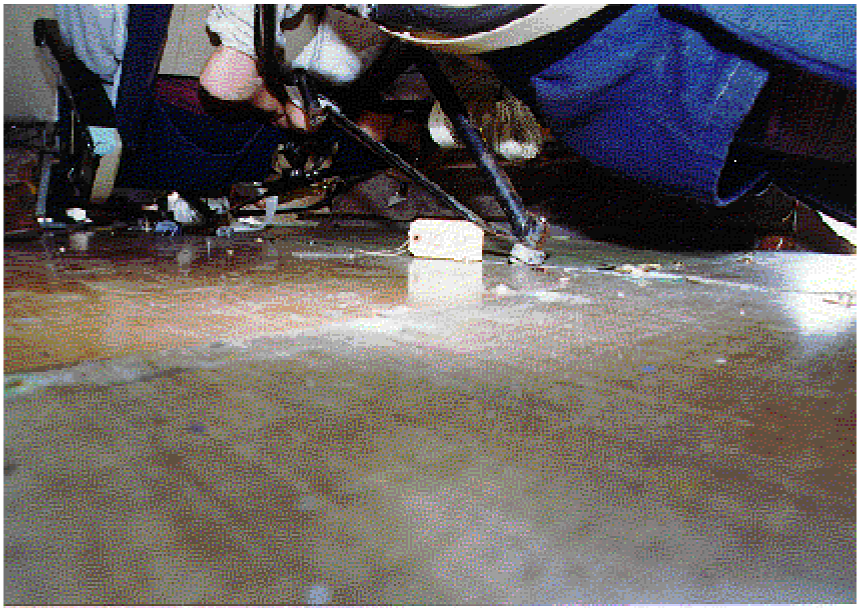

FIGURE 55. ROW 10 COPILOT-SIDE SEAT LEG

FIGURE 56. ROW 10 COPILOT-SIDE SEAT BACK

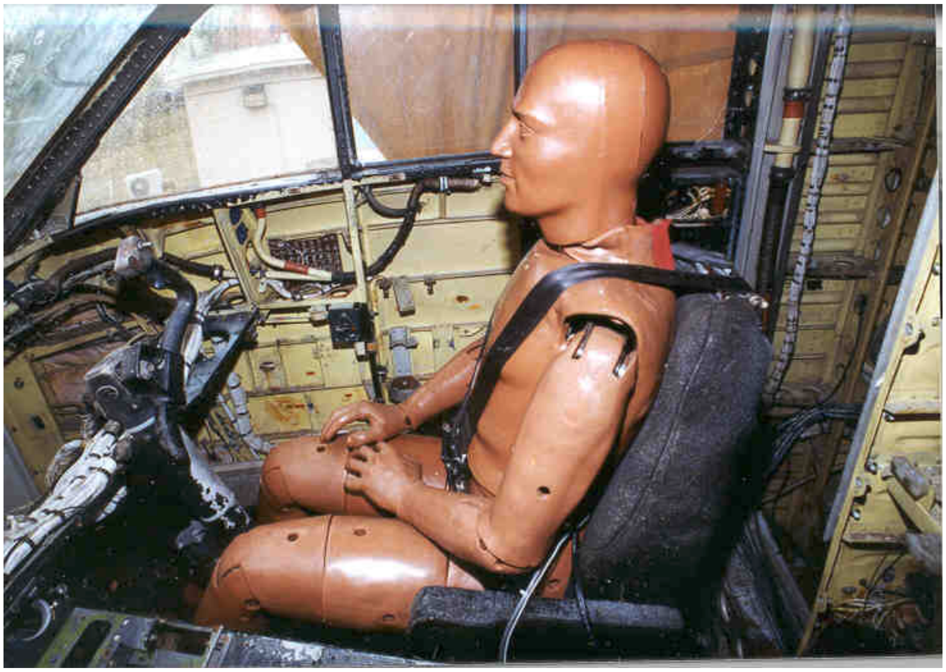

FIGURE 57. COPILOT ATD POSTTEST SIDE VIEW

FIGURE 58. ROW 1 ATD POSTTEST SIDE VIEW

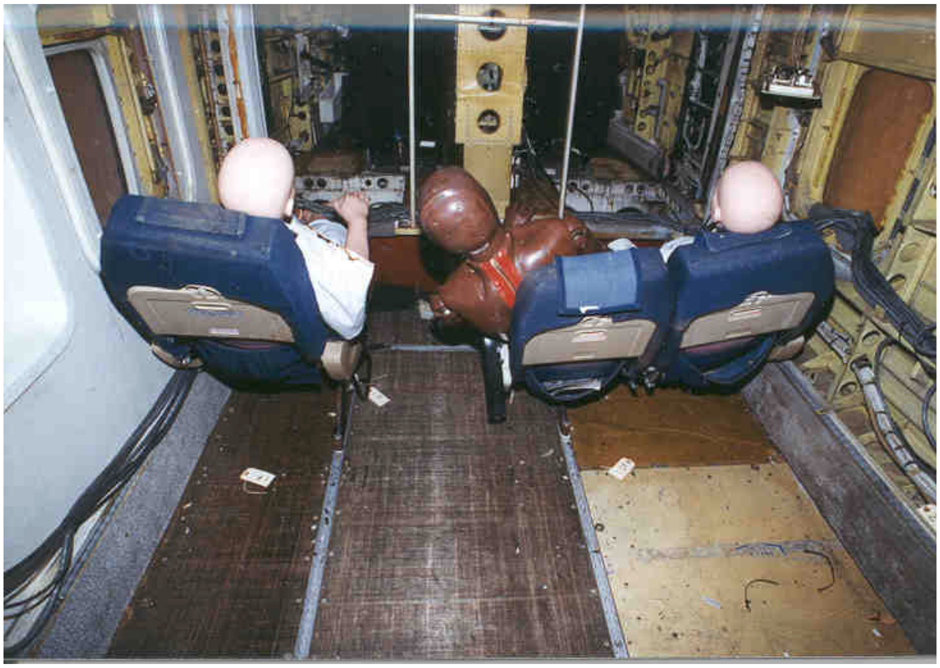

FIGURE 59. ROW 1 ATD POSTTEST AFT VIEW

FIGURE 60. ROW 3 ATD POSTTEST FRONT VIEW

FIGURE 61. ROW 3 ATD POSTTEST AFT VIEW

FIGURE 62. ROW 4 ATD POSTTEST FRONT VIEW

FIGURE 63. ROW 4 ATD POSTTEST SIDE VIEW

FIGURE 64. ROW 4 ATD POSTTEST AFT VIEW

FIGURE 65. ROW 6 ATD POSTTEST AFT VIEW

FIGURE 66. ROW 8 ATD POSTTEST FRONT VIEW

FIGURE 67. ROW 9 ATD POSTTEST SIDE VIEW

CONCLUDING REMARKS

1. The Shorts 3-30 airplane was dropped from a height of 14 feet which resulted in an impact velocity of 30 ft/sec.

2. In general the fuselage experienced G_{max} levels of approximately 90 g's with a impact pulse duration of 15 ms.

3. The lower fuselage experienced very little deformation. Although the fuselage did crack open aft of the main spar, a survivable volume was maintained for the occupants.

4. The seat tracks remained attached to the fuselage.

5. The crew seats remained undamaged. Twenty-three of the 26 passenger seats experienced some form of structural failure.

6. The occupants experienced G_{peak} levels in the range of 31-67 g's with a pulse duration of 21-59 ms. This may be considered a severe impact which would have resulted in moderate to severe injuries to the occupants.

7. All exits remained operable.

8. Nine external windows out of 23 and 13 internal windows out of 23 shattered.

9. The overhead fuel tanks broke loose from their mountings resulting in large quantities of simulated fuel being spilled onto the occupants.

REFERENCES

1. Airplane Safety Research Plan, November 1991, Federal Aviation Administration Technical Center, Atlantic City International Airport, NJ 08405.

2. Vertical Drop Test of a Metro III Airplane, DOT/FAA/CT-93/1, June 1993, Federal Aviation Administration Technical Center, Atlantic City International Airport, NJ 08405.

3. Vertical Drop Test of a Beechcraft 1900C Airliner, DOT/FAA/AR-96/119, May 1998, William J. Hughes FAA Technical Center, Atlantic City International Airport, NJ 08405.

4. SAE International, "Surface Vehicle Recommended Practice," SAE J211/1, Revised March 1995.

5. Airplane Crash Survival Design Guide, Volume II, December 1989, Simula Inc., Phoenix, AZ, 85044.

APPENDIX—DATA FIGURES

ANTHROPOMORPHIC TEST DUMMY DATA

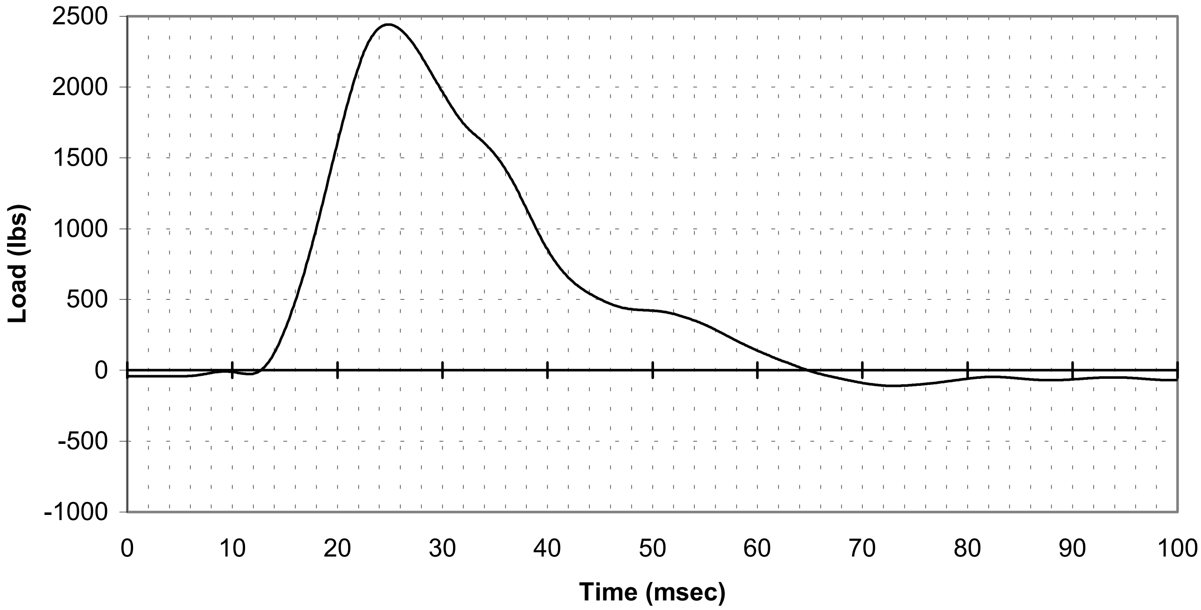

FIGURE A-1. FS 55, ATD #1, LOAD CELL
(channel 209)

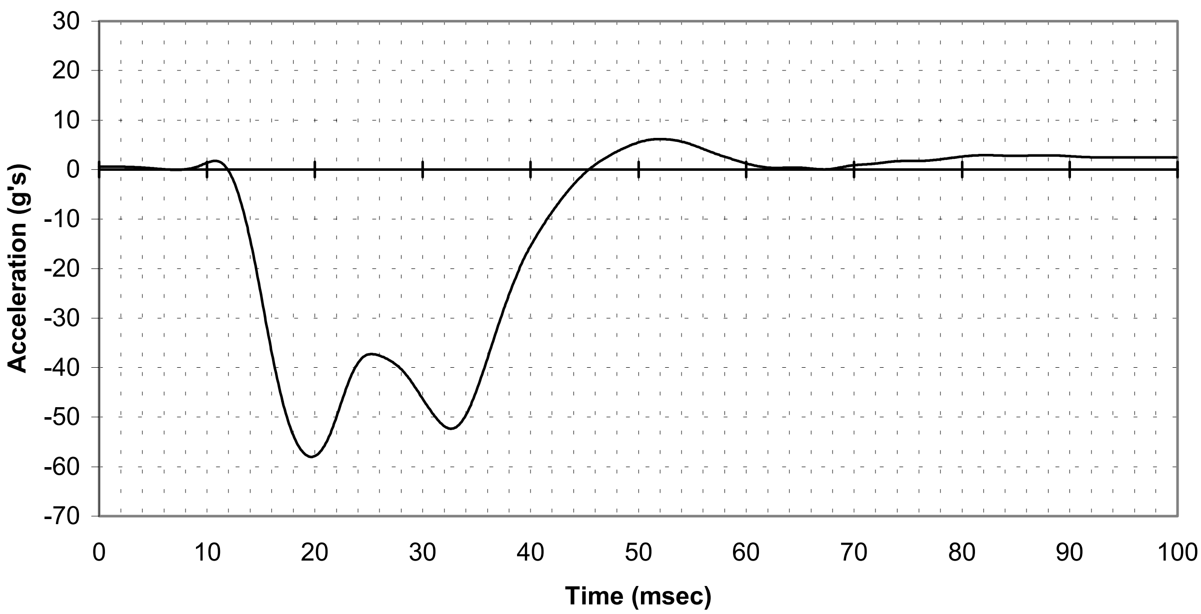

FIGURE A-2. FS 55 ATD #1, ACCELEROMETER Z DIRECTION 100 g
(channel 210)

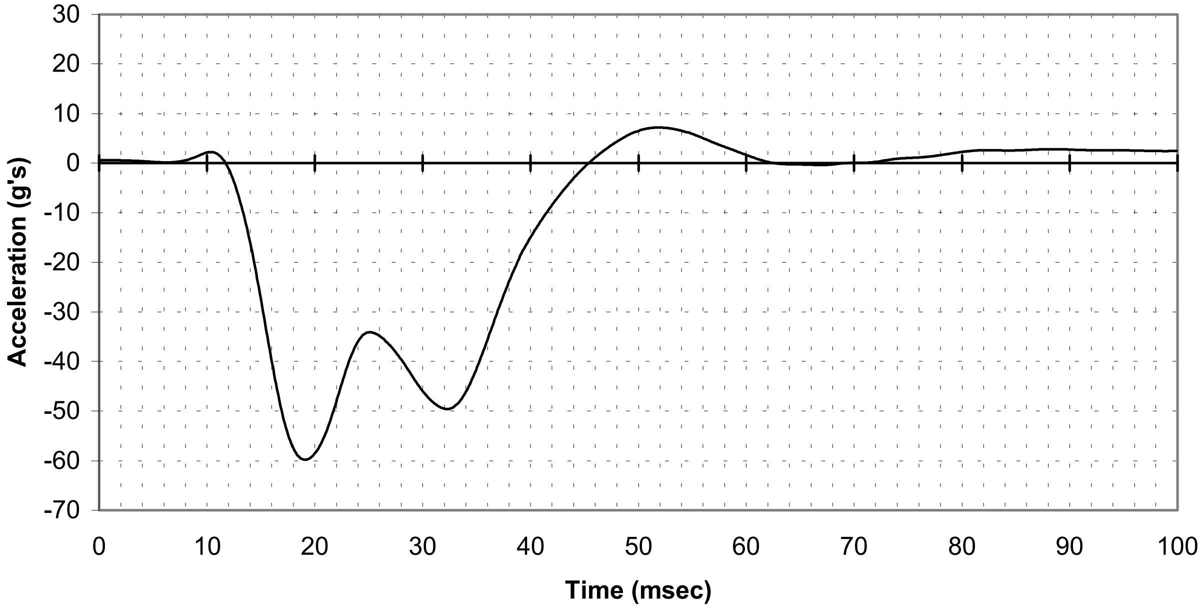

FIGURE A-3. FS 55, ATD #1, ACCELEROMETER Z DIRECTION 750 g
(channel 211)

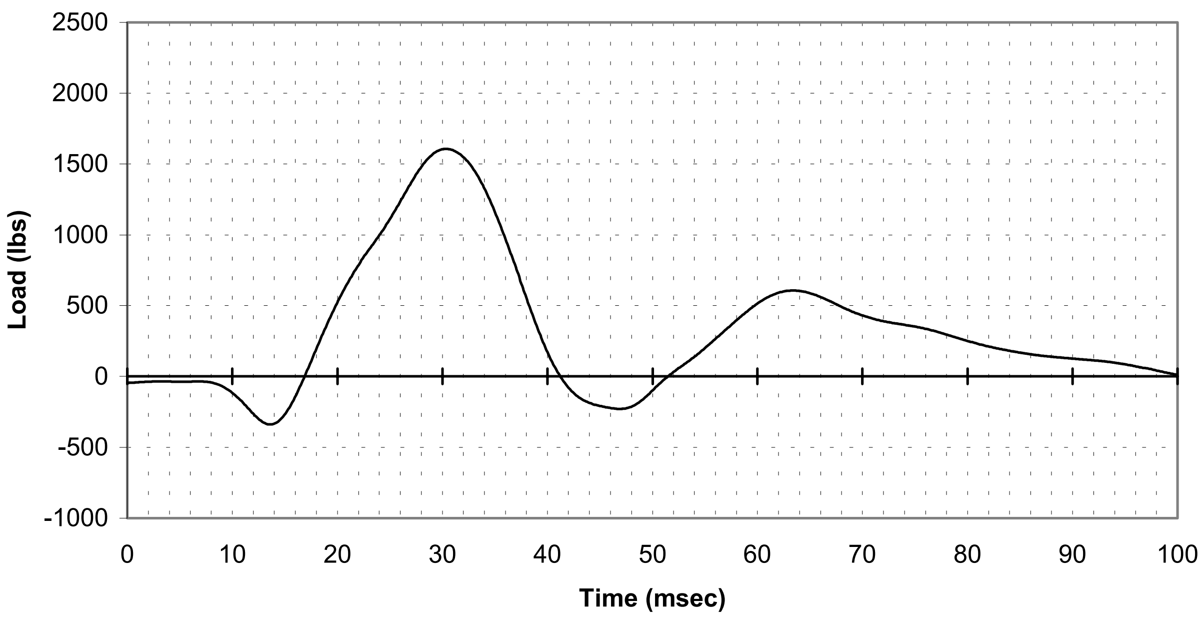

FIGURE A-4. FS 110, ATD #2, LOAD CELL
(channel 212)

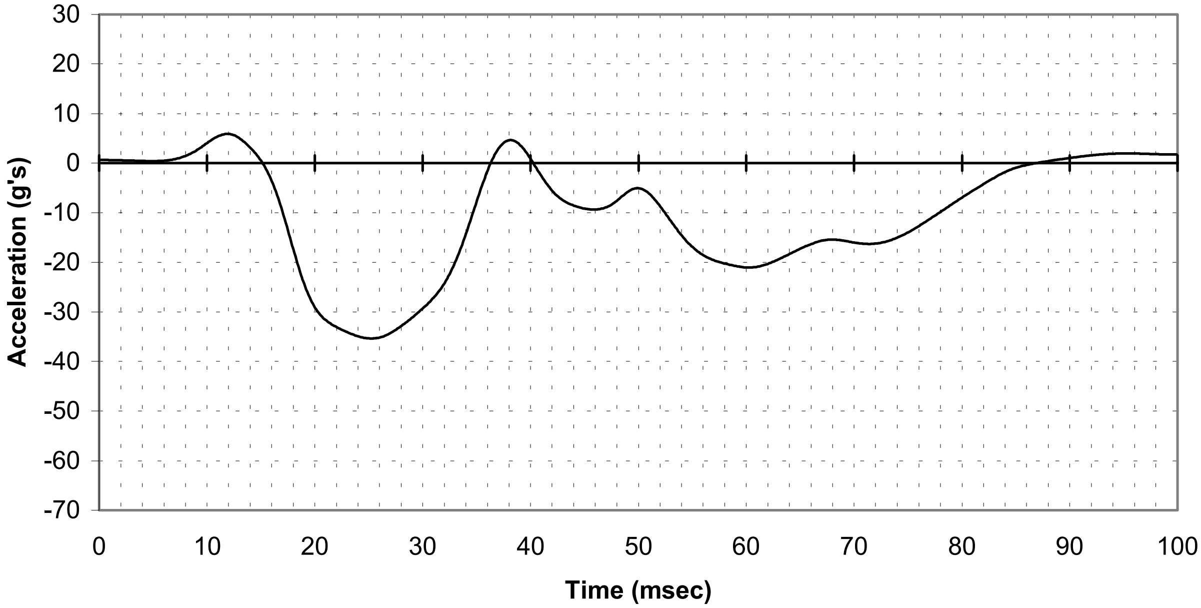

FIGURE A-5. FS 110, ATD #2, ACCELEROMETER Z DIRECTION 100 g
(channel 220)

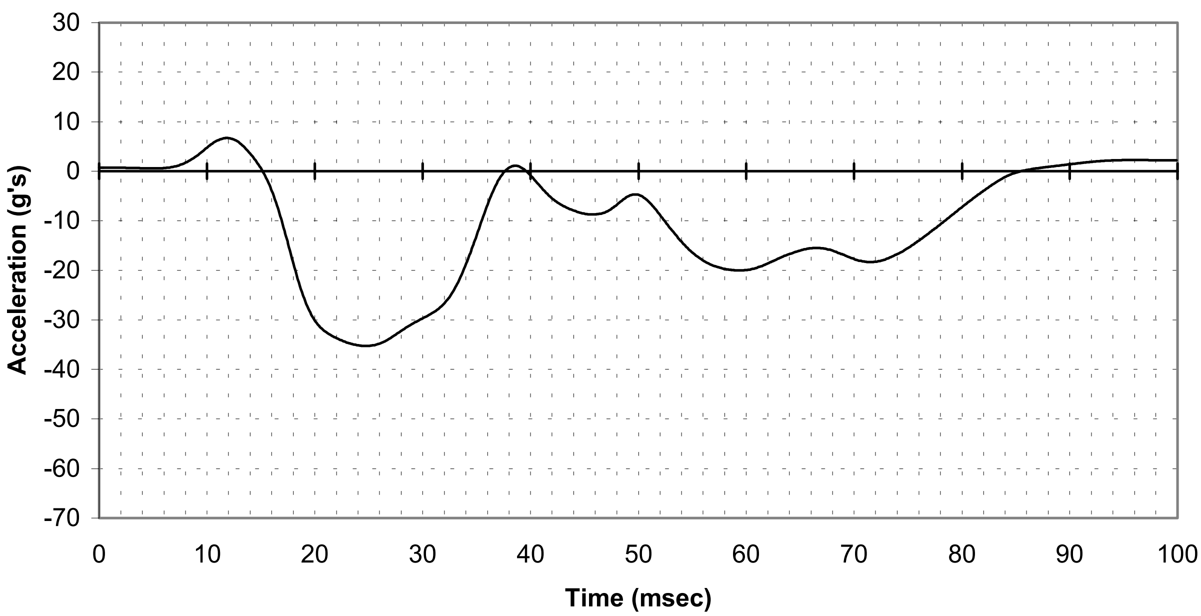

FIGURE A-6. FS 110, ATD#2, ACCELEROMETER Z DIRECTION 750 g
(channel 221)

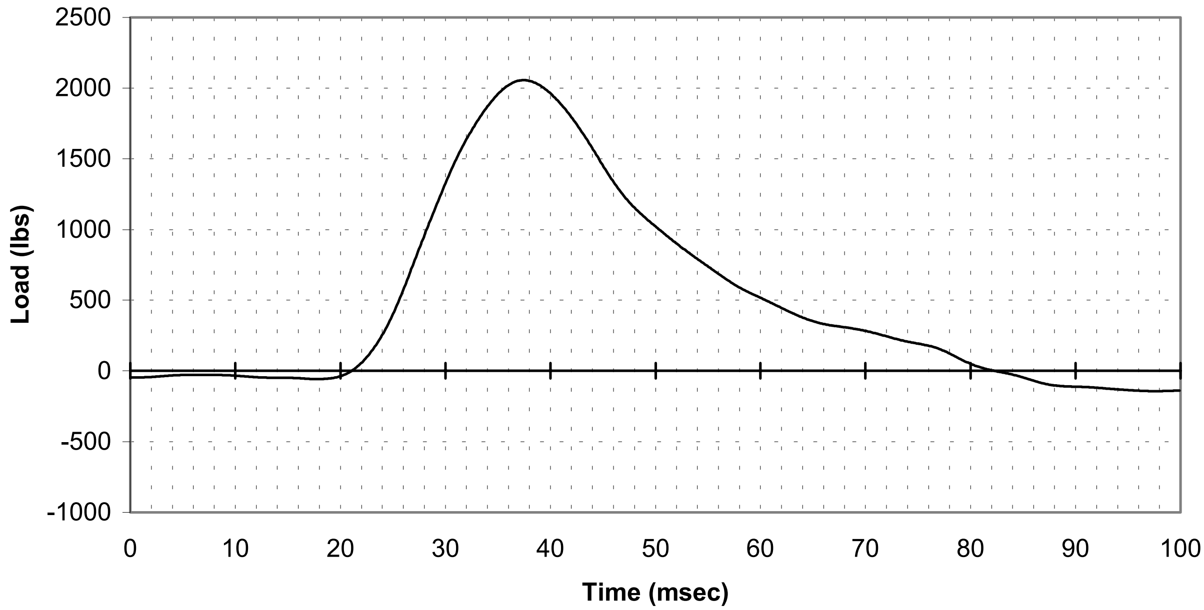

FIGURE A-7. FS 173, ATD #3, LOAD CELL
(channel 228)

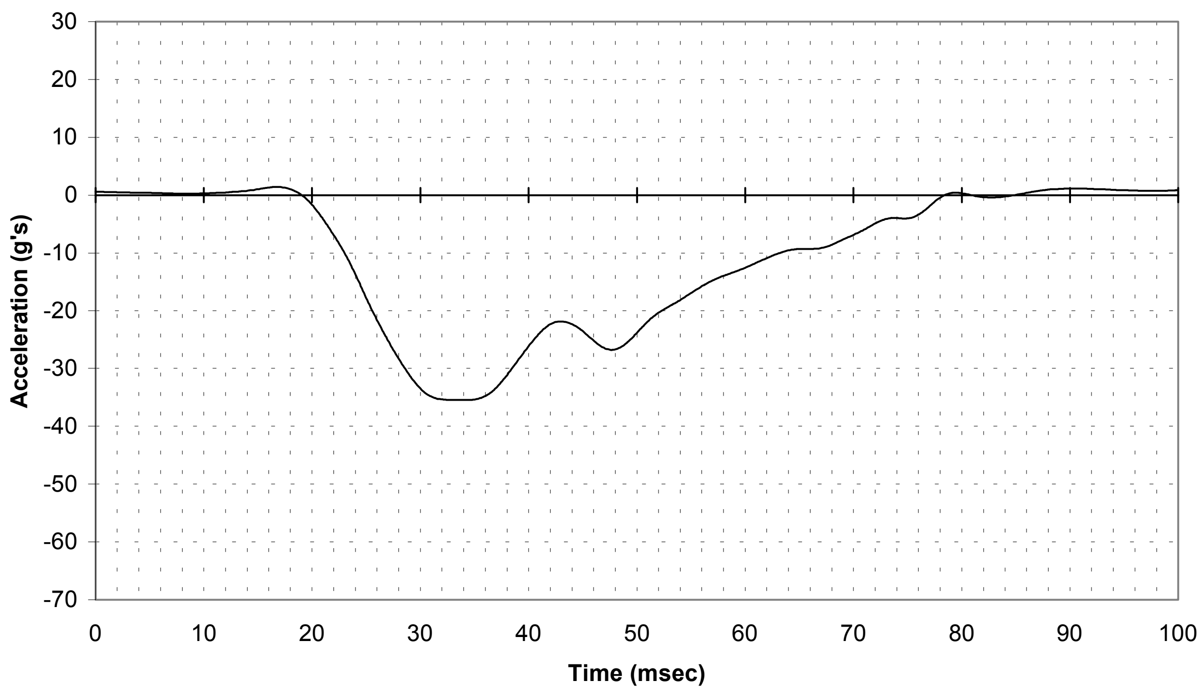

FIGURE A-8. FS 173, ATD #3 ACCELEROMETER Z DIRECTION 100 g
(channel 13)

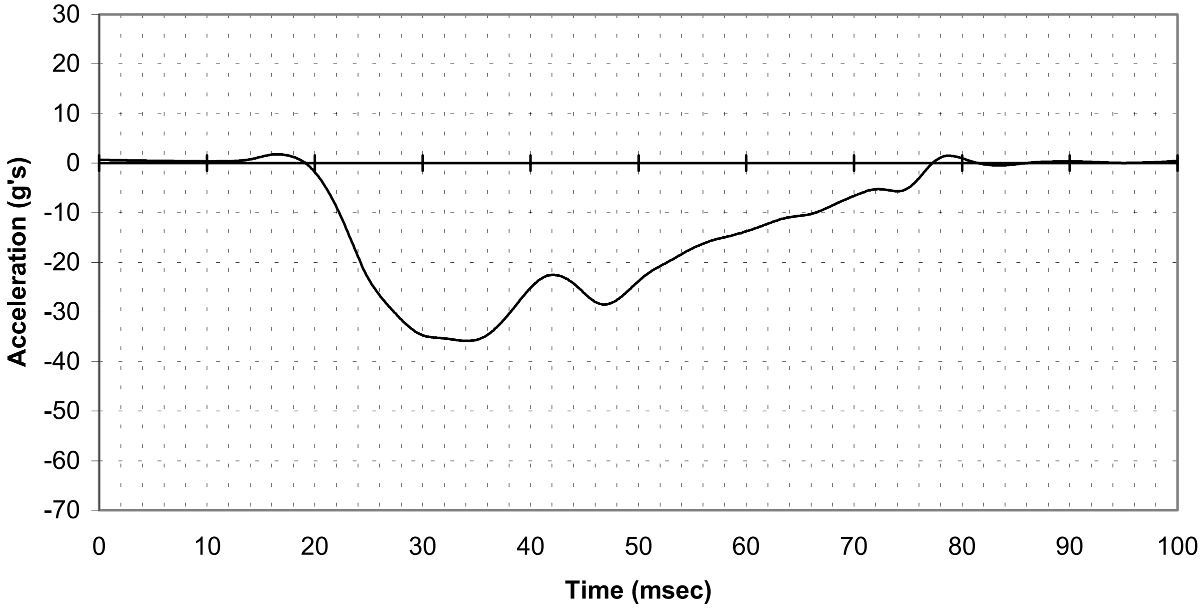

FIGURE A-9. FS 173, ATD #3, ACCELEROMETER Z DIRECTION 750 g
(channel 229)

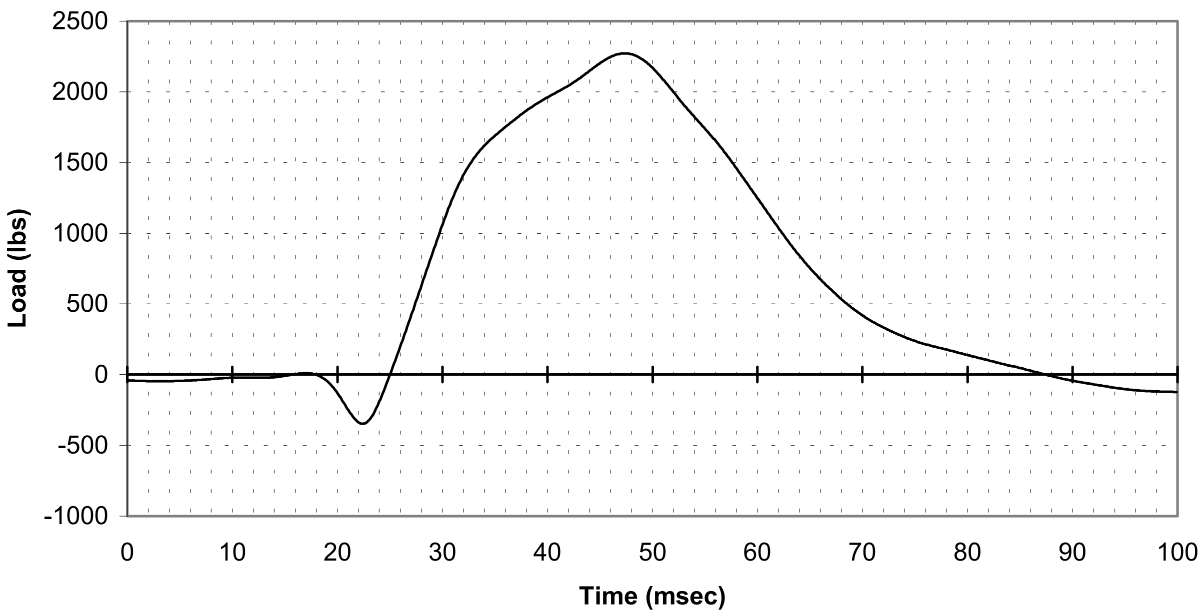

FIGURE A-10. FS 190, ATD #4, LOAD CELL
(channel 301)

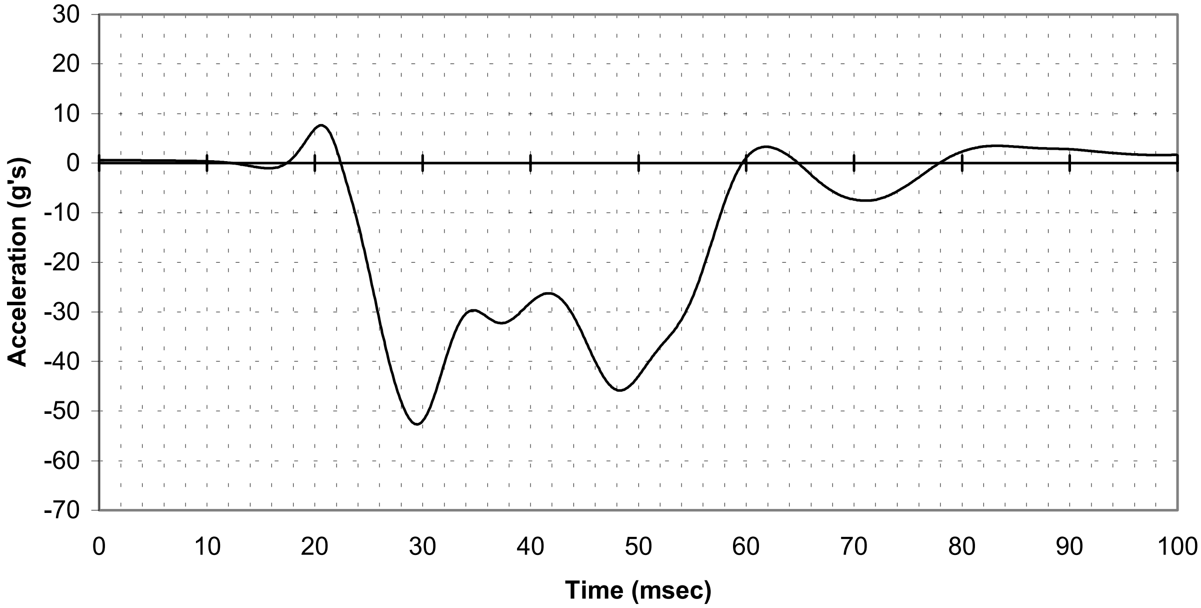

FIGURE A-11. FS 190, ATD #4, ACCELEROMETER Z DIRECTION 100 g (channel 302)

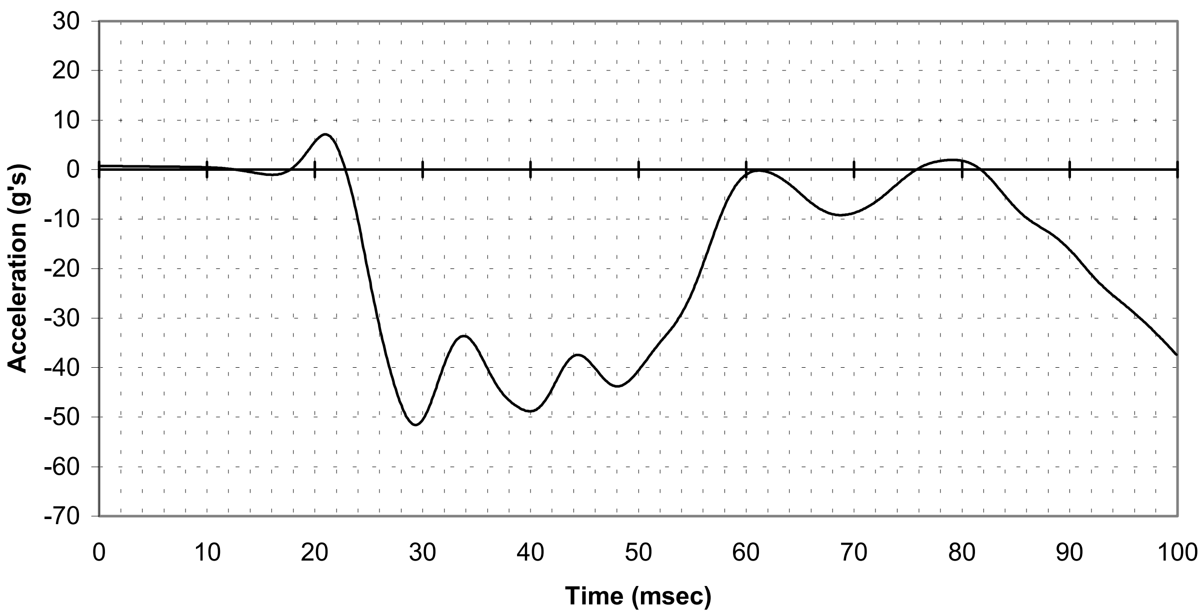

FIGURE A-12. FS 190, ATD #4, ACCELEROMETER Z DIRECTION 750 g (channel 303)

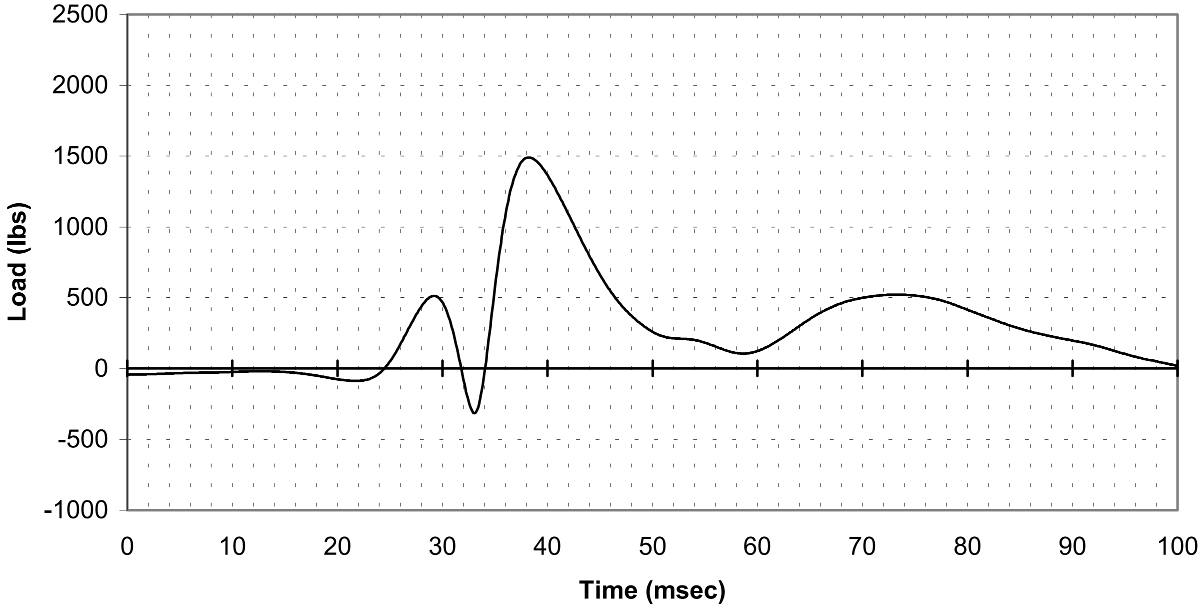

FIGURE A-13. FS 292, ATD #5, LOAD CELL
(channel 412)

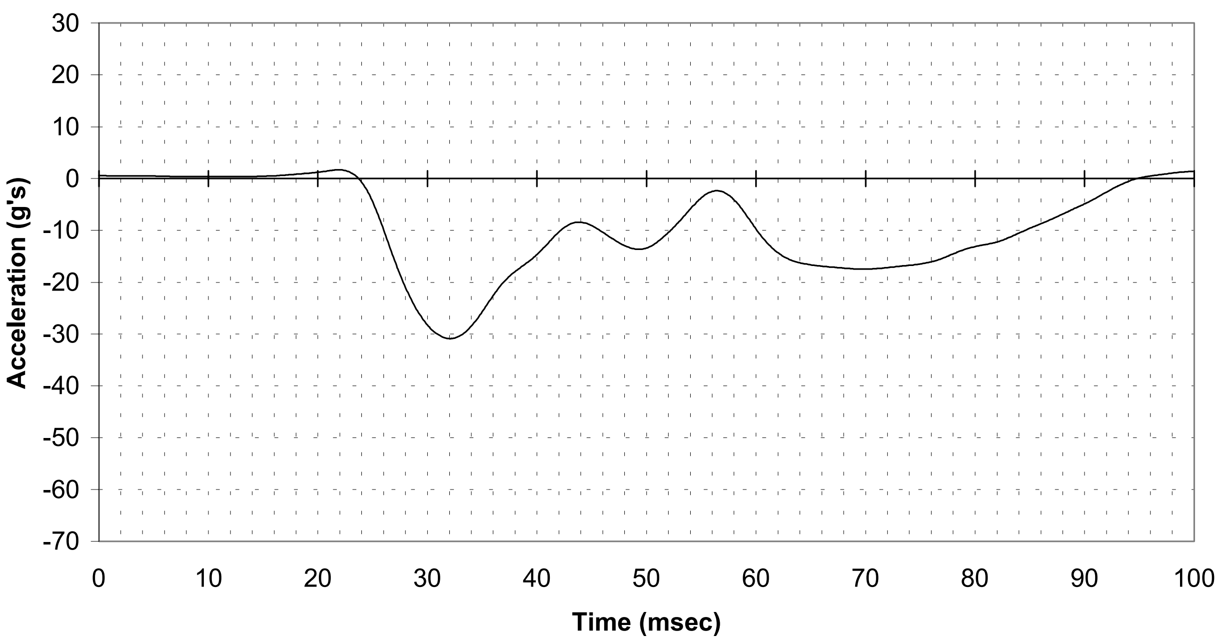

FIGURE A-14. FS 292, ATD #5, ACCELEROMETER Z DIRECTION 100 g
(channel 24)

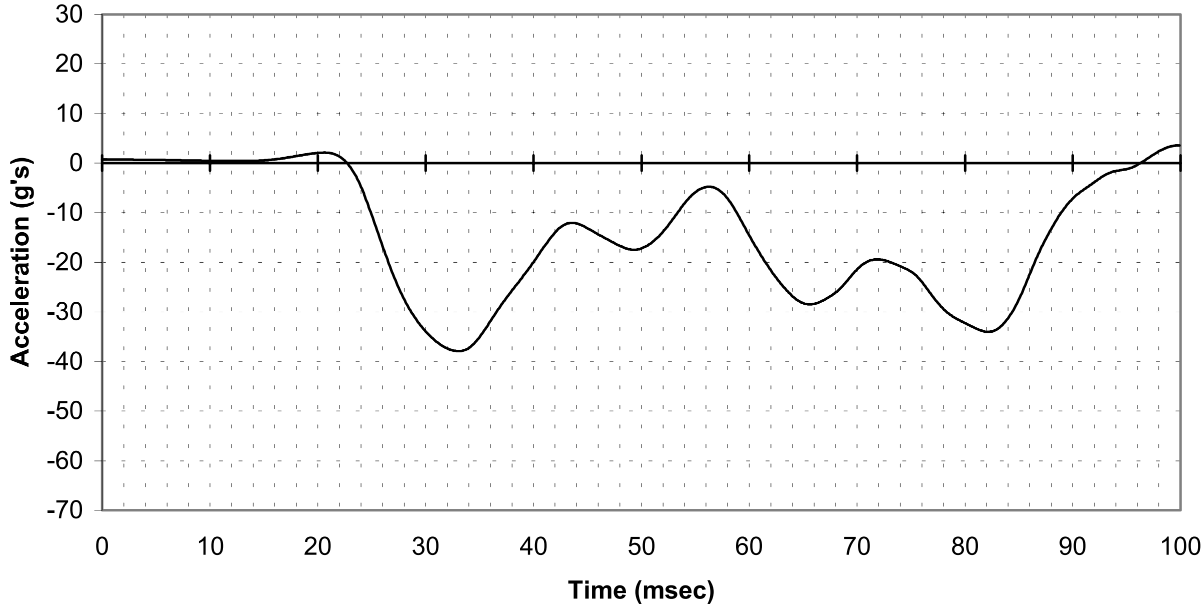

FIGURE A-15. FS 292, ATD #5, ACCELEROMETER Z DIRECTION 750 g
(channel 416)

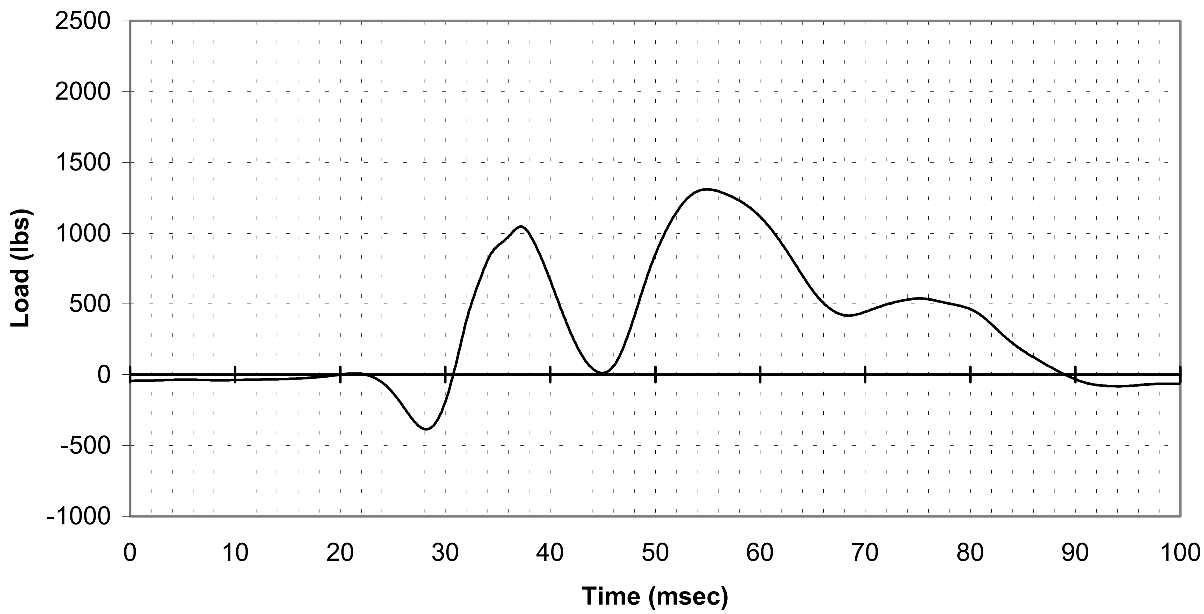

FIGURE A-16. FS 315, ATD #6, LOAD CELL
(channel 413)

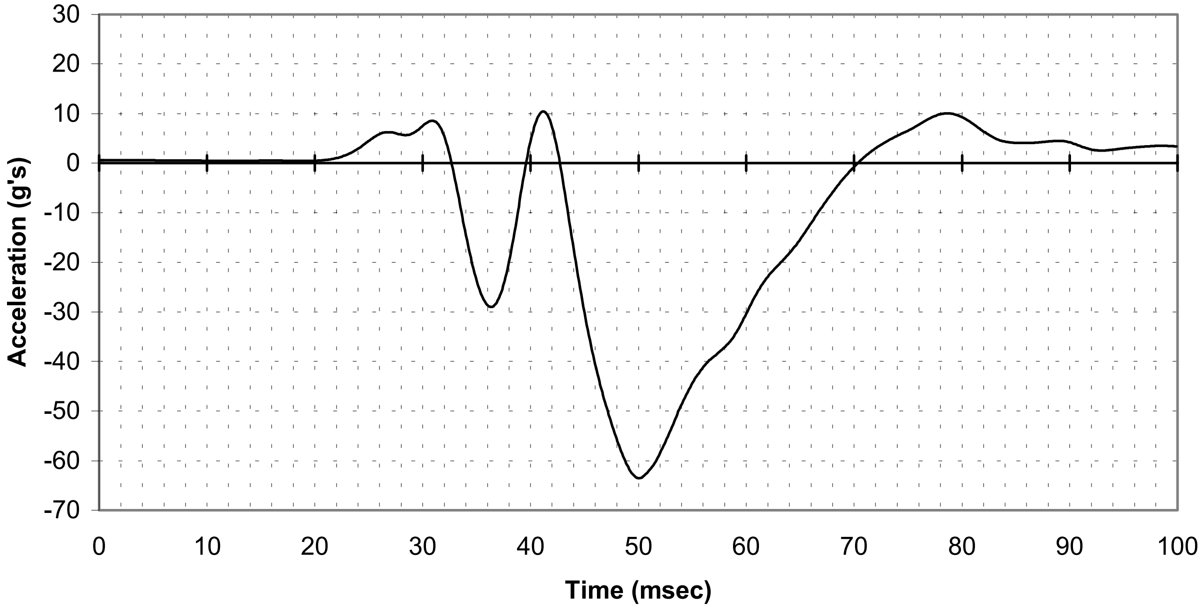

FIGURE A-17. FS 315, ATD #6, ACCELEROMETER Z DIRECTION 100 g
(channel 414)

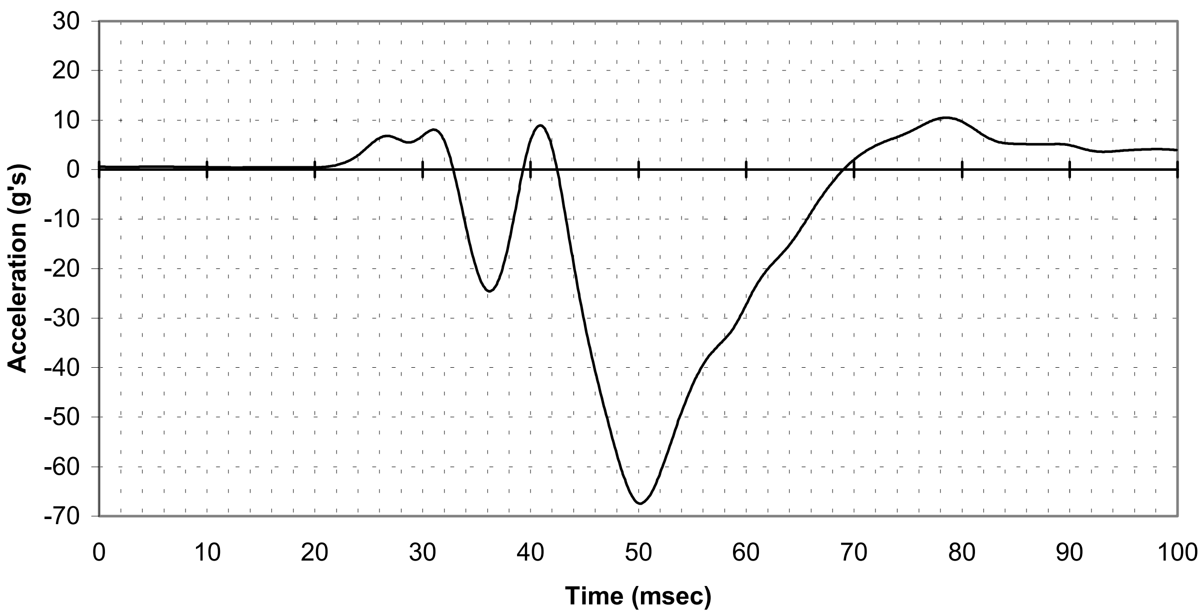

FIGURE A-18. FS 315, ATD #6, ACCELEROMETER Z DIRECTION 750 g
(channel 415)

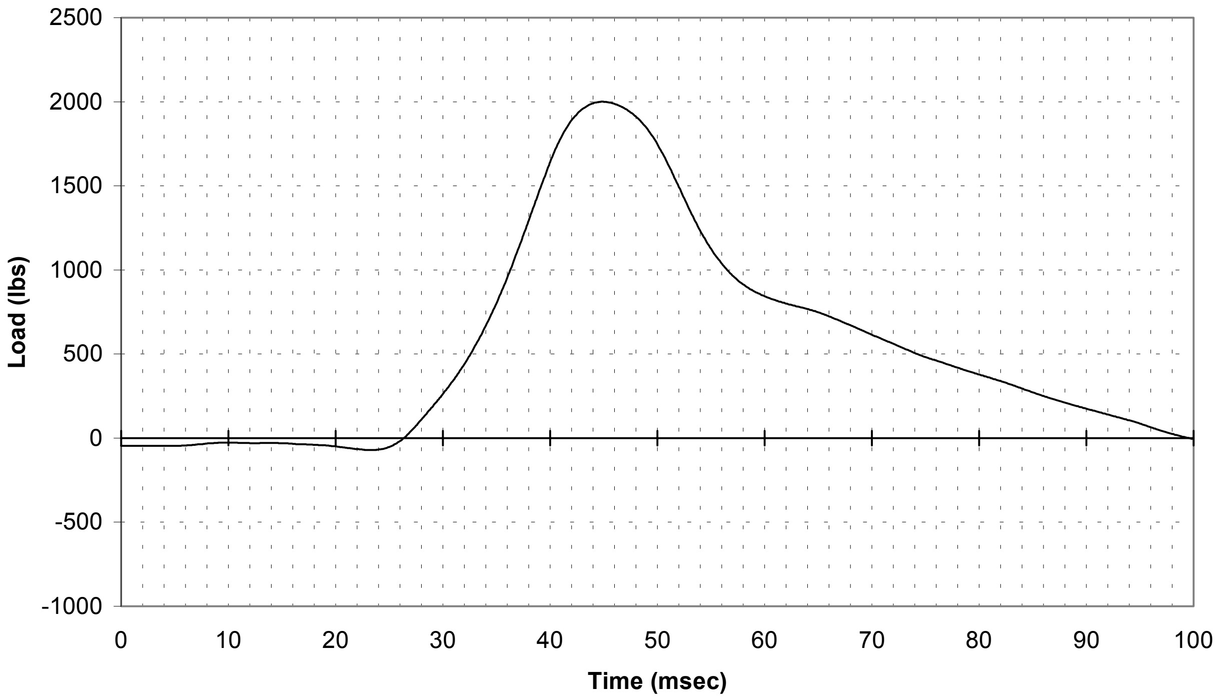

FIGURE A-19. FS 357, ATD #7, LOAD CELL
(channel 424)

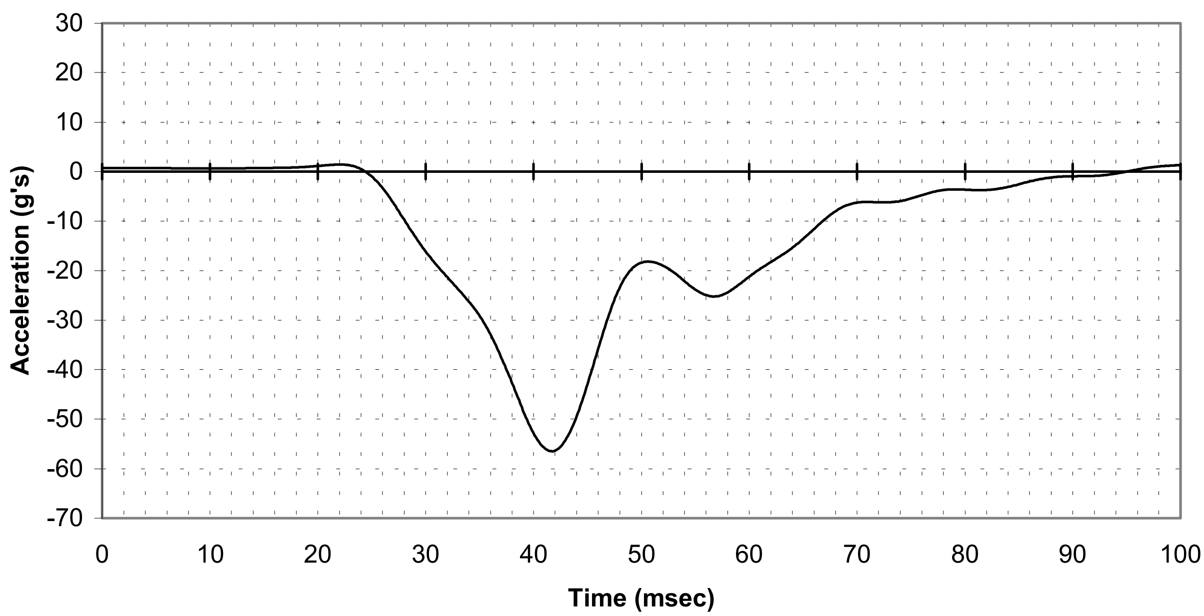

FIGURE A-20. FS 357, ATD #7, ACCELEROMETER Z DIRECTION 100 g
(channel 425)

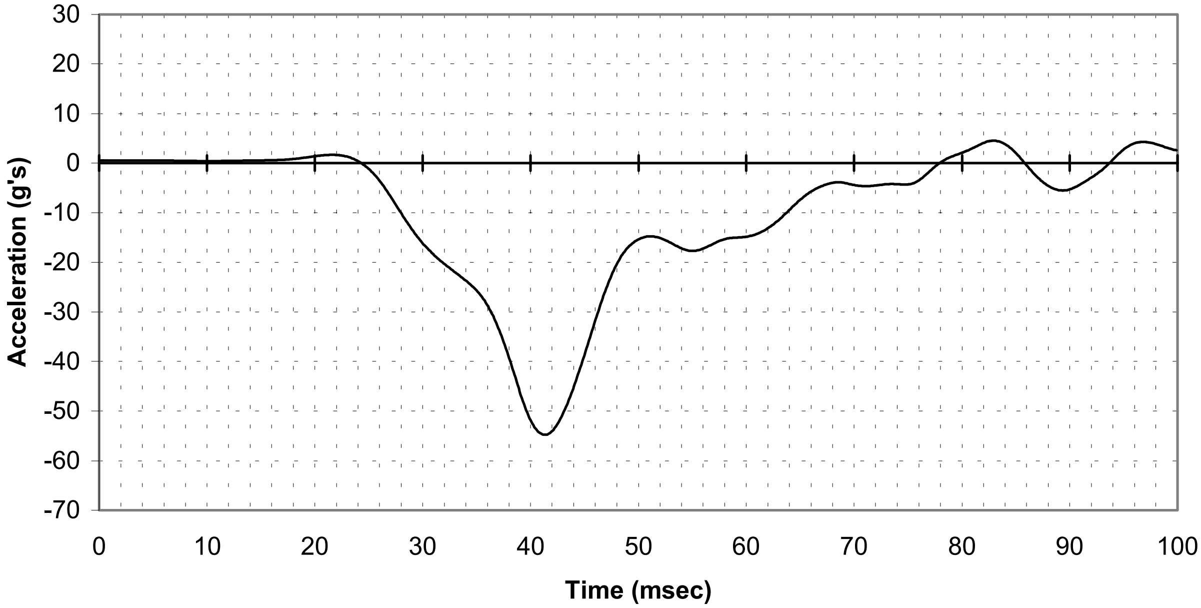

FIGURE A-21. FS 357, ATD #7, ACCELEROMETER Z DIRECTION 750 g
(channel 426)

SIDE WALL DATA

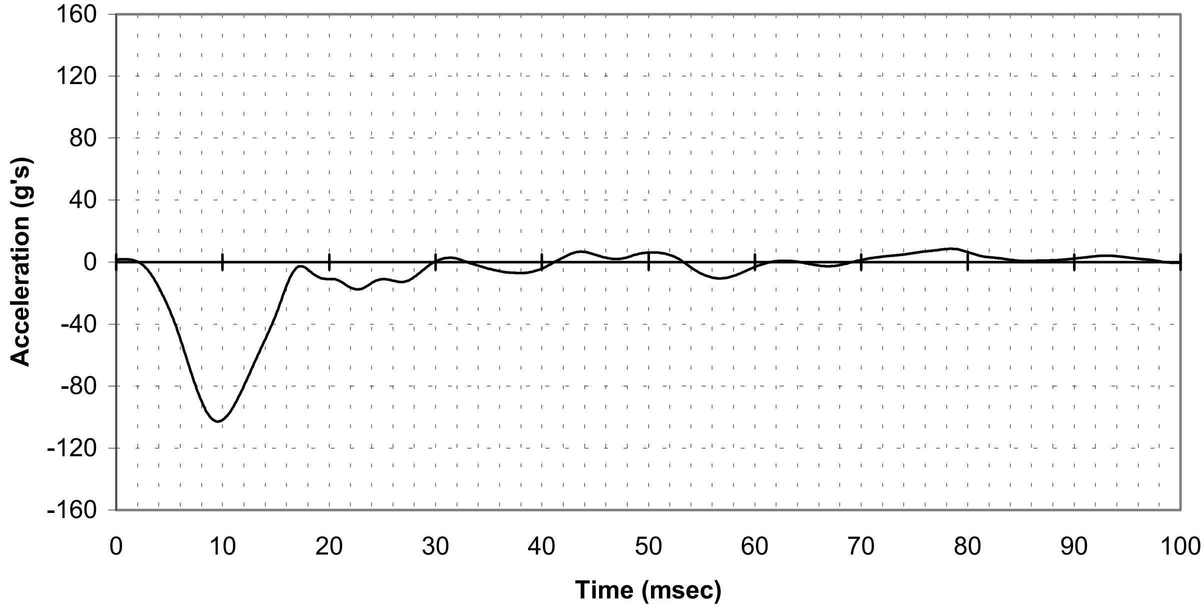

FIGURE A-22. FS 89, LEFT-SIDE WALL, ACCELEROMETER Z DIRECTION (channel 216)

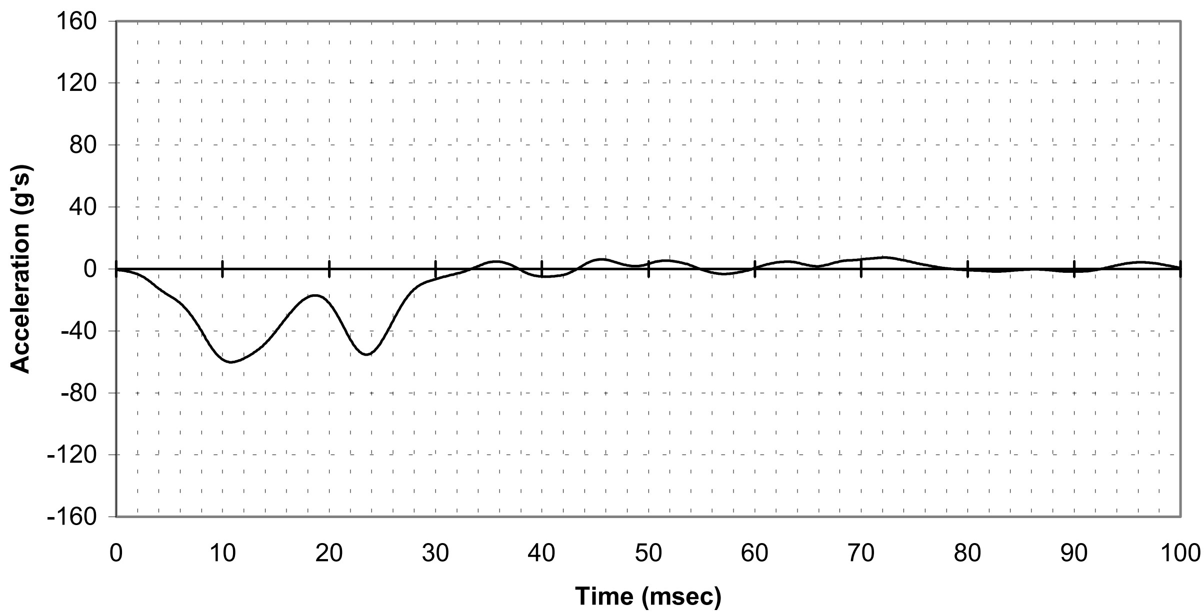

FIGURE A-23. FS 89, RIGHT-SIDE WALL, ACCELEROMETER Z DIRECTION (channel 223)

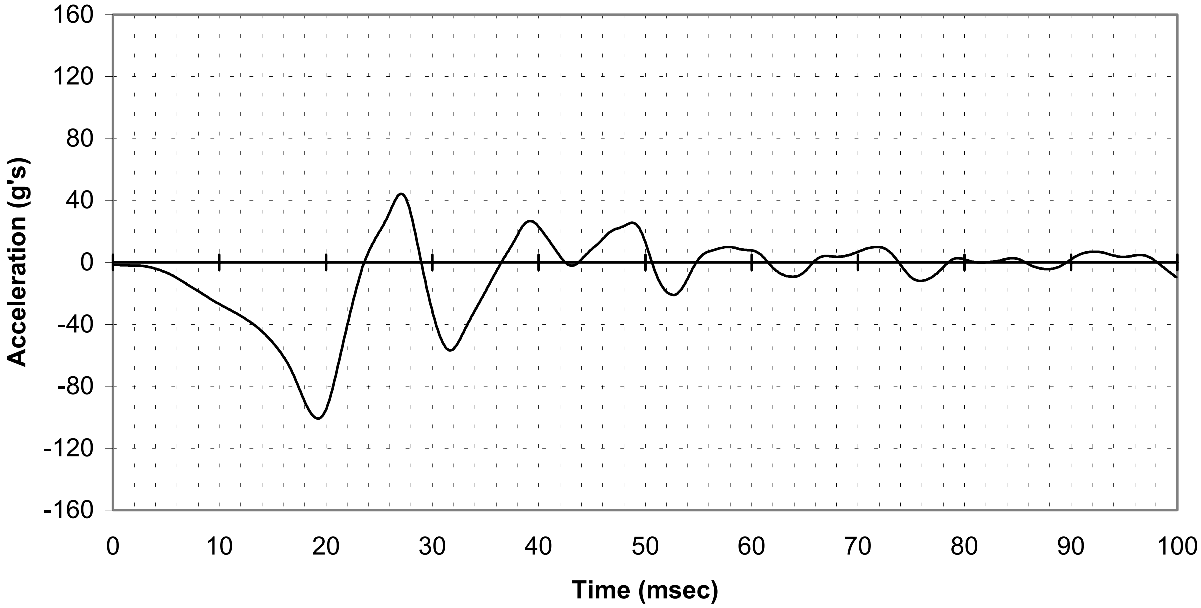

FIGURE A-24. FS 161, LEFT-SIDE WALL, ACCELEROMETER Z DIRECTION (channel 224)

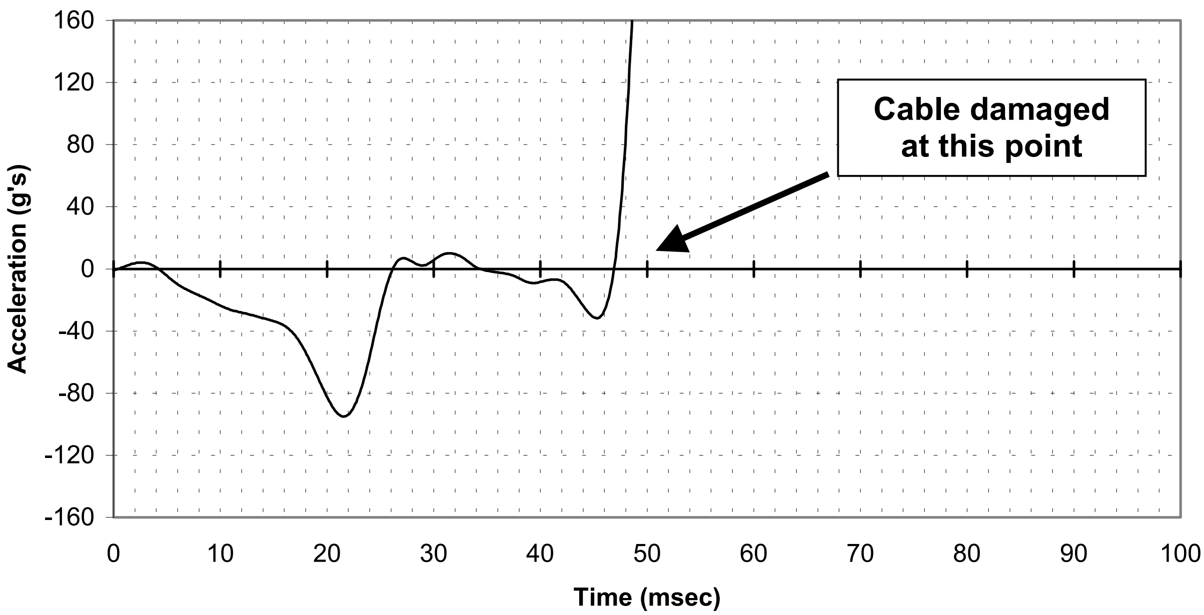

FIGURE A-25. FS 161, RIGHT-SIDE WALL, ACCELEROMETER Z DIRECTION (channel 231)

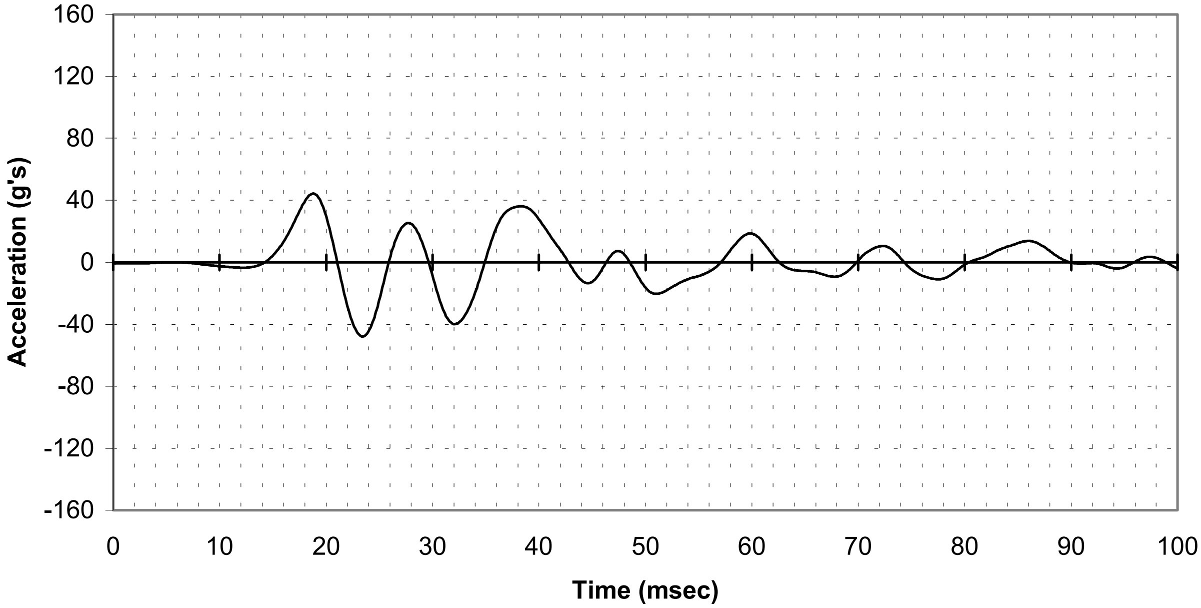

FIGURE A-26. FS 264, LEFT-SIDE WALL, ACCELEROMETER Y DIRECTION (channel 405)

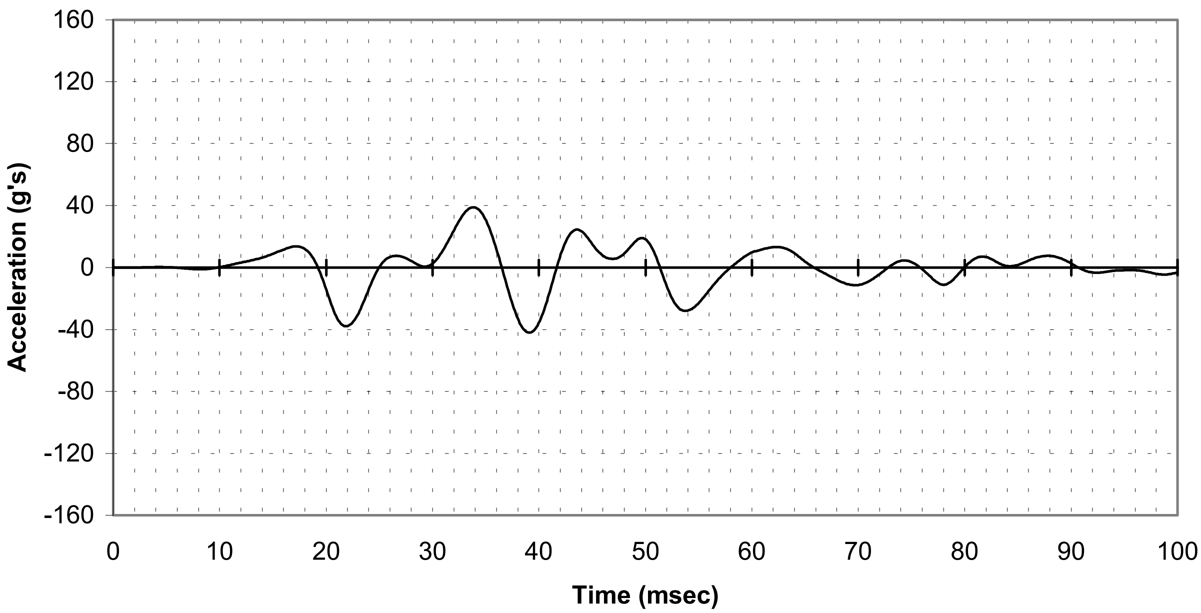

FIGURE A-27. FS 264, RIGHT-SIDE WALL, ACCELEROMETER Y DIRECTION (channel 418)

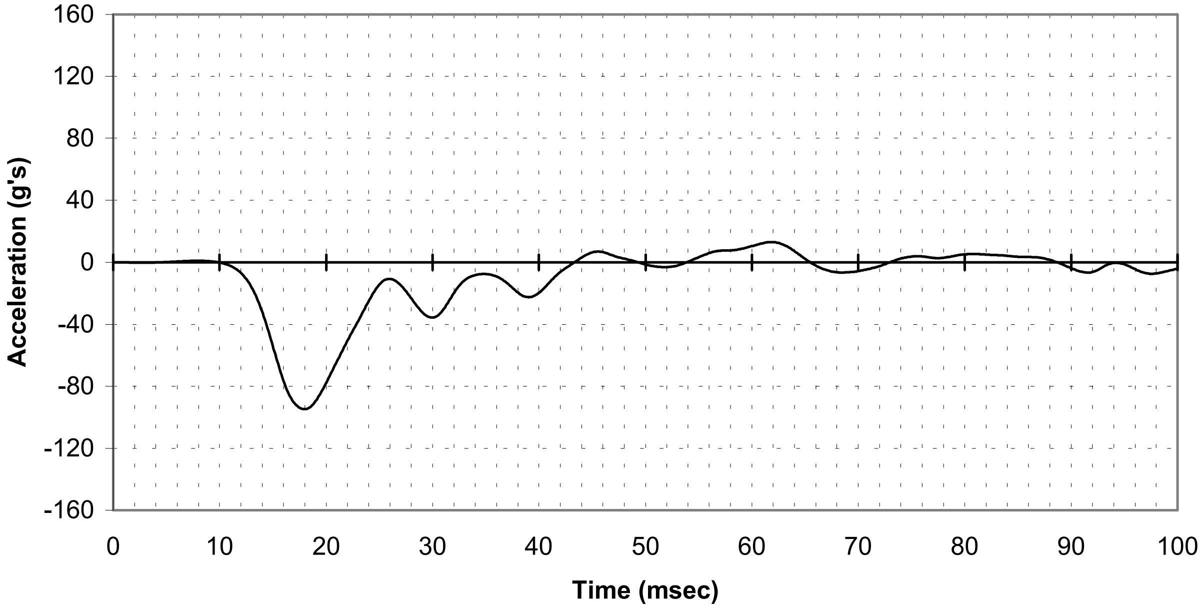

FIGURE A-28. FS 264, LEFT-SIDE WALL, ACCELEROMETER Z DIRECTION (channel 406)

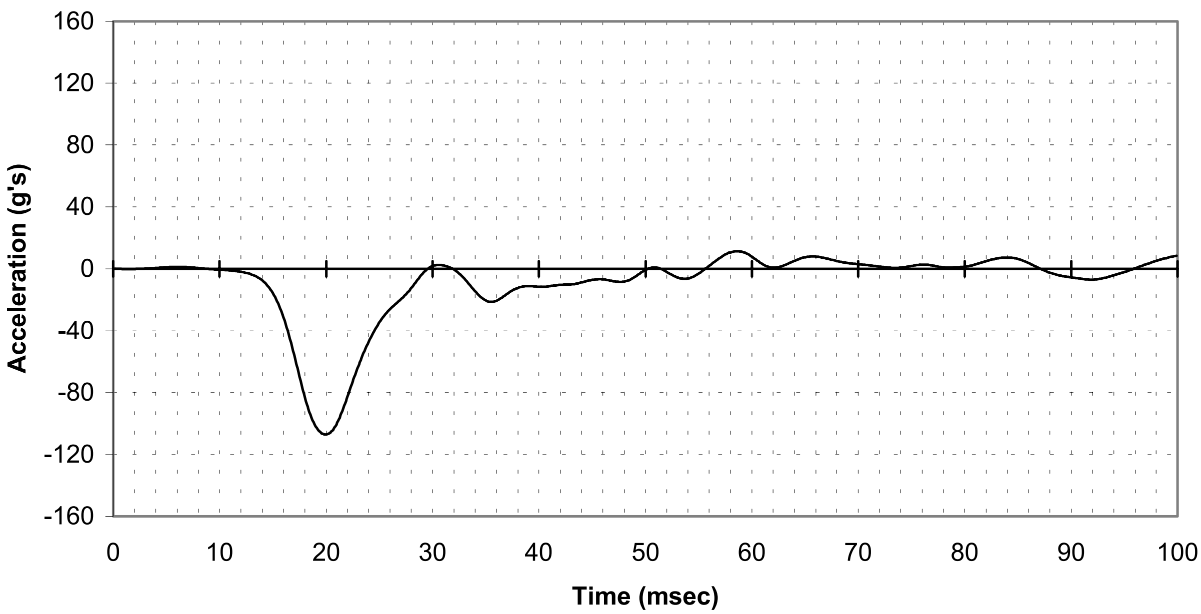

FIGURE A-29. FS 264, RIGHT-SIDE WALL, ACCELEROMETER Z DIRECTION (channel 419)

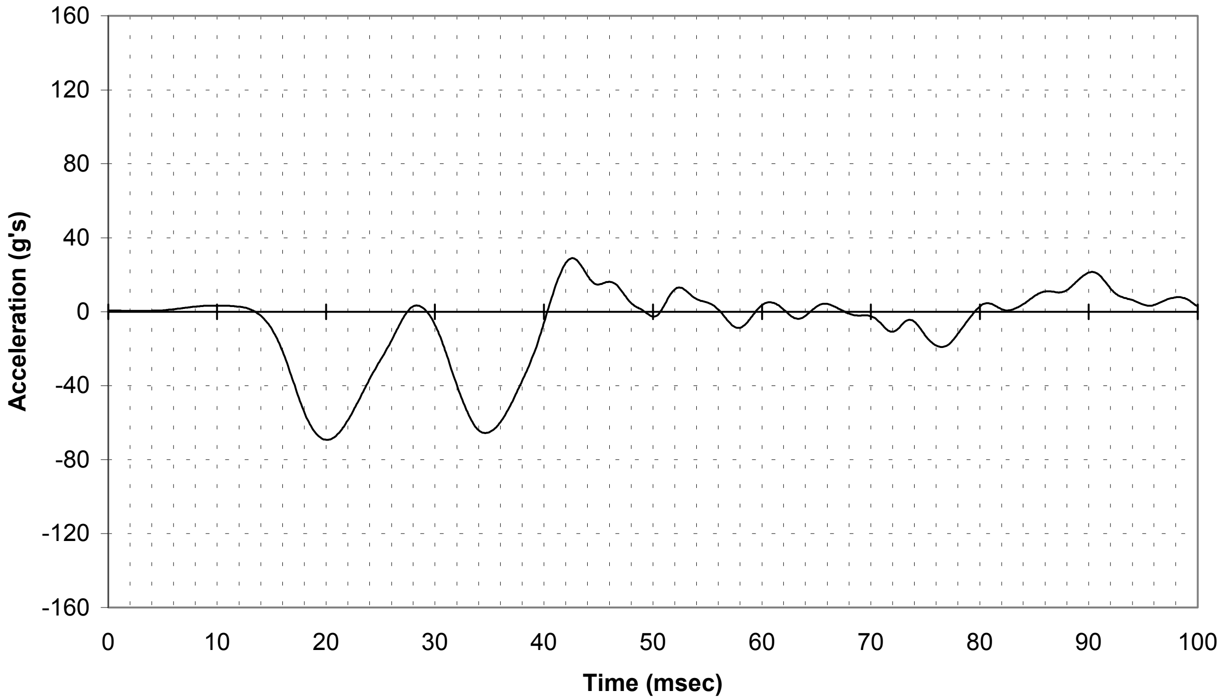

FIGURE A-30. FS 340, LEFT-SIDE WALL, ACCELEROMETER Z DIRECTION (channel 420)

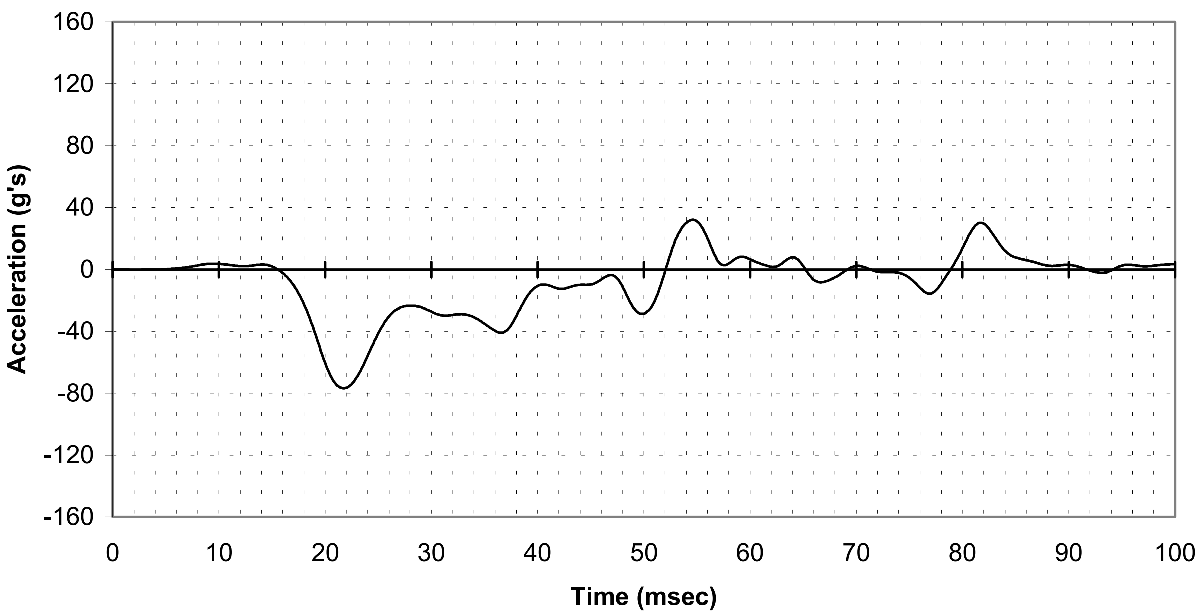

FIGURE A-31. FS 340, RIGHT-SIDE WALL, ACCELEROMETER Z DIRECTION (channel 315)

SIDE WALL SEAT TRACK DATA

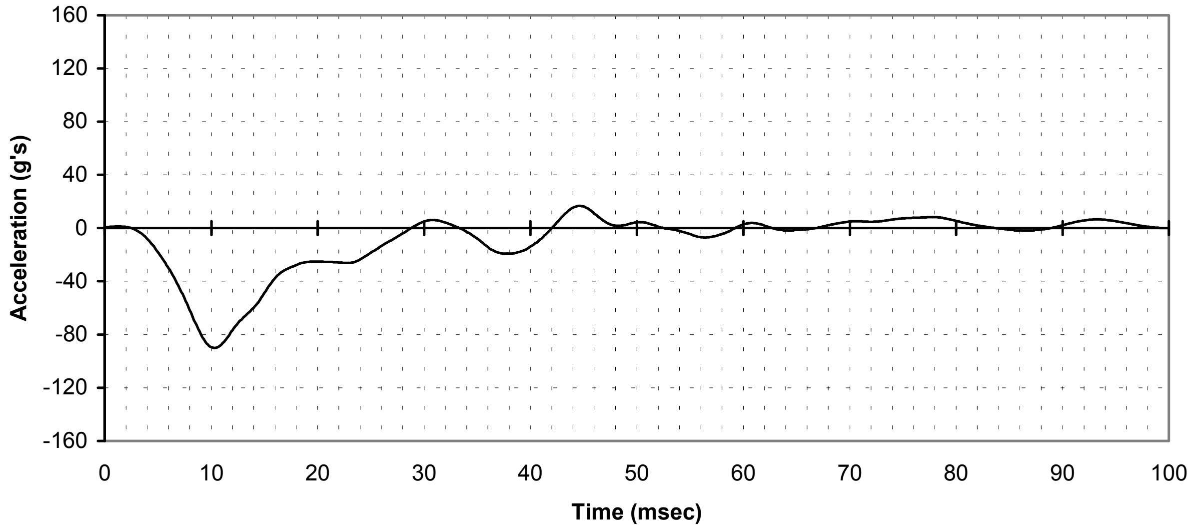

FIGURE A-32. FS 89, LEFT-SIDE WALL SEAT TRACK, ACCELEROMETER Z DIRECTION (channel 217)

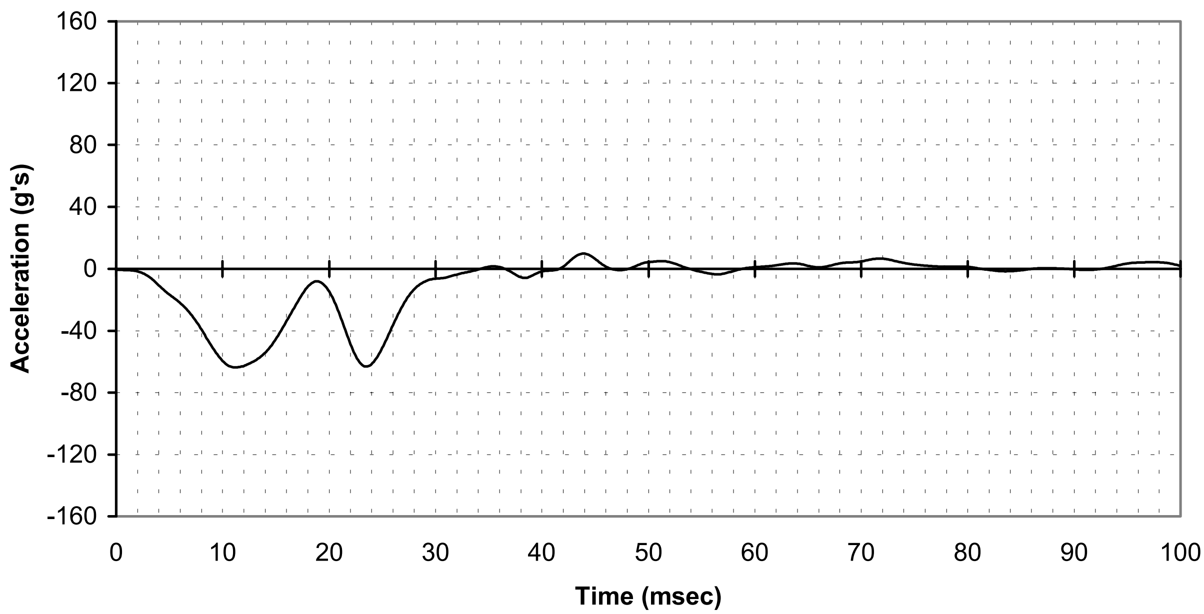

FIGURE A-33. FS 89, RIGHT-SIDE WALL SEAT TRACK, ACCELEROMETER Z DIRECTION (channel 222)

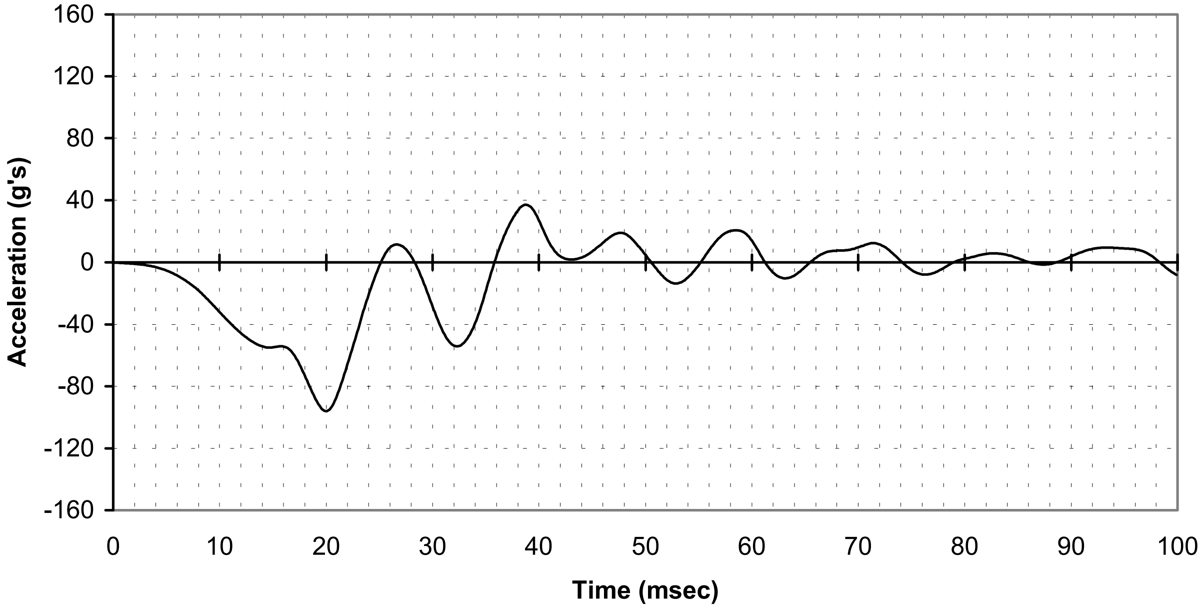

FIGURE A-34. FS 161, LEFT-SIDE WALL SEAT TRACK, ACCELEROMETER Z DIRECTION (channel 225)

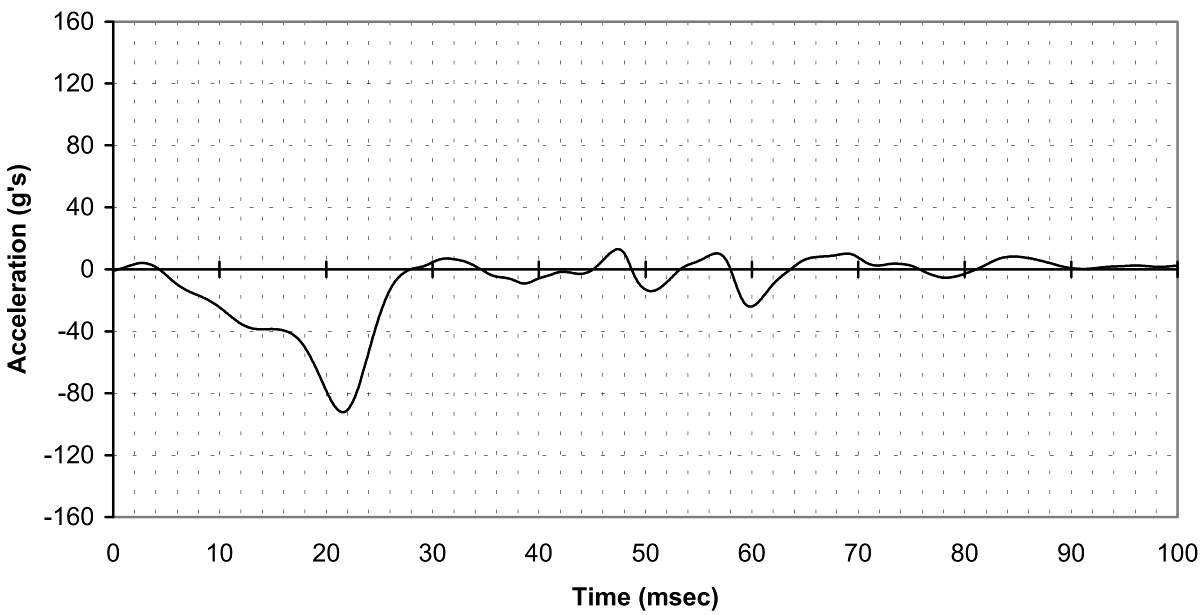

FIGURE A-35. FS 161, RIGHT-SIDE WALL SEAT TRACK, ACCELEROMETER Z DIRECTION (channel 230)

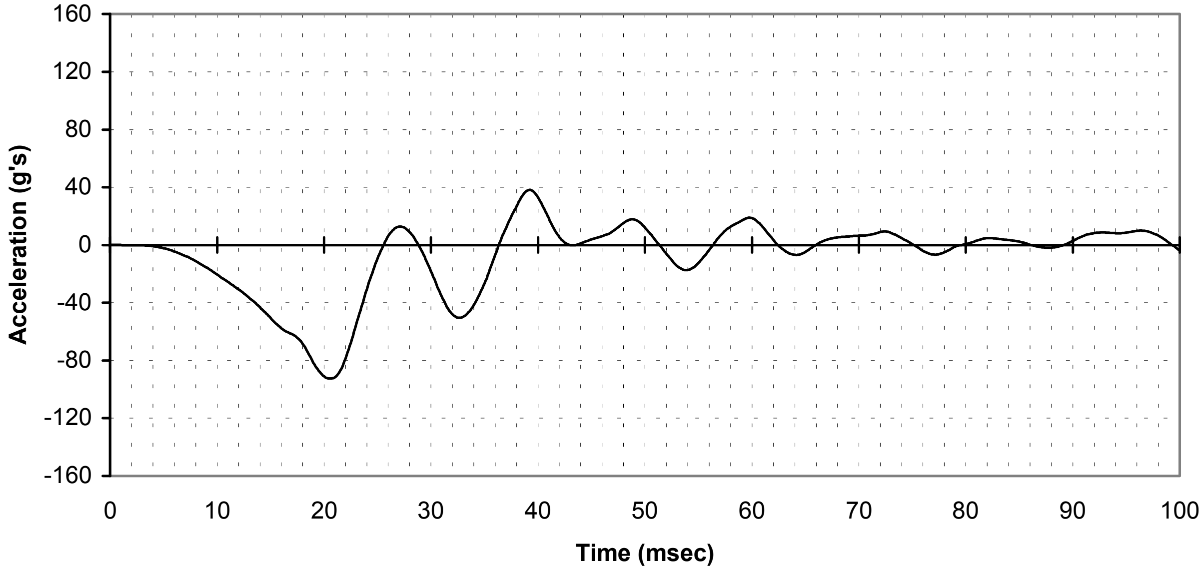

FIGURE A-36. FS 187, LEFT-SIDE WALL SEAT TRACK, ACCELEROMETER Z DIRECTION (channel 14)

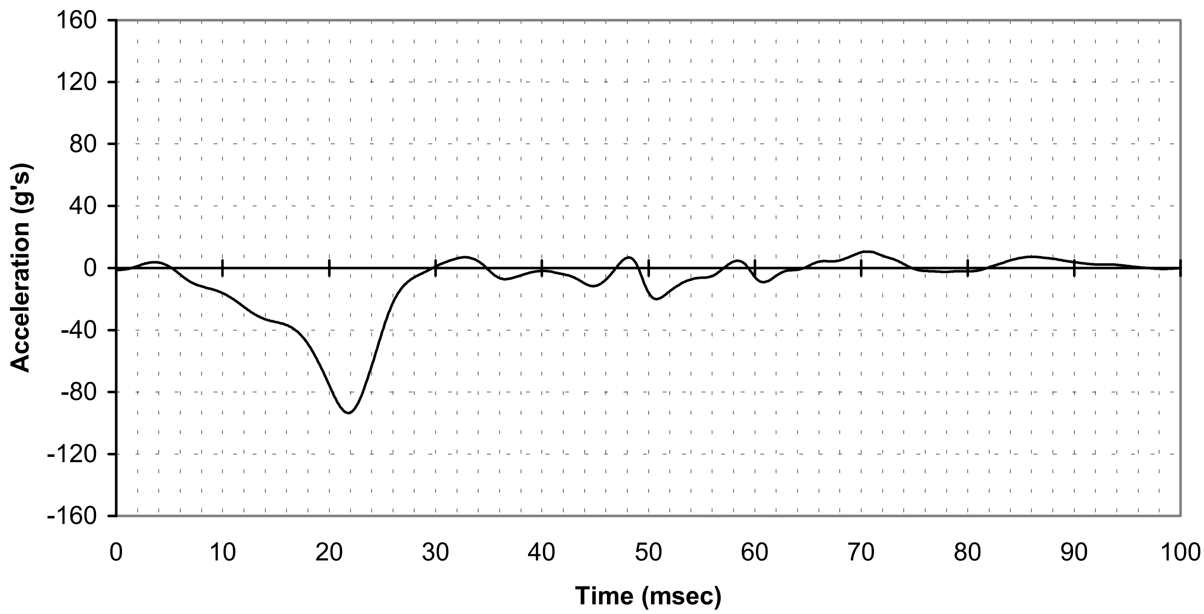

FIGURE A-37. FS 187, RIGHT-SIDE WALL SEAT TRACK, ACCELEROMETER Z DIRECTION (channel 17)

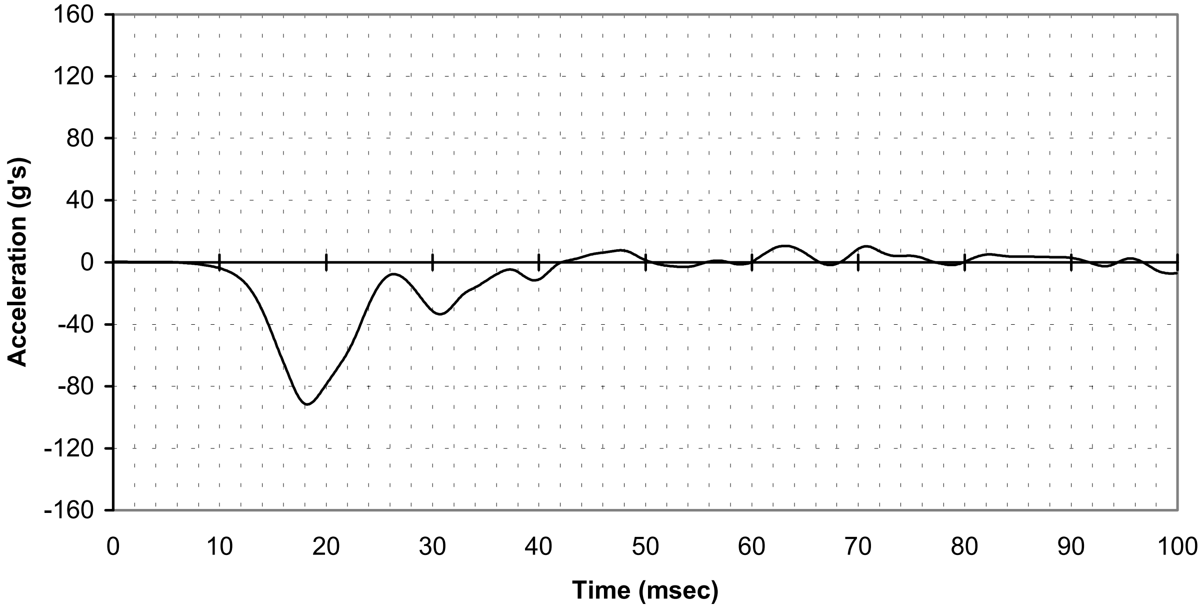

FIGURE A-38. FS 238, LEFT-SIDE WALL SEAT TRACK, ACCELEROMETER Z DIRECTION (channel 18)

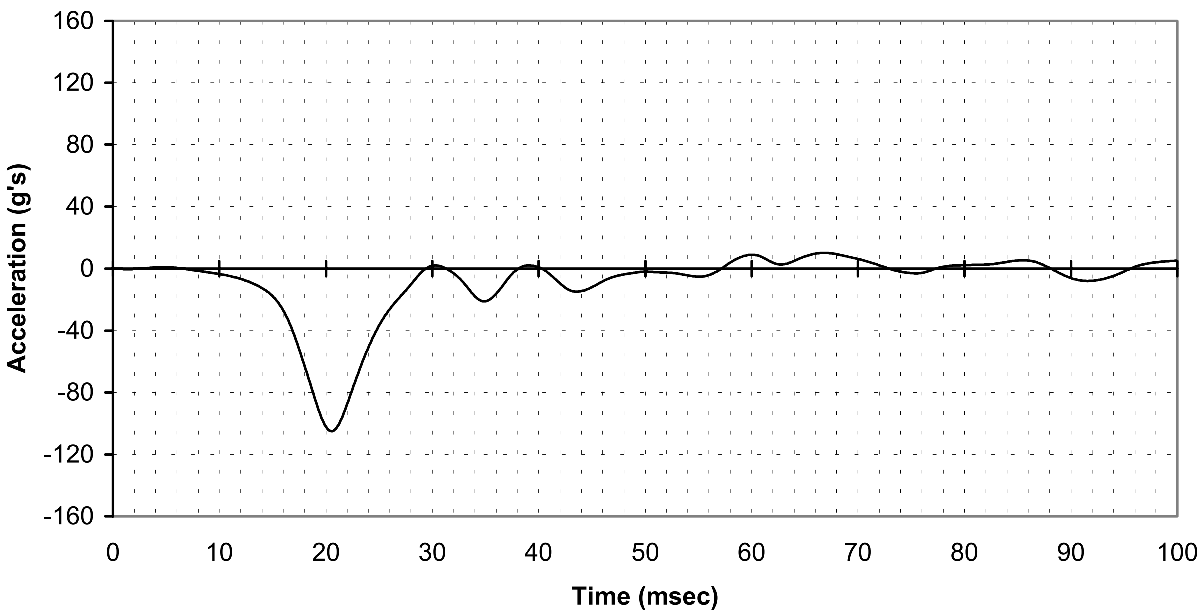

FIGURE A-39. FS 238, RIGHT-SIDE WALL SEAT TRACK, ACCELEROMETER Z DIRECTION (channel 21)

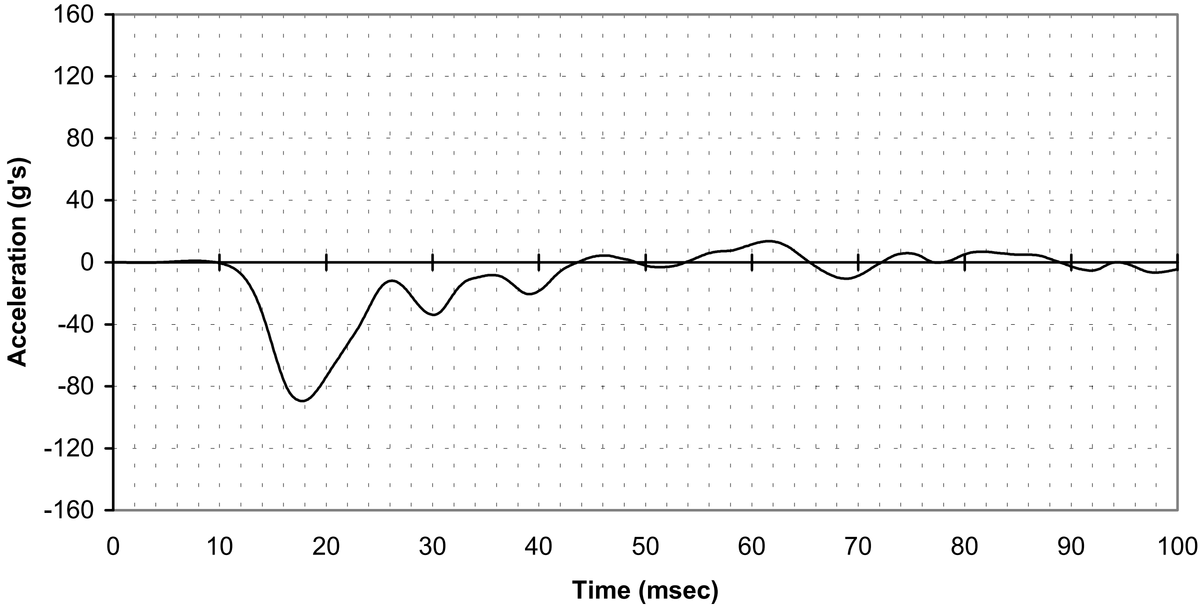

FIGURE A-40. FS 264, LEFT-SIDE WALL SEAT TRACK, ACCELEROMETER Z DIRECTION (channel 407)

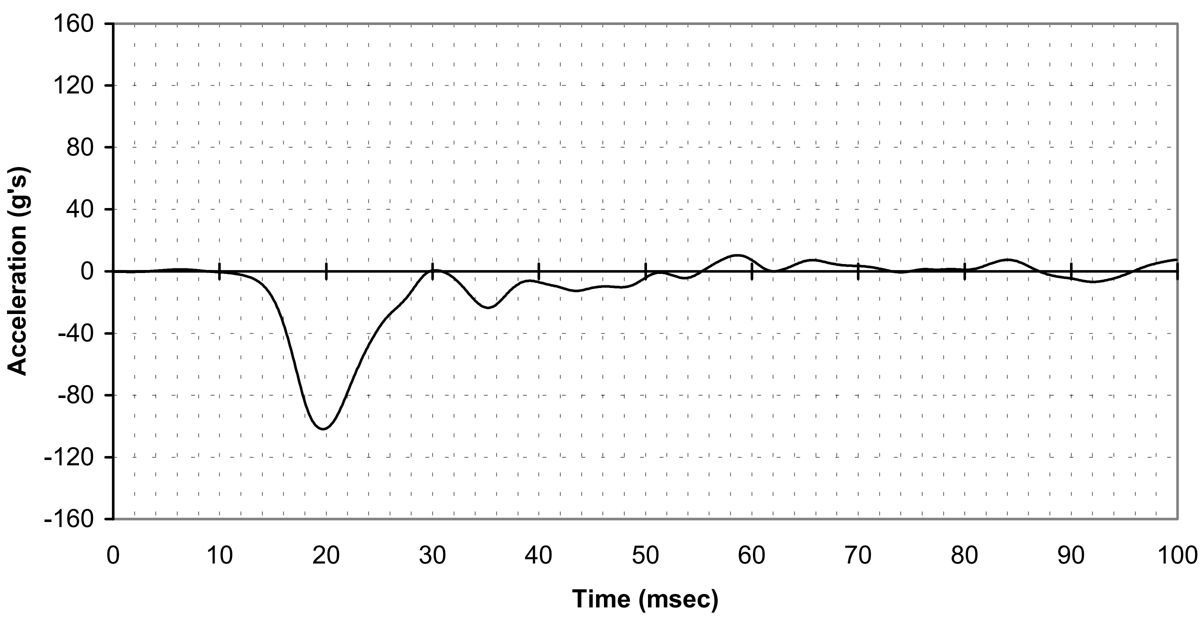

FIGURE A-41. FS 264, RIGHT-SIDE WALL SEAT TRACK, ACCELEROMETER Z DIRECTION (channel 417)

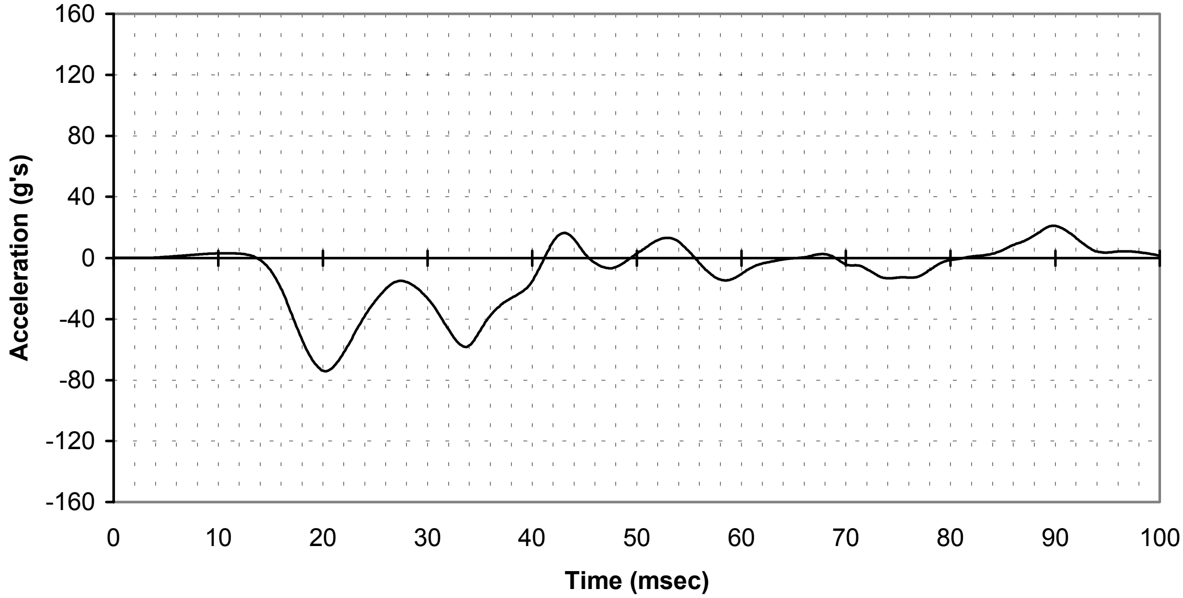

FIGURE A-42. FS 340, LEFT-SIDE WALL SEAT TRACK, ACCELEROMETER Z DIRECTION (channel 421)

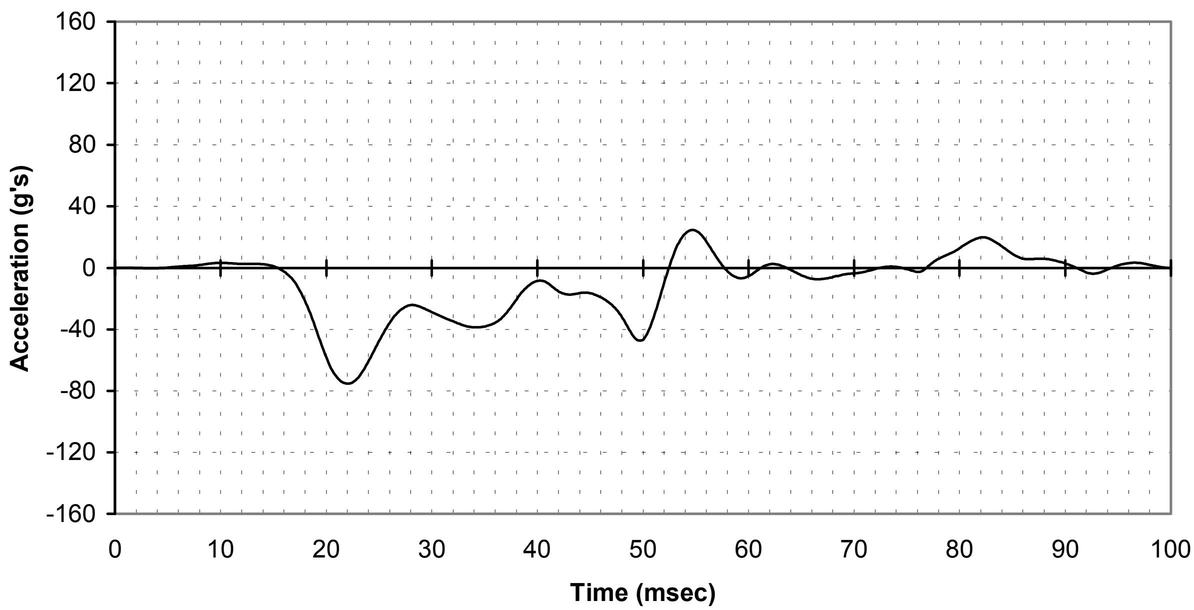

FIGURE A-43. FS 340, RIGHT-SIDE WALL SEAT TRACK, ACCELEROMETER Z DIRECTION (channel 314)

FLOOR SEAT TRACK DATA

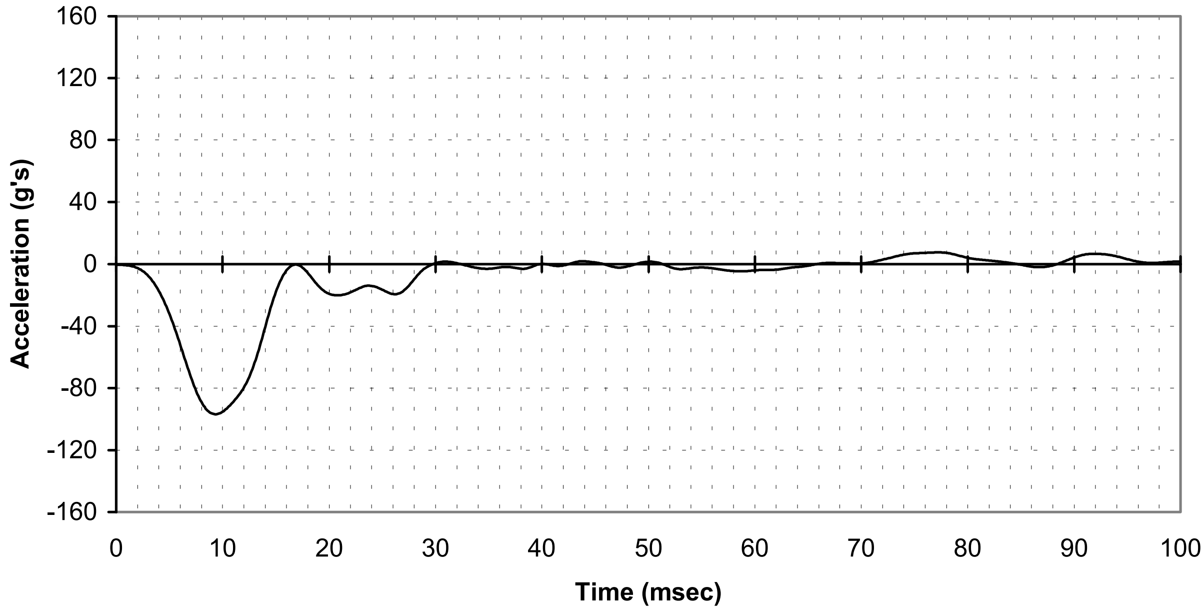

FIGURE A-44. FS 89, LEFT FLOOR SEAT TRACK, ACCELEROMETER Z DIRECTION (channel 218)

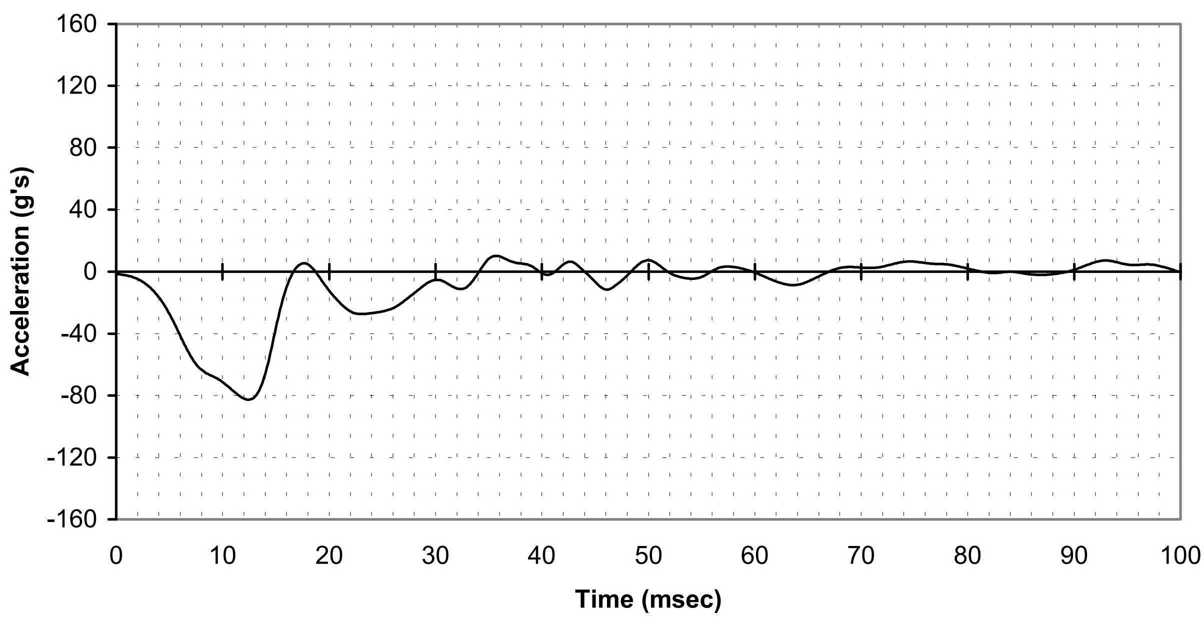

FIGURE A-45. FS 89, RIGHT FLOOR SEAT TRACK, ACCELEROMETER Z DIRECTION (channel 219)

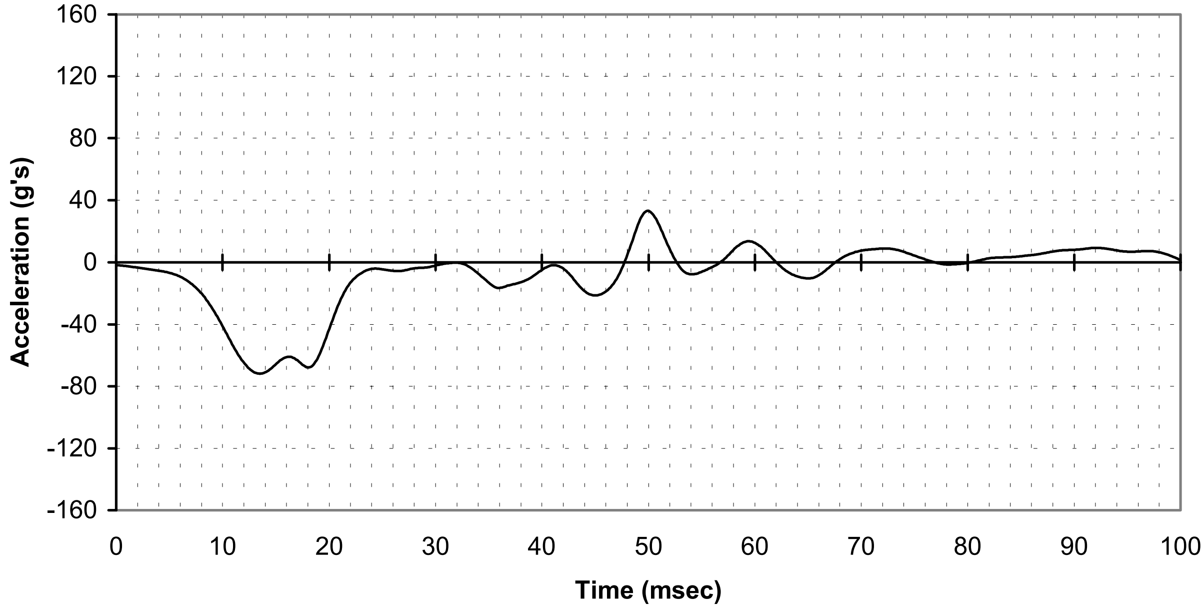

FIGURE A-46. FS 161, LEFT FLOOR SEAT TRACK, ACCELEROMETER Z DIRECTION (channel 226)

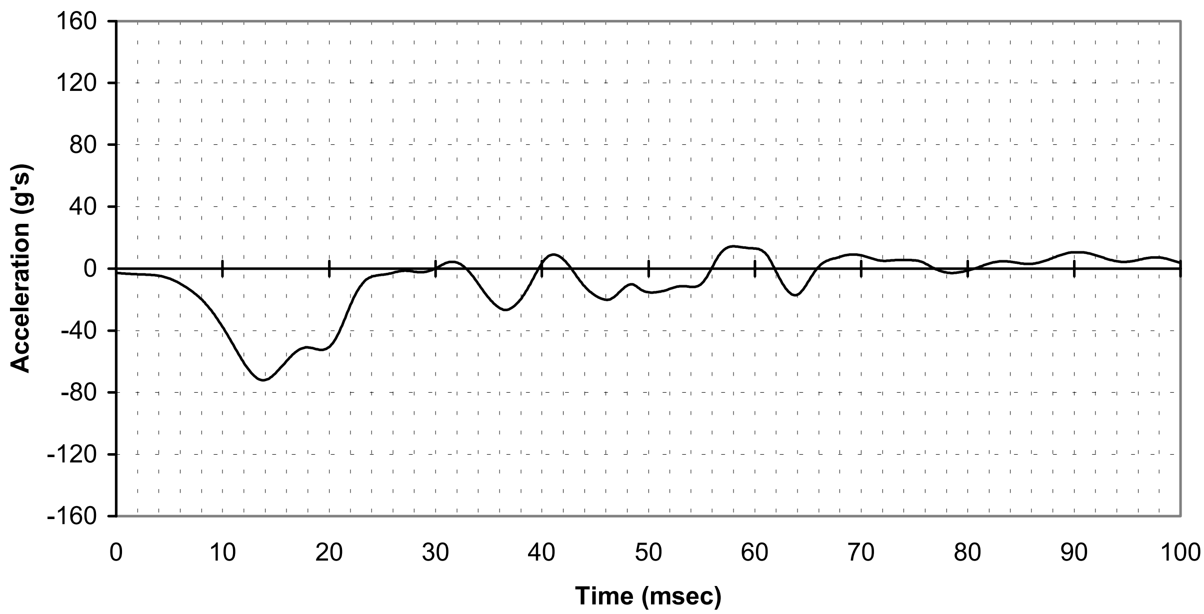

FIGURE A-47. FS 161, RIGHT FLOOR SEAT TRACK, ACCELEROMETER Z DIRECTION (channel 227)

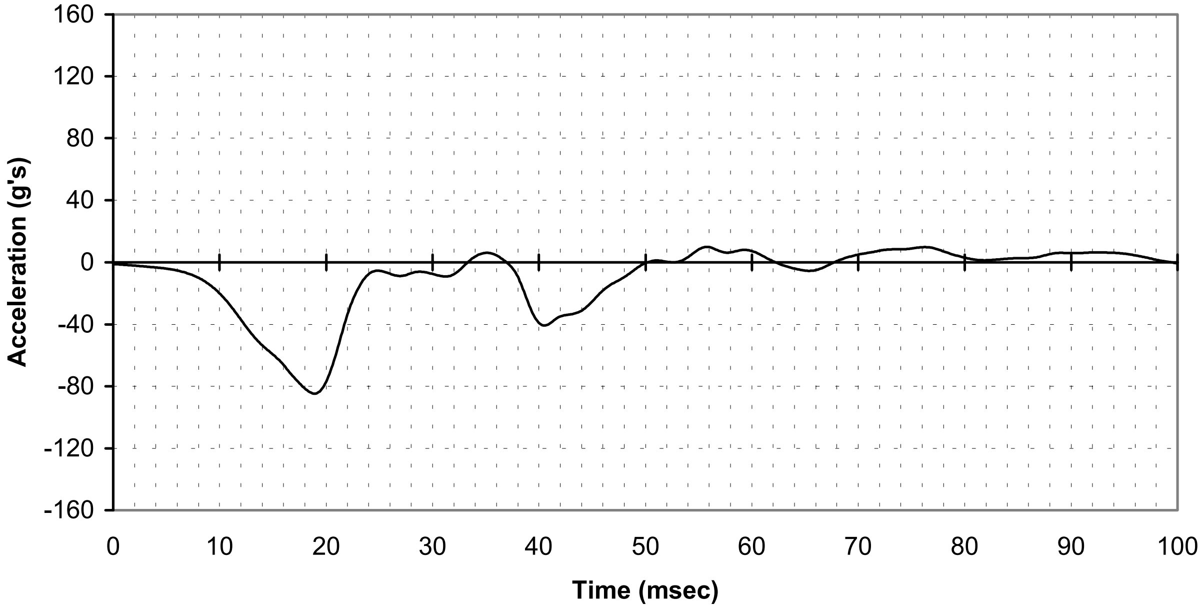

FIGURE A-48. FS 187, LEFT FLOOR SEAT TRACK, ACCELEROMETER Z DIRECTION (channel 15)

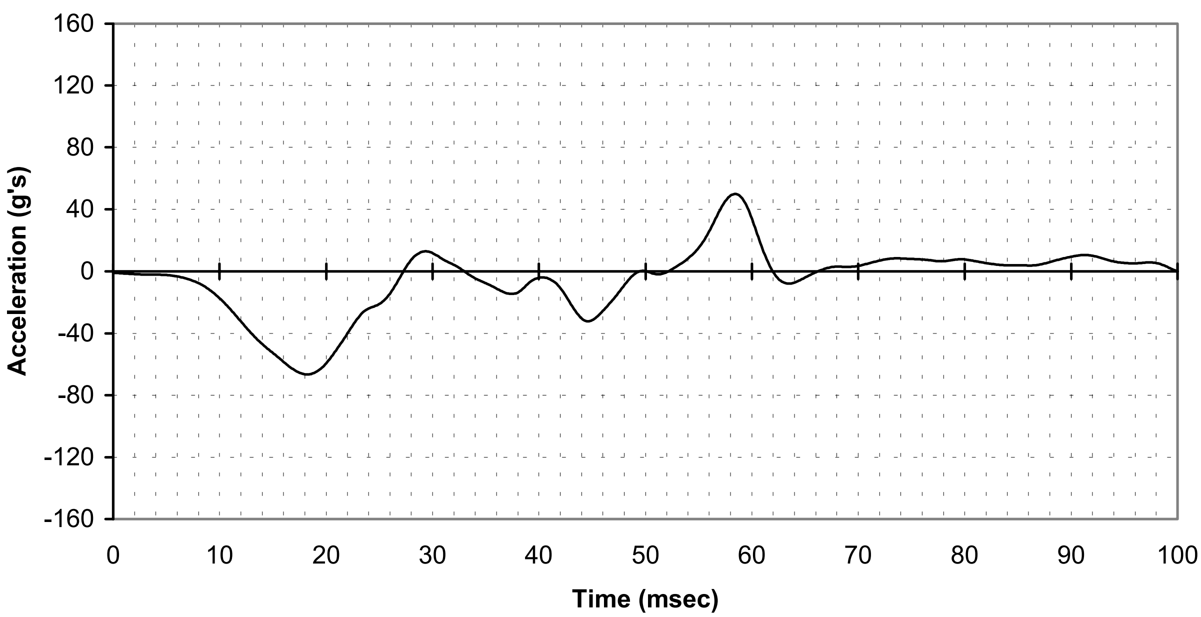

FIGURE A-49. FS 187, RIGHT FLOOR SEAT TRACK, ACCELEROMETER Z DIRECTION (channel 16)

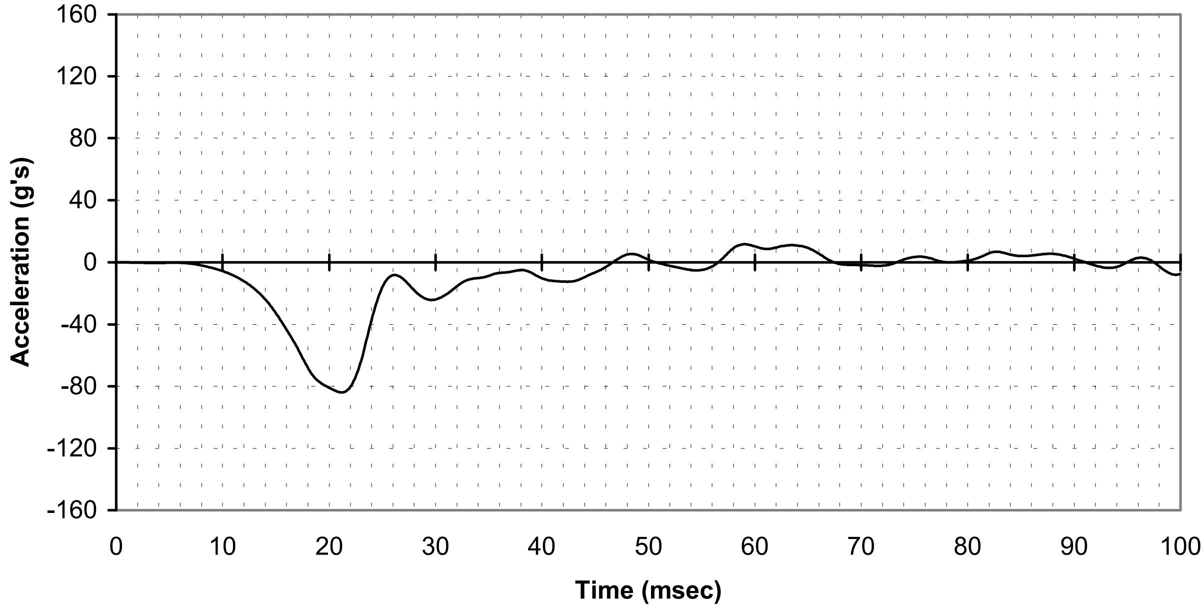

FIGURE A-50. FS 238, LEFT FLOOR SEAT TRACK, ACCELEROMETER Z DIRECTION (channel 19)

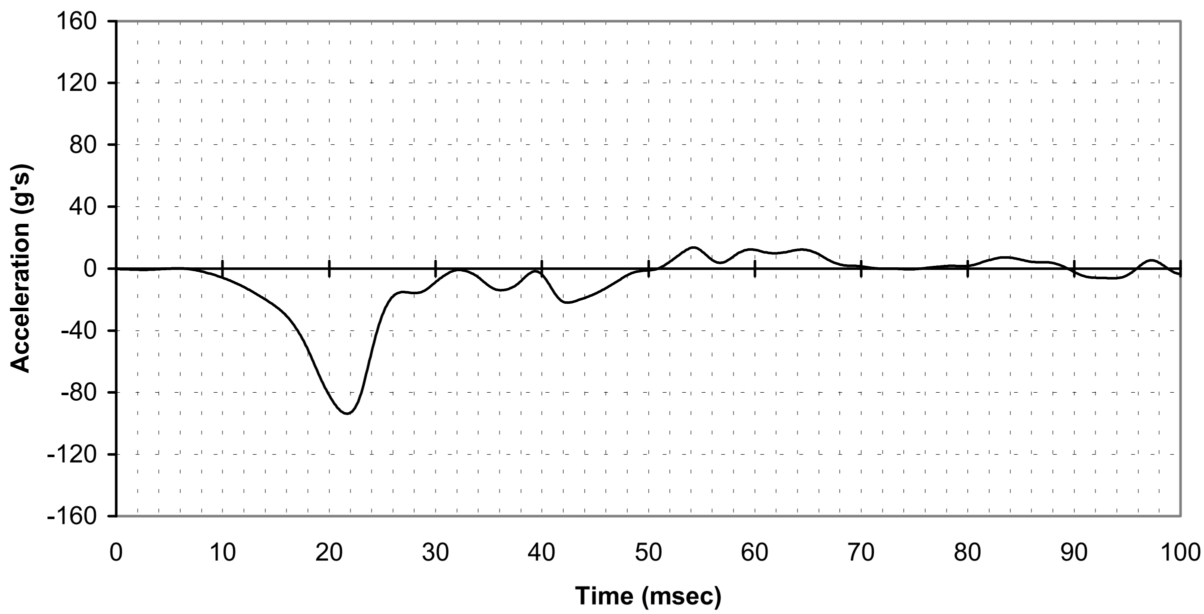

FIGURE A-51. FS 238, RIGHT FLOOR SEAT TRACK, ACCELEROMETER Z DIRECTION (channel 20)

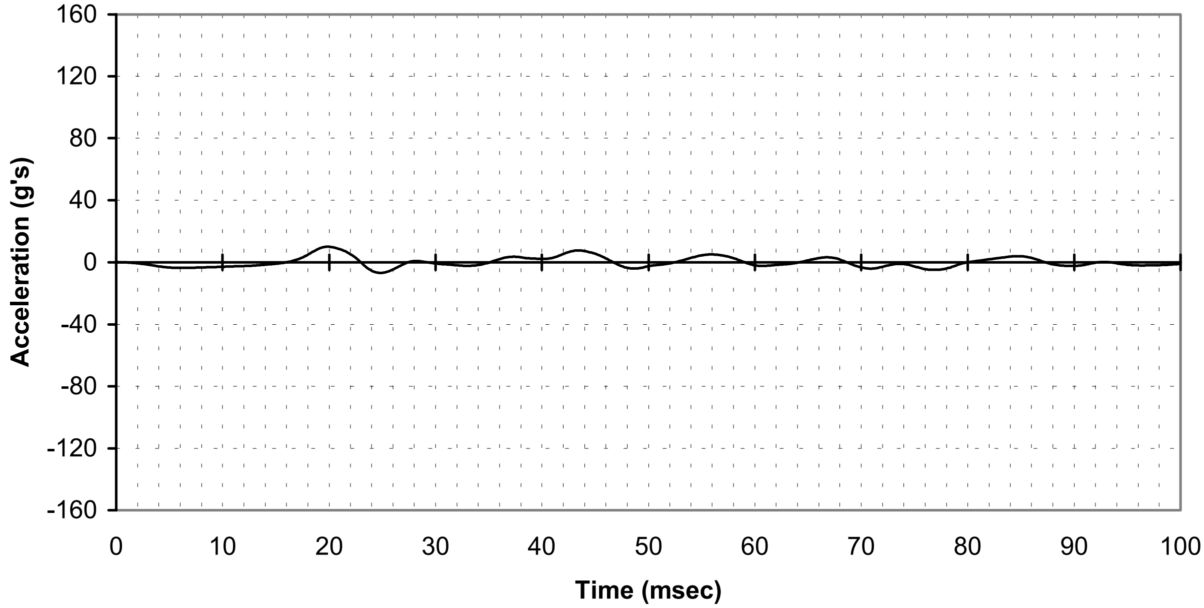

FIGURE A-52. FS 264, LEFT FLOOR SEAT TRACK, ACCELEROMETER X DIRECTION (channel 408)

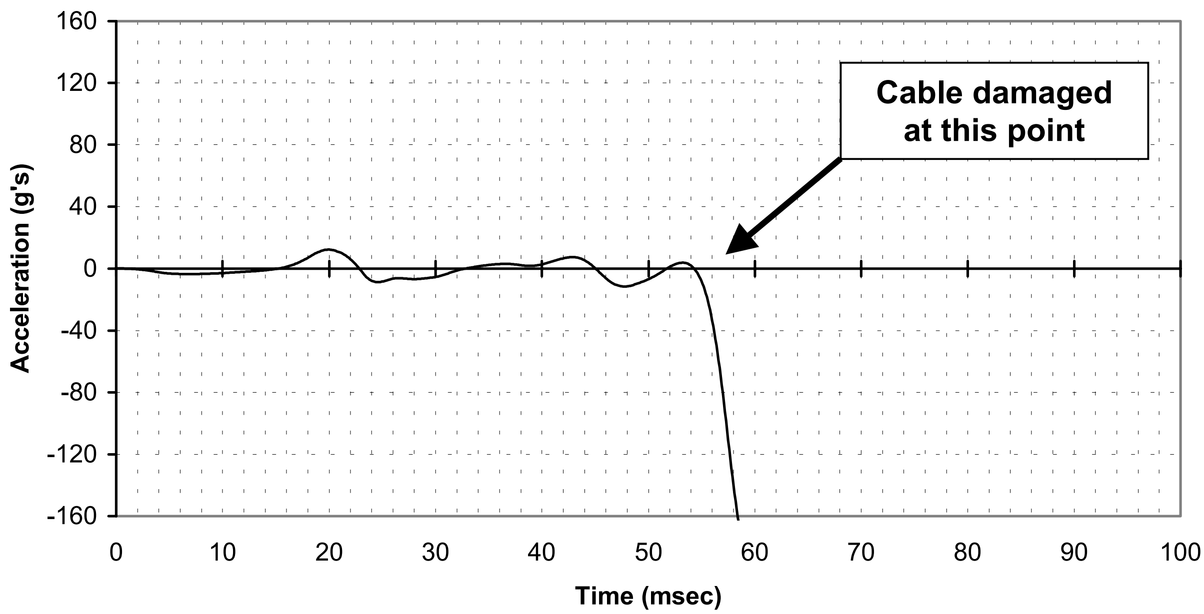

FIGURE A-53. FS 264, RIGHT FLOOR SEAT TRACK, ACCELEROMETER X DIRECTION (channel 410)

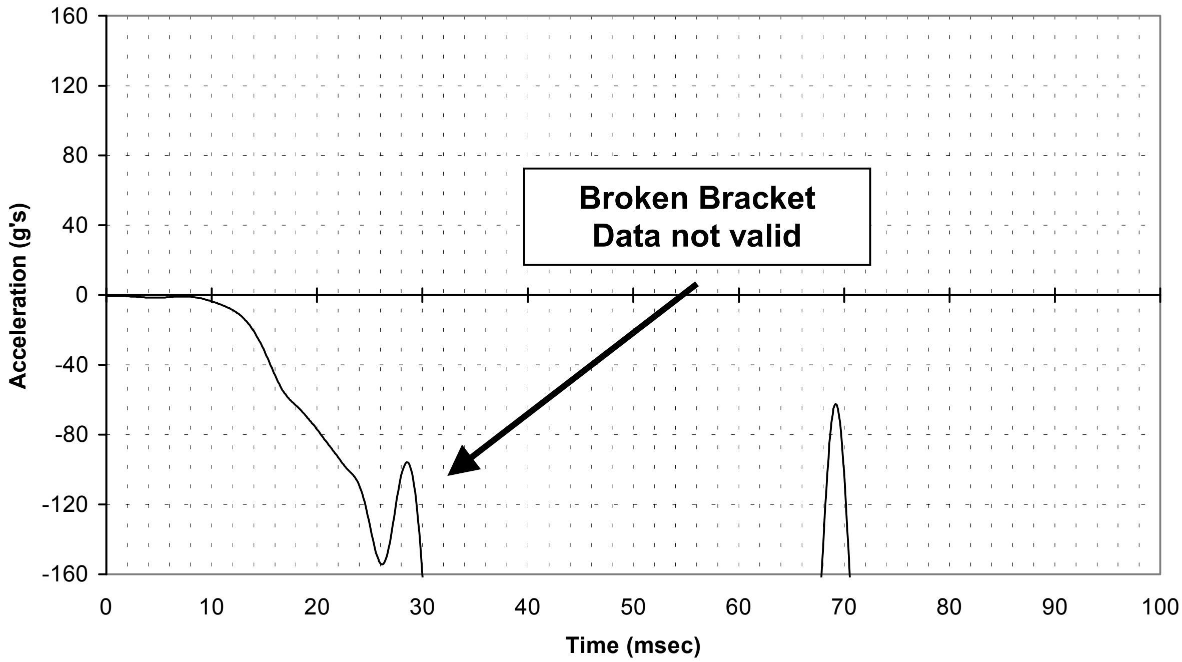

FIGURE A-54. FS 264, LEFT FLOOR SEAT TRACK, ACCELEROMETER Z DIRECTION (channel 409)

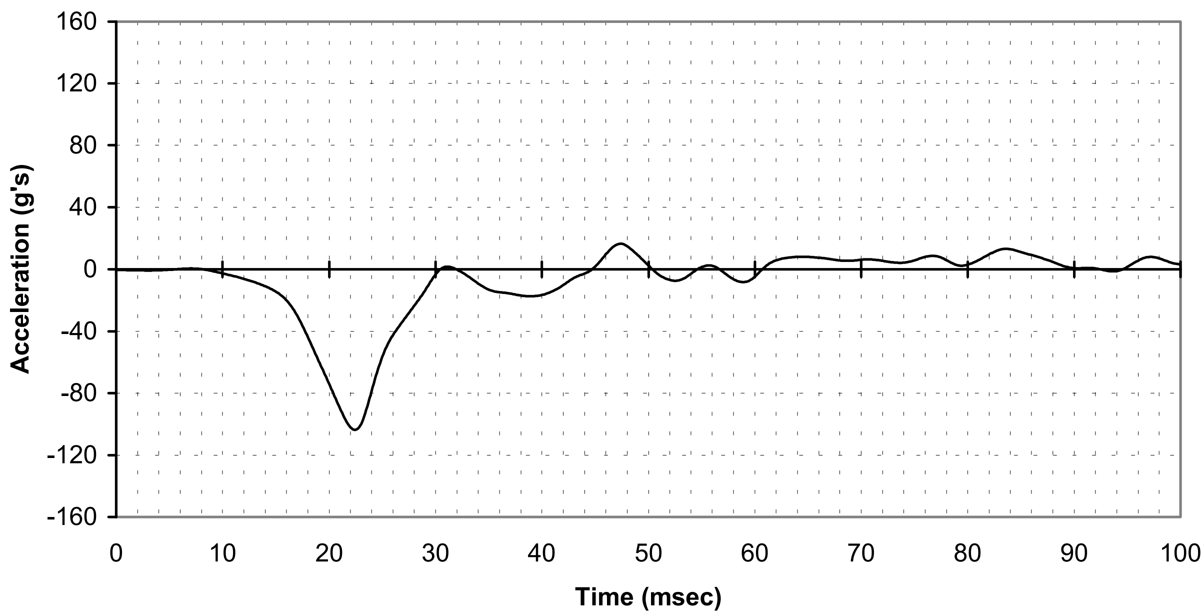

FIGURE A-55. FS 264, RIGHT FLOOR SEAT TRACK, ACCELEROMETER Z DIRECTION (channel 411)

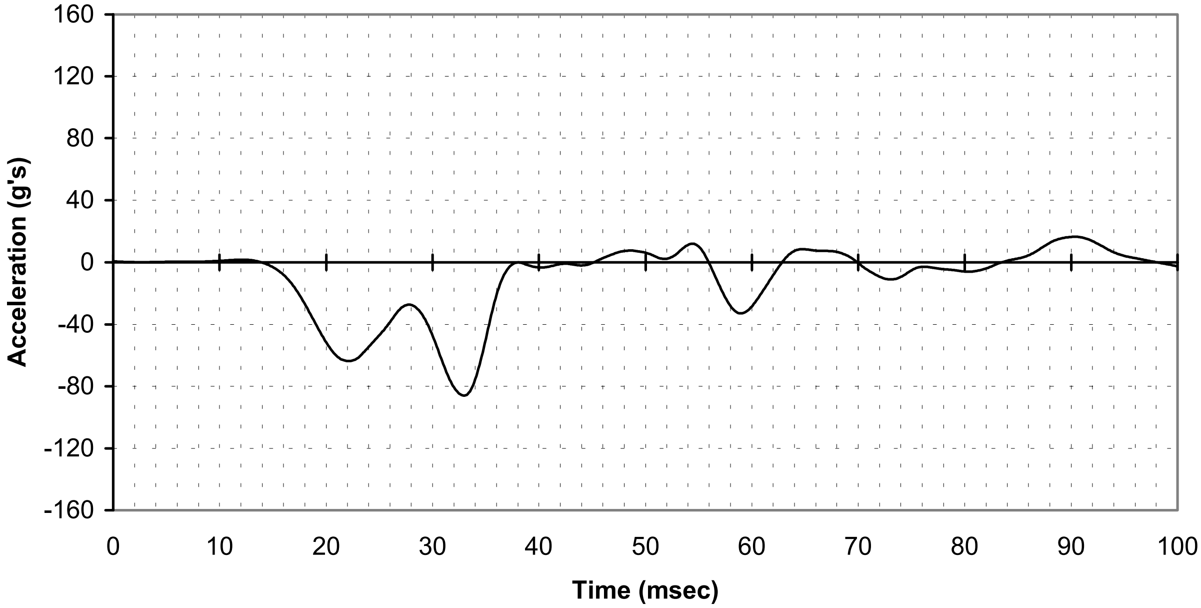

FIGURE A-56. FS 340, LEFT FLOOR SEAT TRACK, ACCELEROMETER Z DIRECTION (channel 422)

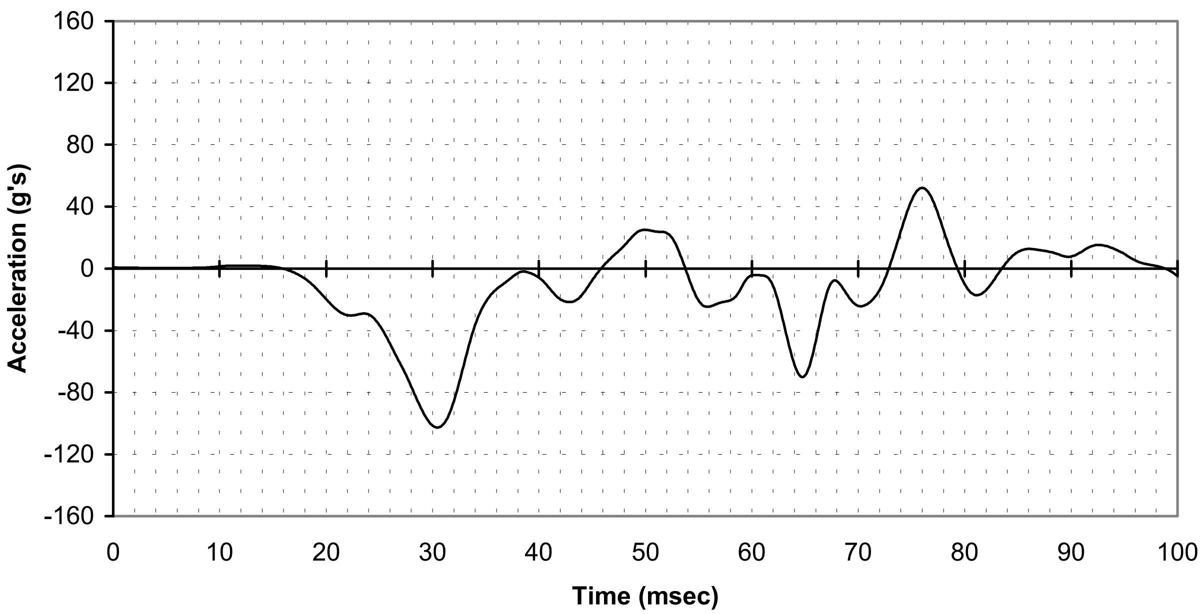

FIGURE A-57. FS 340, RIGHT FLOOR SEAT TRACK, ACCELEROMETER Z DIRECTION (channel 313)

FRONT SPAR DATA

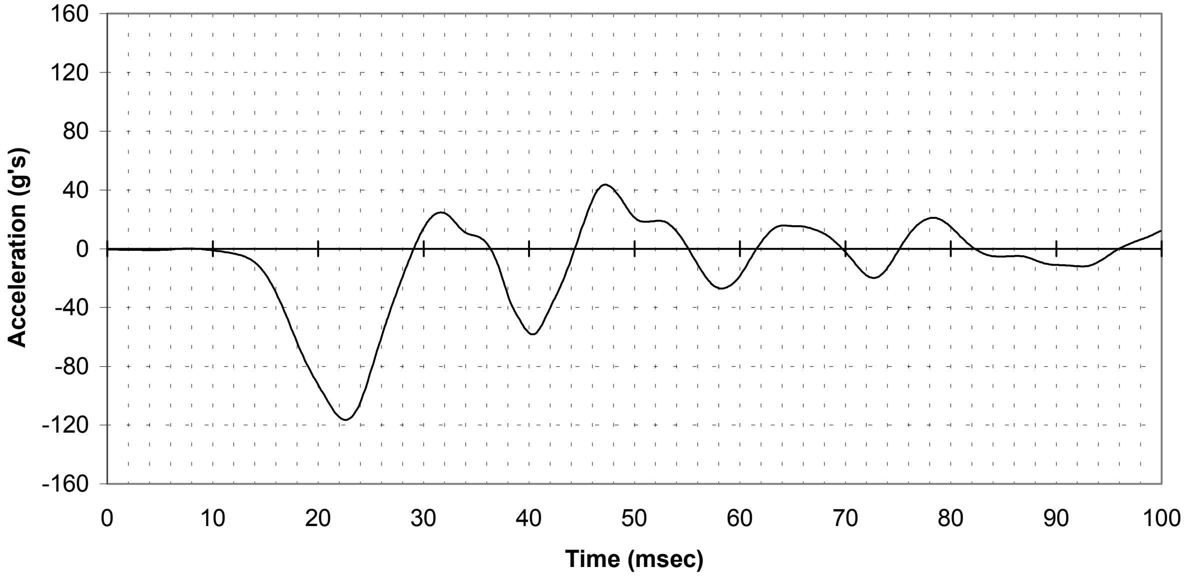

FIGURE A-58. FS 238, LEFT FRONT SPAR, ACCELEROMETER Z DIRECTION (channel 305)

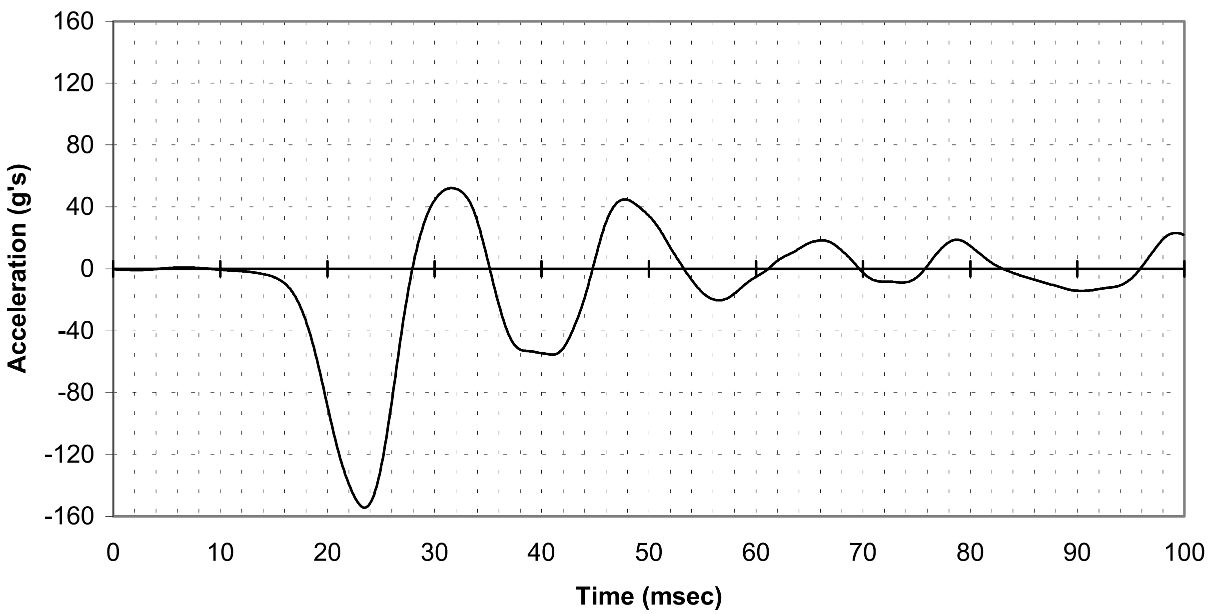

FIGURE A-59. FS 238, RIGHT FRONT SPAR, ACCELEROMETER Z DIRECTION (channel 306)

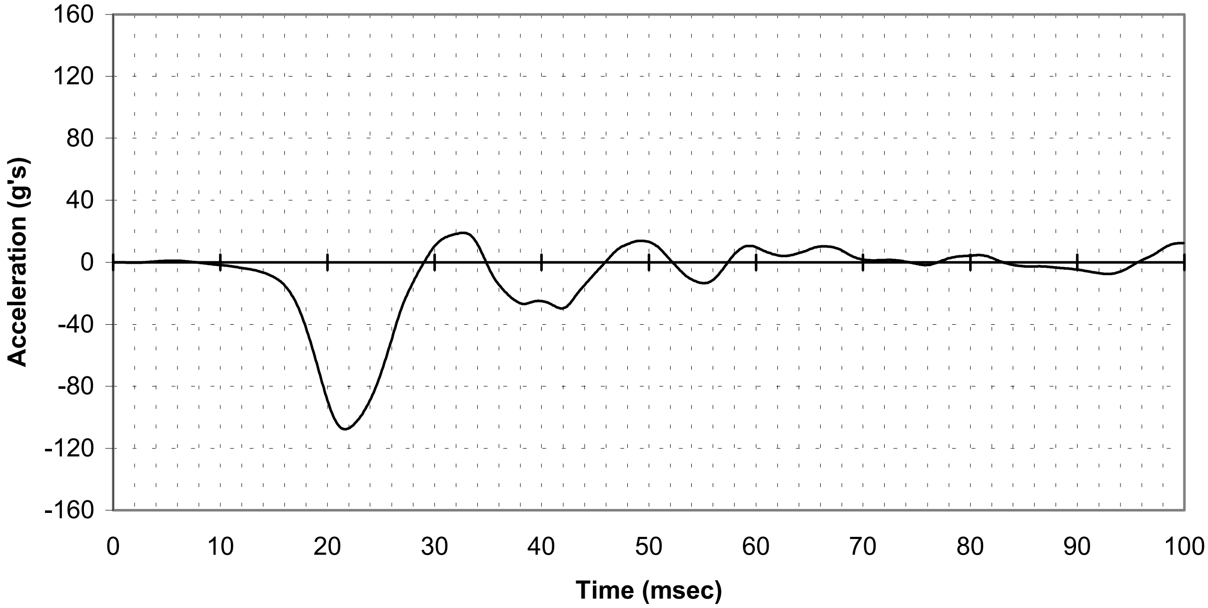

FIGURE A-60. FS 238, RIGHT FRONT SPAR, ACCELEROMETER Z DIRECTION
(channel 22)

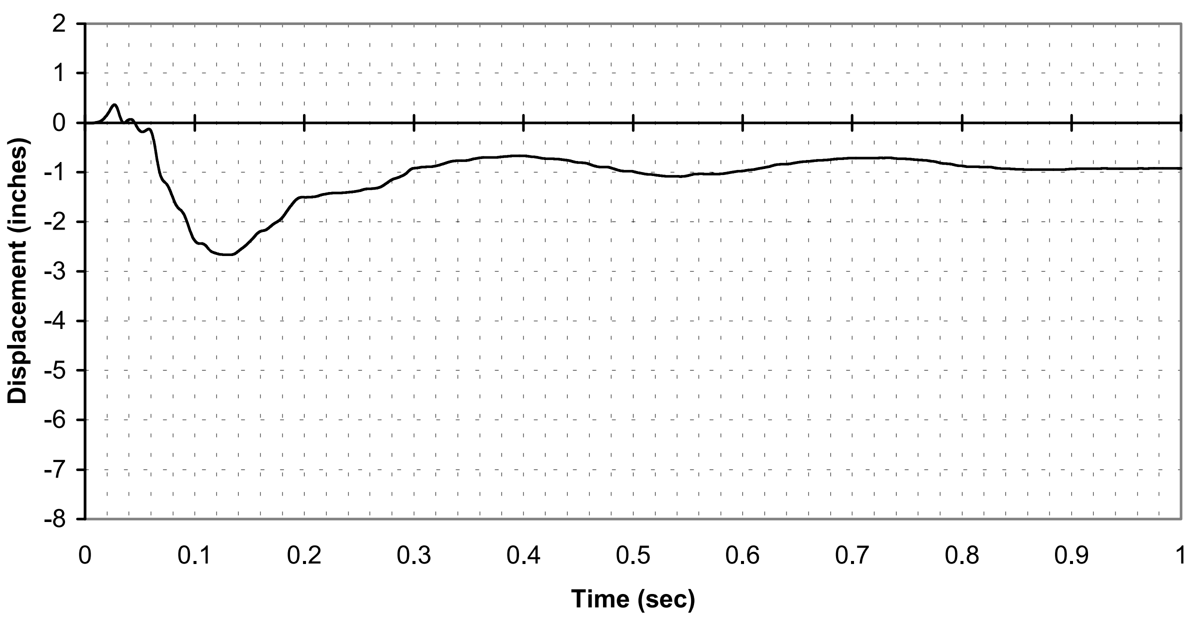

FIGURE A-61. FS 238, LEFT FRONT SPAR, STRING POTENTIOMETER
(channel 307)

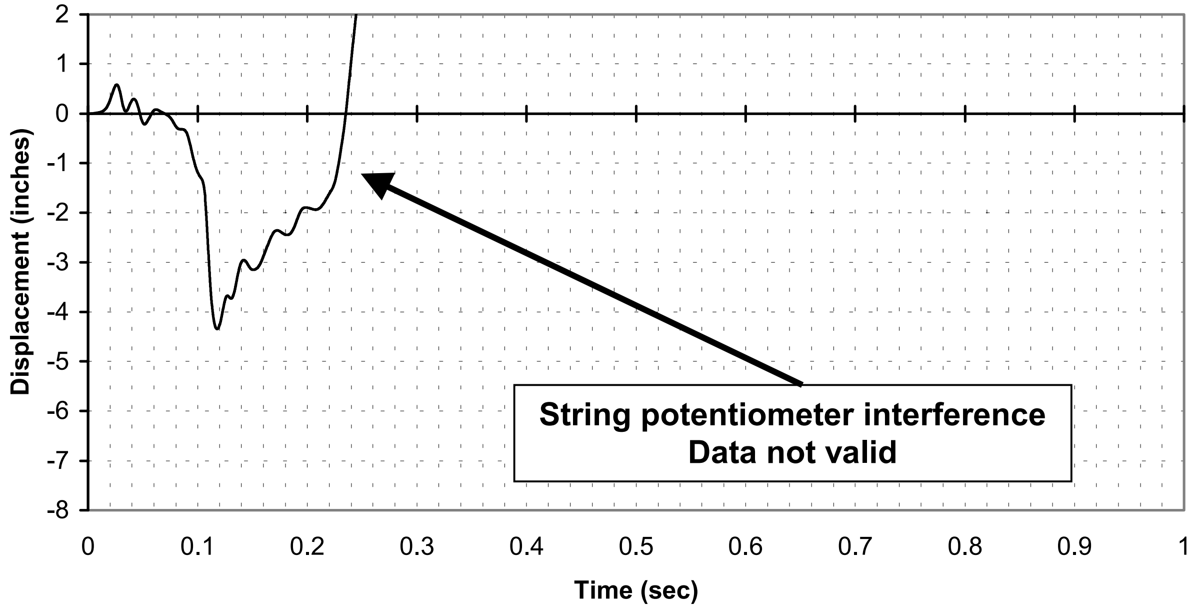

FIGURE A-62. FS 238, RIGHT FRONT SPAR, STRING POTENTIOMETER (channel 308)

REAR SPAR DATA

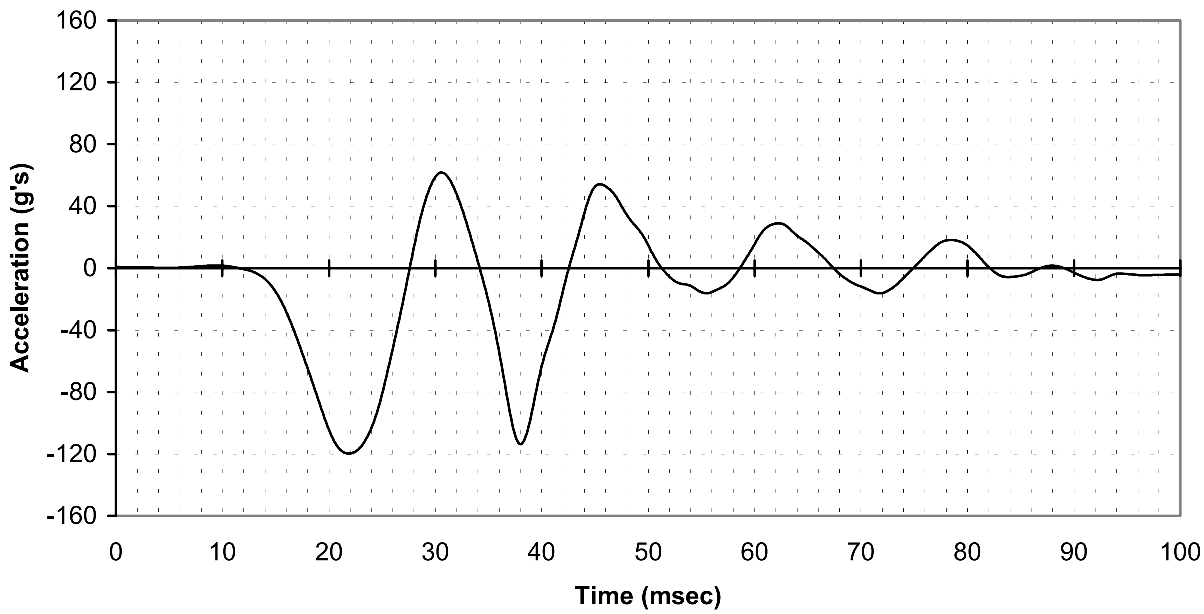

FIGURE A-63. FS 264, LEFT REAR SPAR, ACCELEROMETER Z DIRECTION
(channel 309)

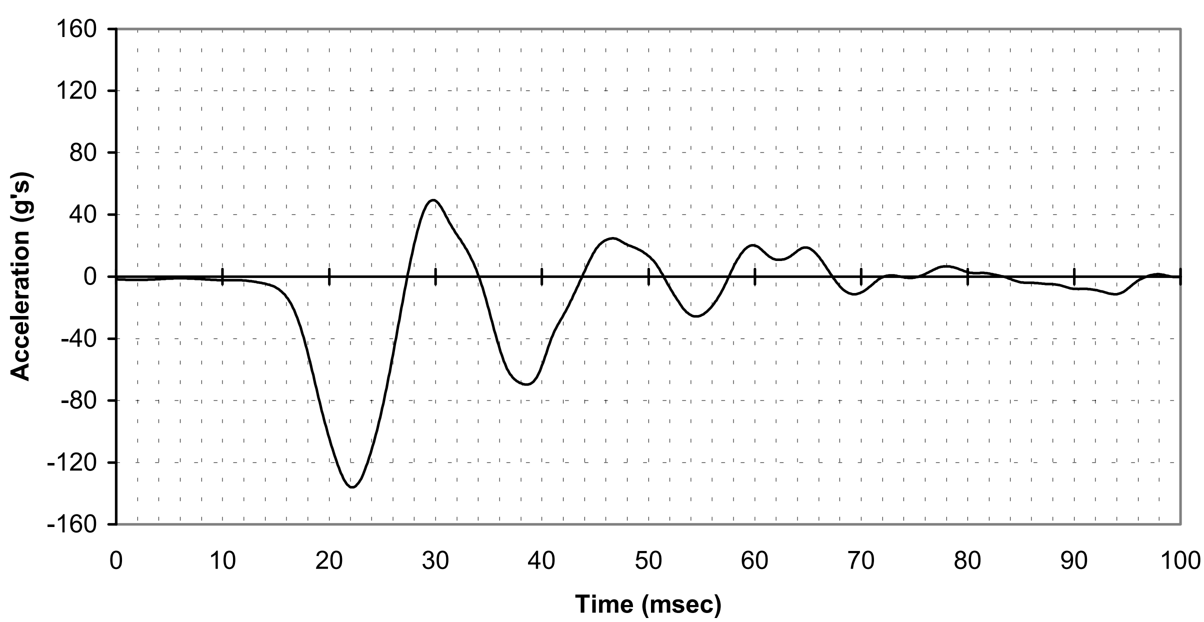

FIGURE A-64. FS 264, RIGHT REAR SPAR, ACCELEROMETER Z DIRECTION
(channel 310)

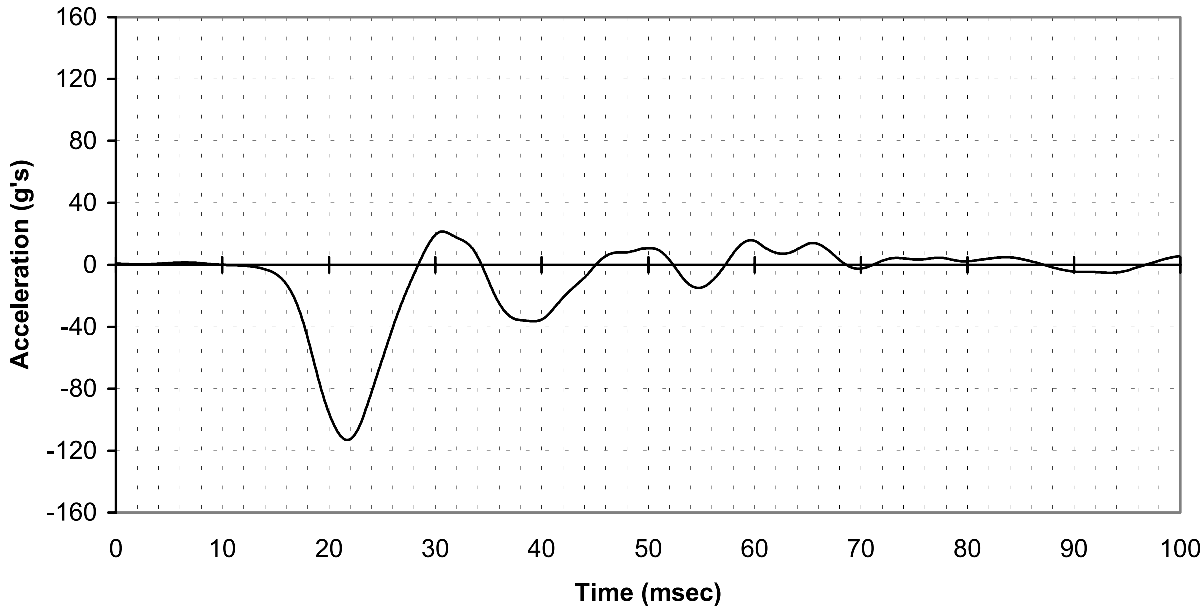

FIGURE A-65. FS 264, RIGHT REAR SPAR, ACCELEROMETER Z DIRECTION
(channel 23)

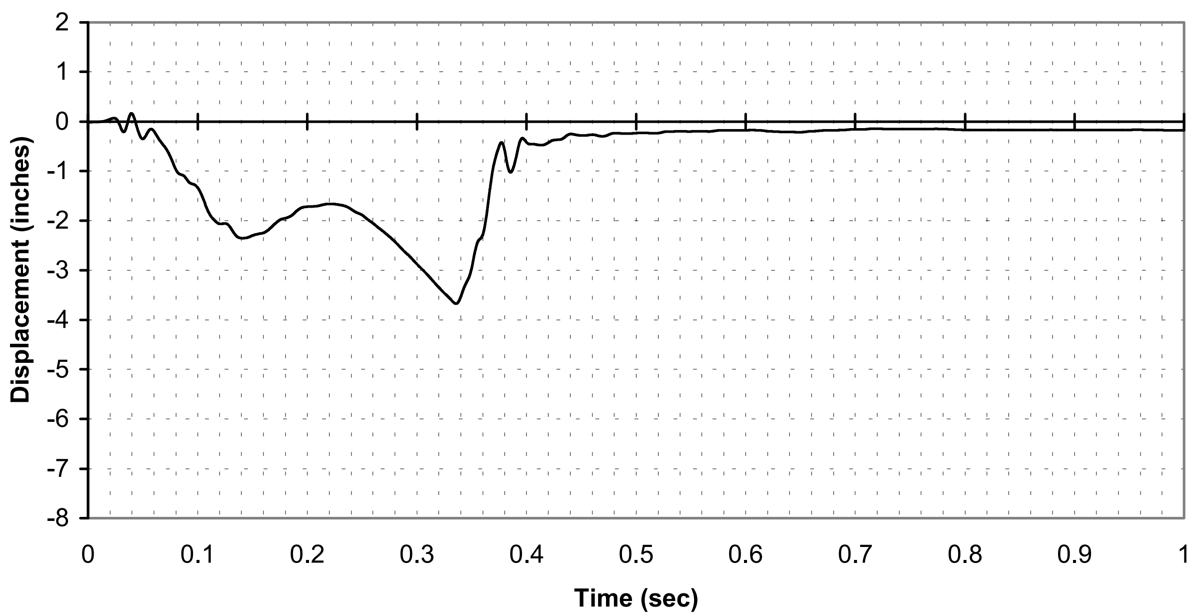

FIGURE A-66. FS 264, LEFT REAR SPAR, STRING POTENTIOMETER
(channel 311)

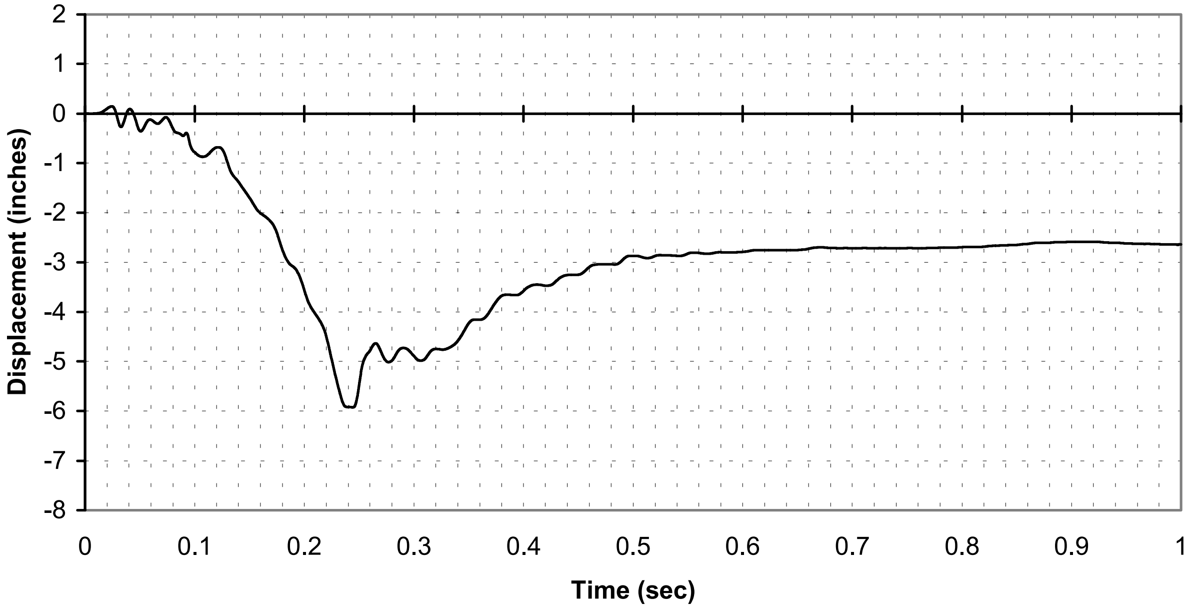

FIGURE A-67. FS 264, RIGHT REAR SPAR, STRING POTENTIOMETER
(channel 423)

OUTSIDE SPAR DATA

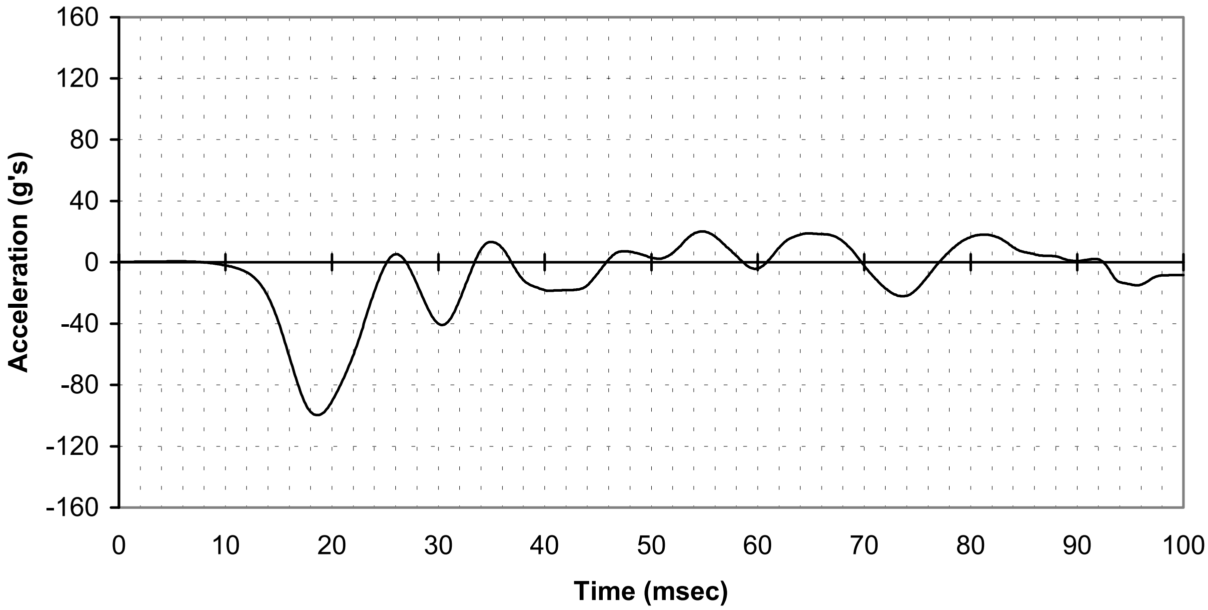

FIGURE A-68. LEFT OUTSIDE SPAR, ACCELEROMETER Z DIRECTION
(channel 104)

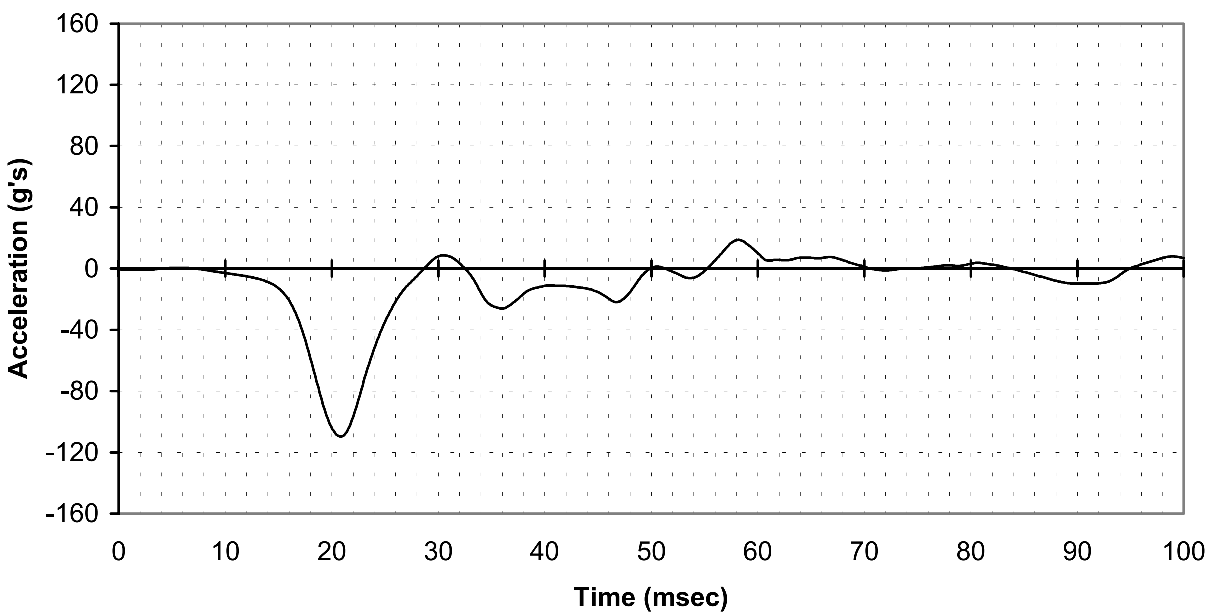

FIGURE A-69. RIGHT OUTSIDE SPAR, ACCELEROMETER Z DIRECTION
(channel 404)

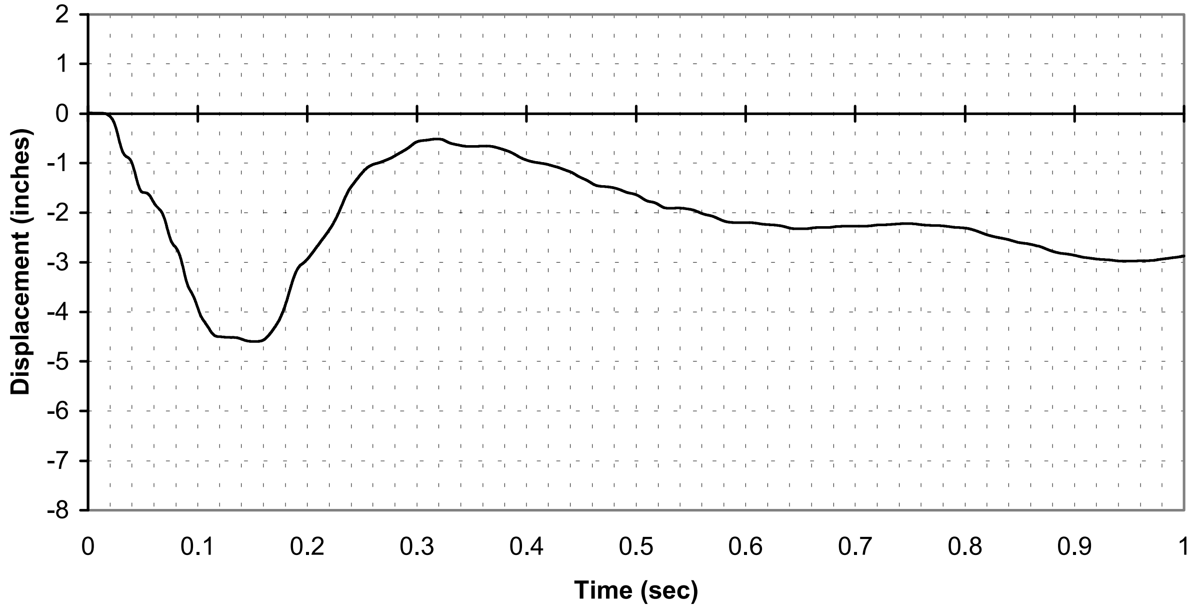

FIGURE A-70. LEFT OUTSIDE SPAR, STRING POTENTIOMETER
(channel 112)

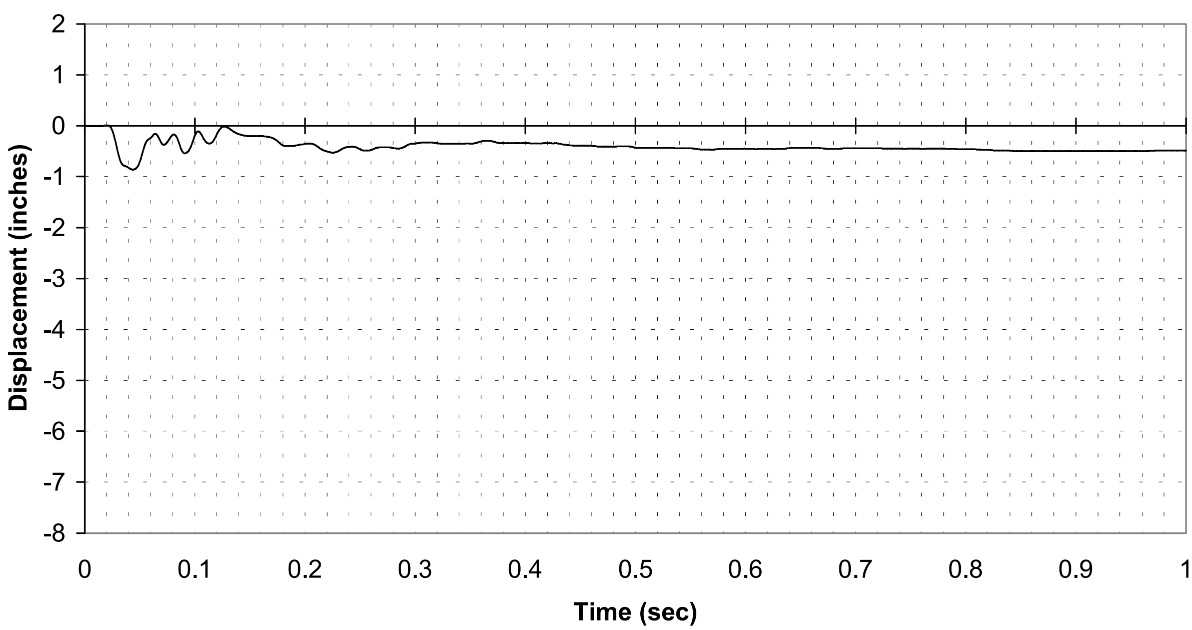

FIGURE A-71. RIGHT OUTSIDE SPAR, STRING POTENTIOMETER
(channel 431)

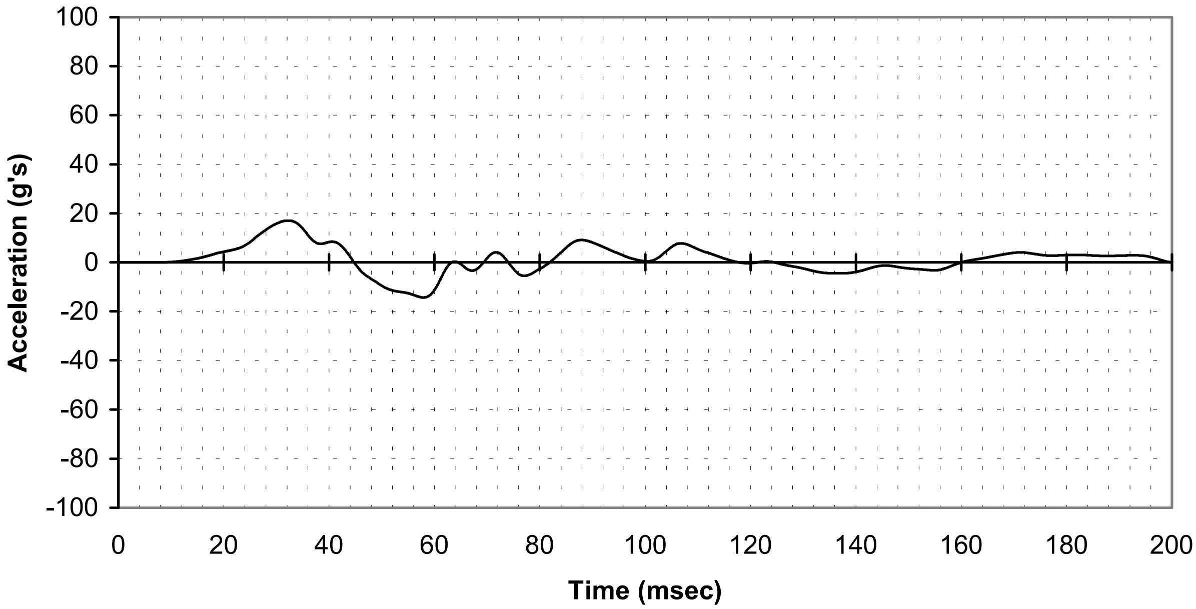

FIGURE A-72. LEFT STRUT, ACCELEROMETER X DIRECTION
(channel 109)

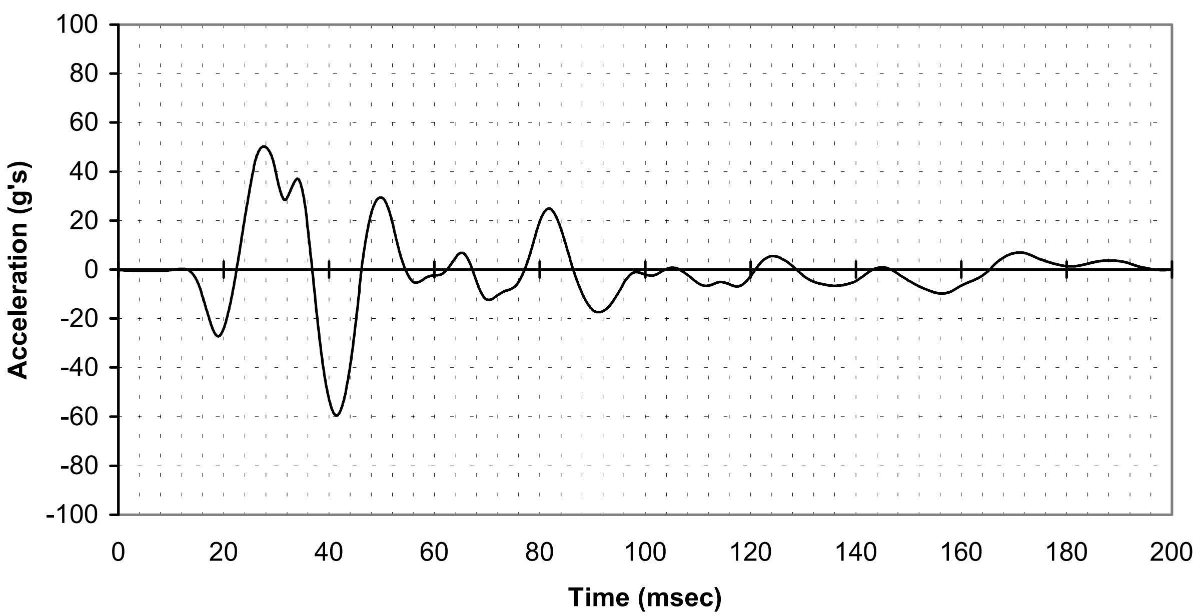

FIGURE A-73. LEFT STRUT, ACCELEROMETER Y DIRECTION
(channel 110)

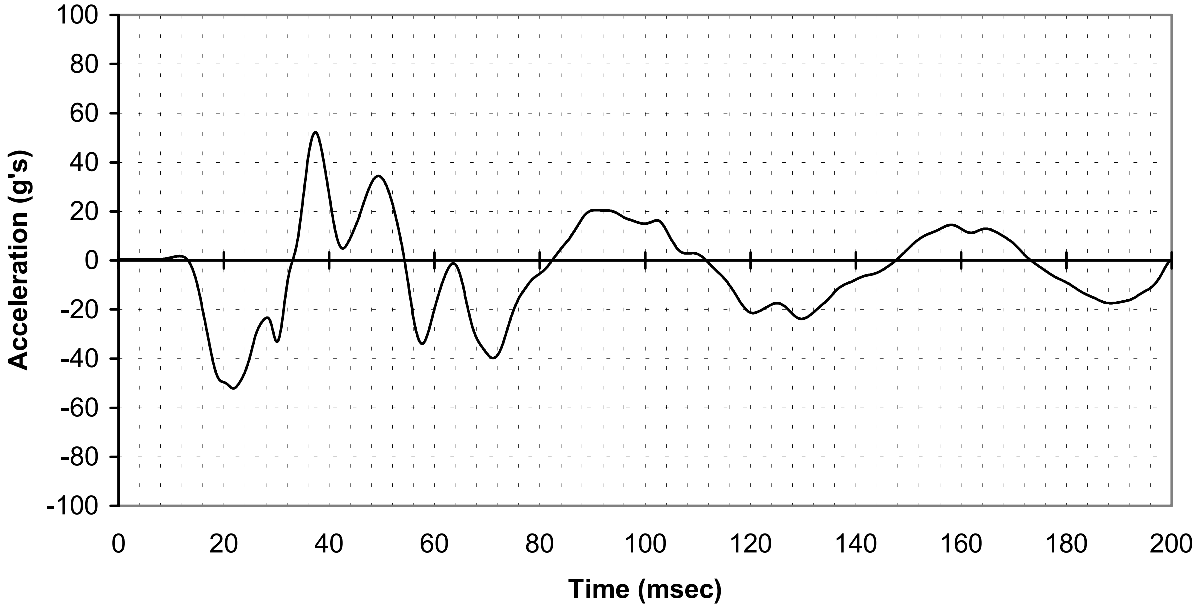

FIGURE A-74. LEFT STRUT, ACCELEROMETER Z DIRECTION
(channel 111)

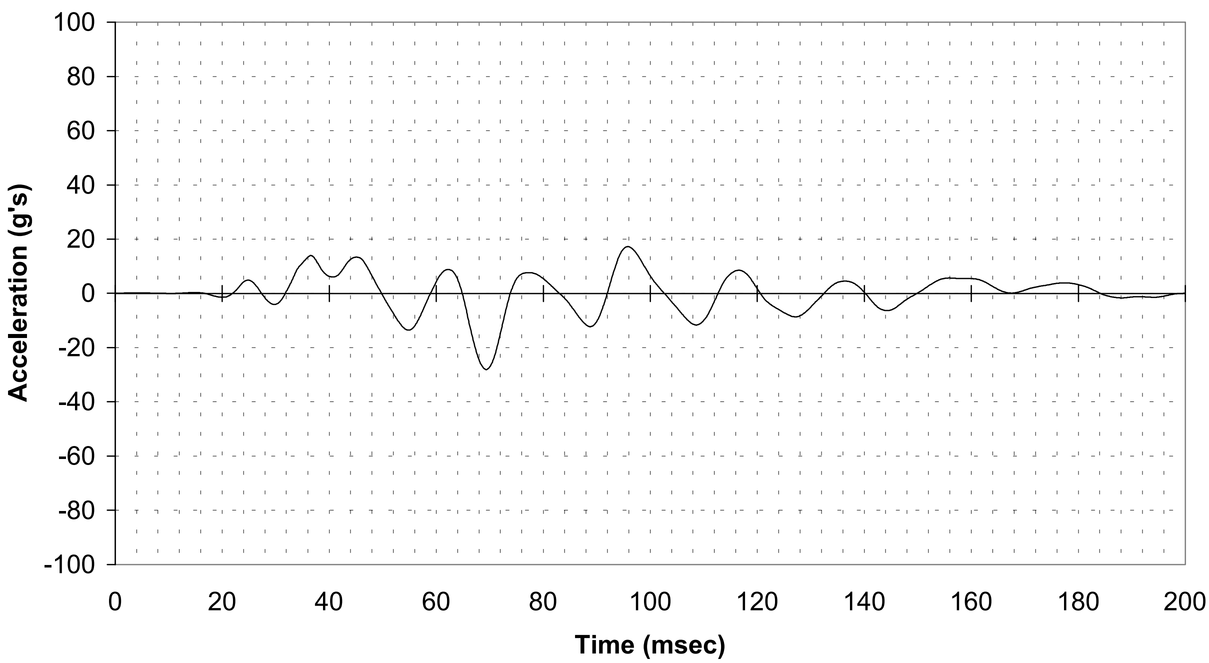

FIGURE A-75. RIGHT STRUT, ACCELEROMETER X DIRECTION
(channel 428)

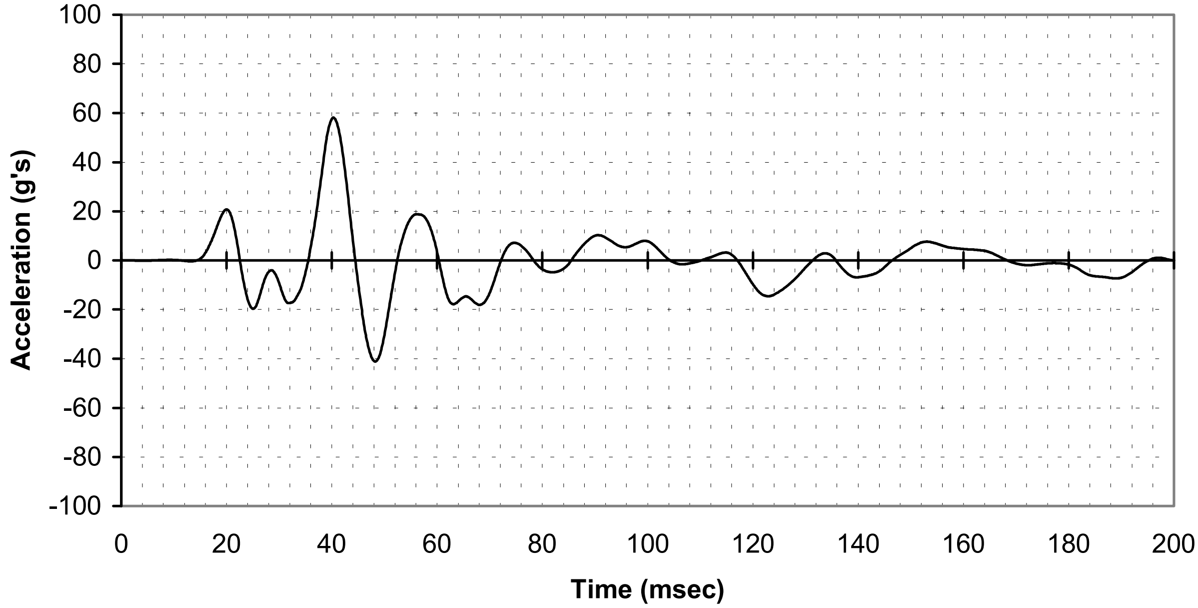

FIGURE A-76. RIGHT STRUT, ACCELEROMETER Y DIRECTION
(channel 429)

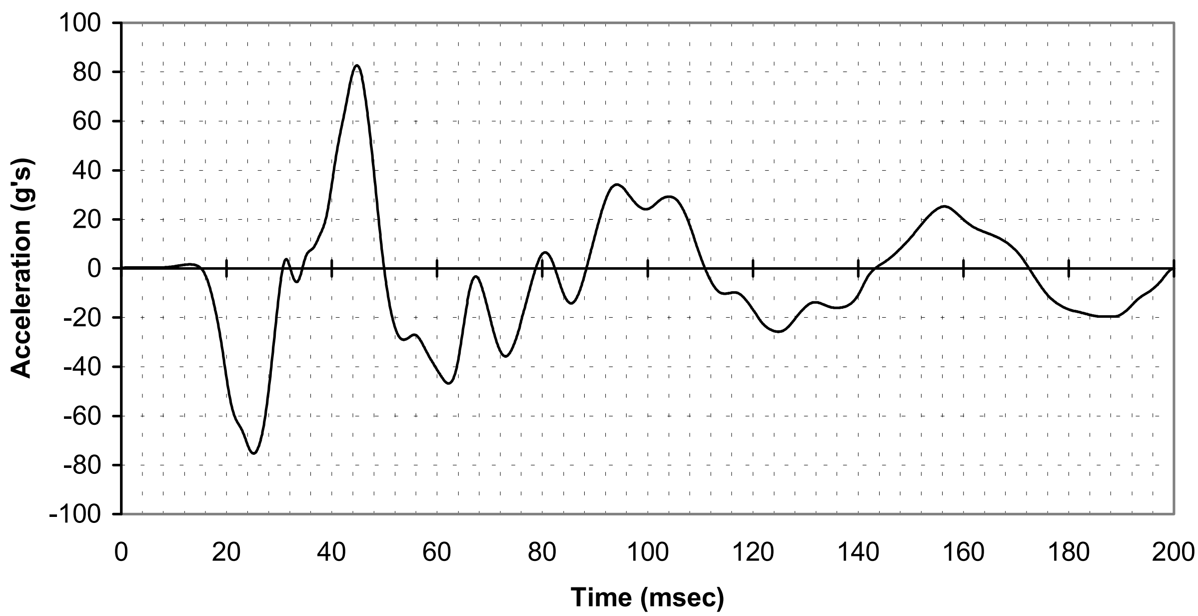

FIGURE A-77. RIGHT STRUT, ACCELEROMETER Z DIRECTION
(channel 430)

ENGINE DATA

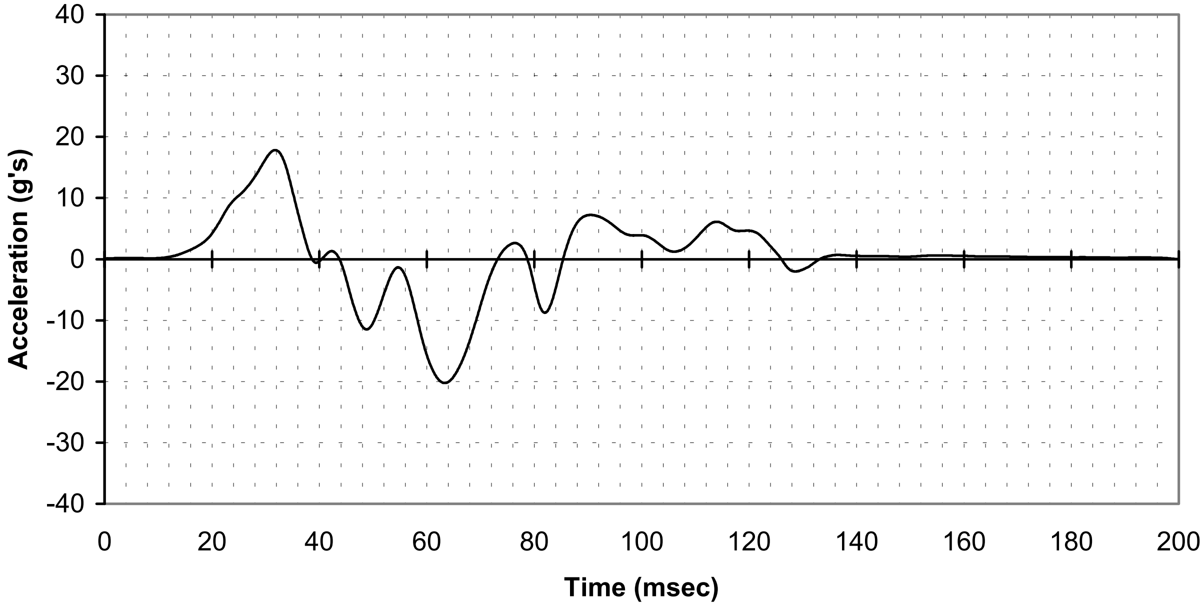

FIGURE A-78. LEFT ENGINE, ACCELEROMETER X DIRECTION
(channel 101)

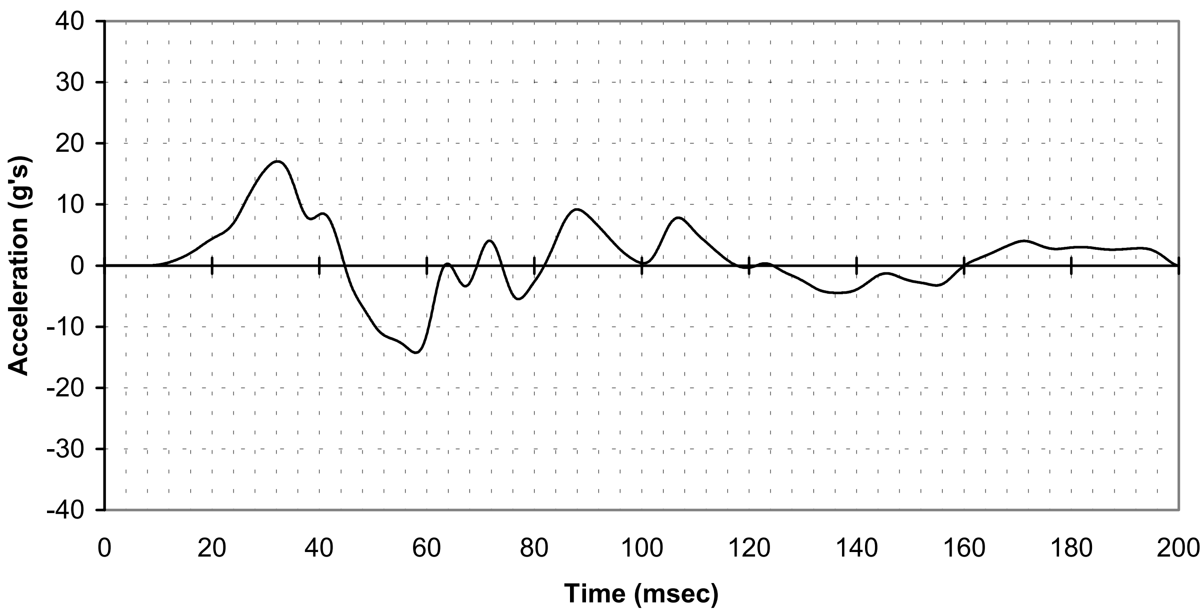

FIGURE A-79. RIGHT ENGINE, ACCELEROMETER X DIRECTION
(channel 401)

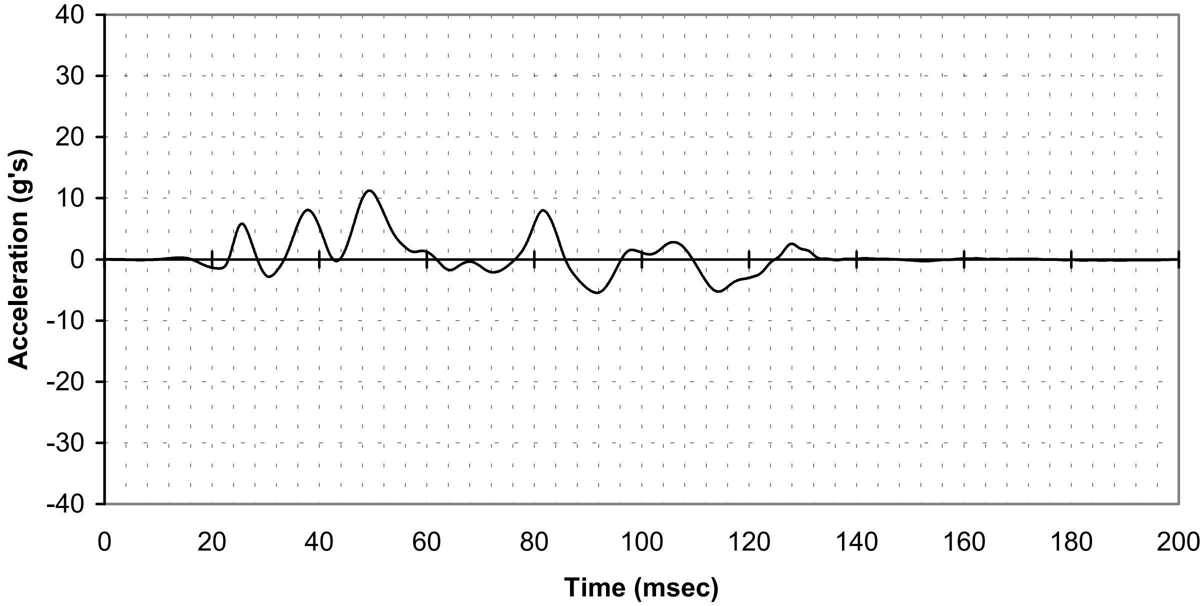

FIGURE A-80. LEFT ENGINE, ACCELEROMETER Y DIRECTION
(channel 102)

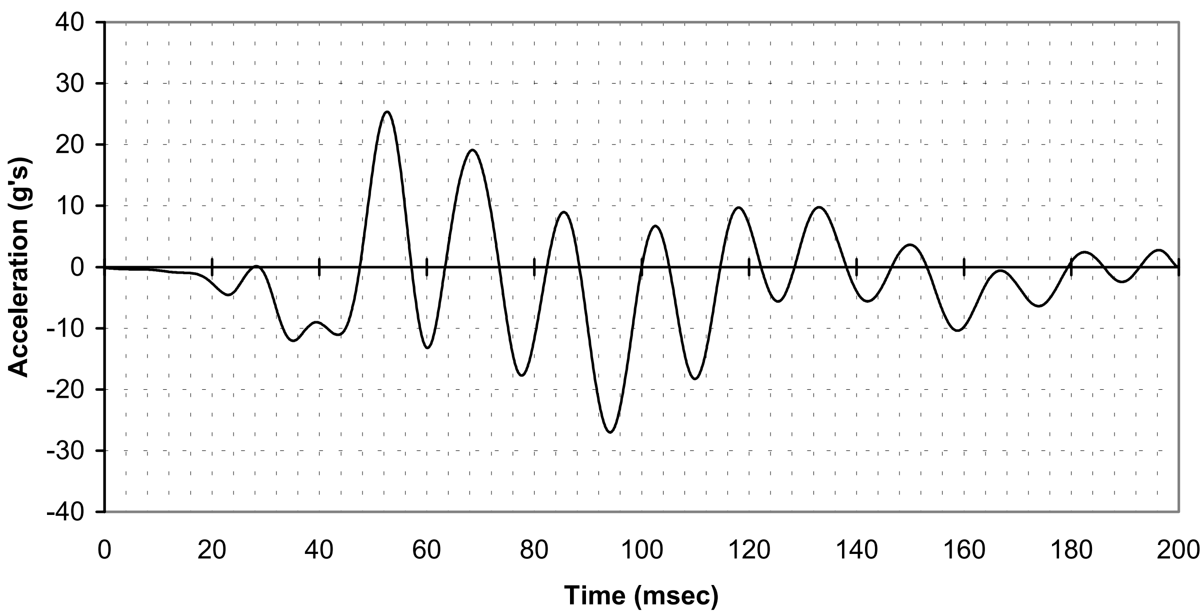

FIGURE A-81. RIGHT ENGINE, ACCELEROMETER Y DIRECTION
(channel 402)

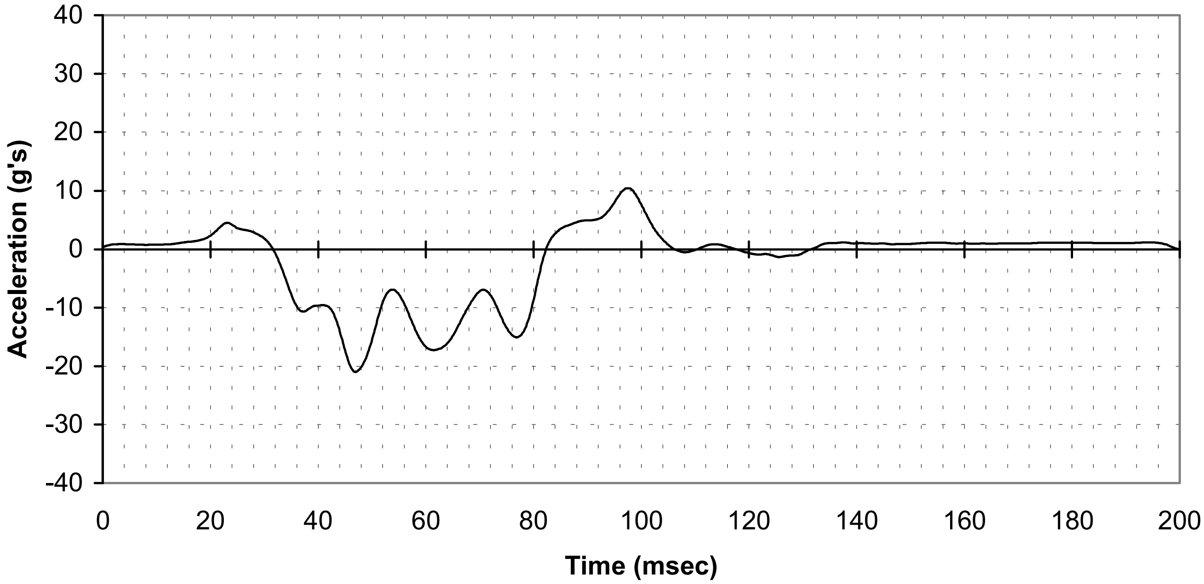

FIGURE A-82. LEFT ENGINE, ACCELEROMETER Z DIRECTION
(channel 103)

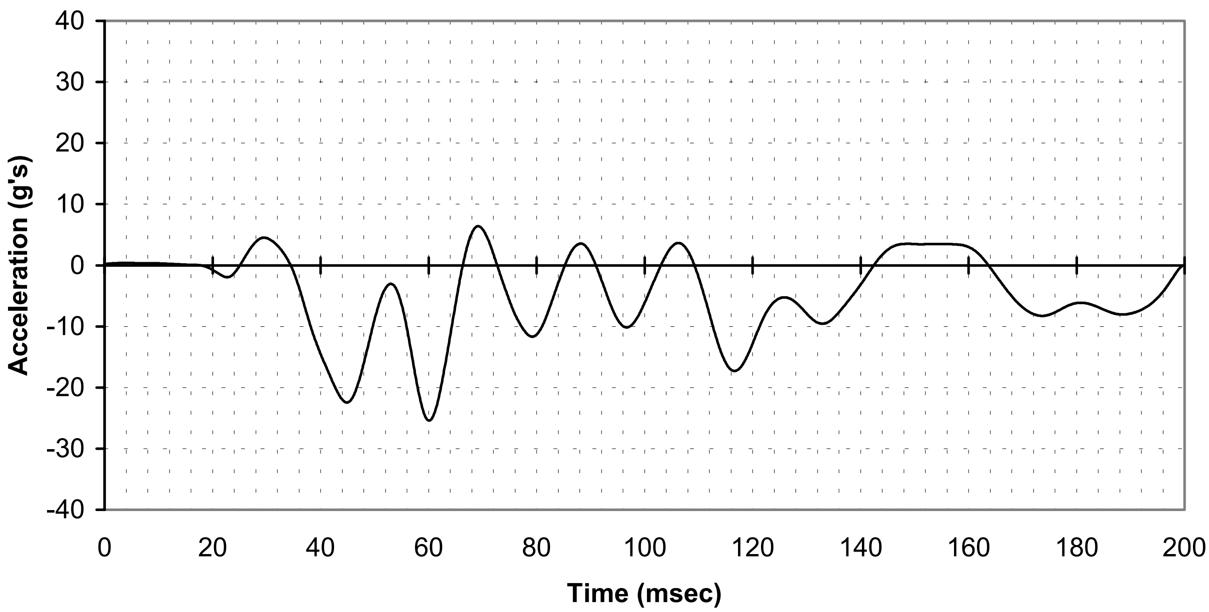

FIGURE A-83. RIGHT ENGINE, ACCELEROMETER Z DIRECTION
(channel 403)

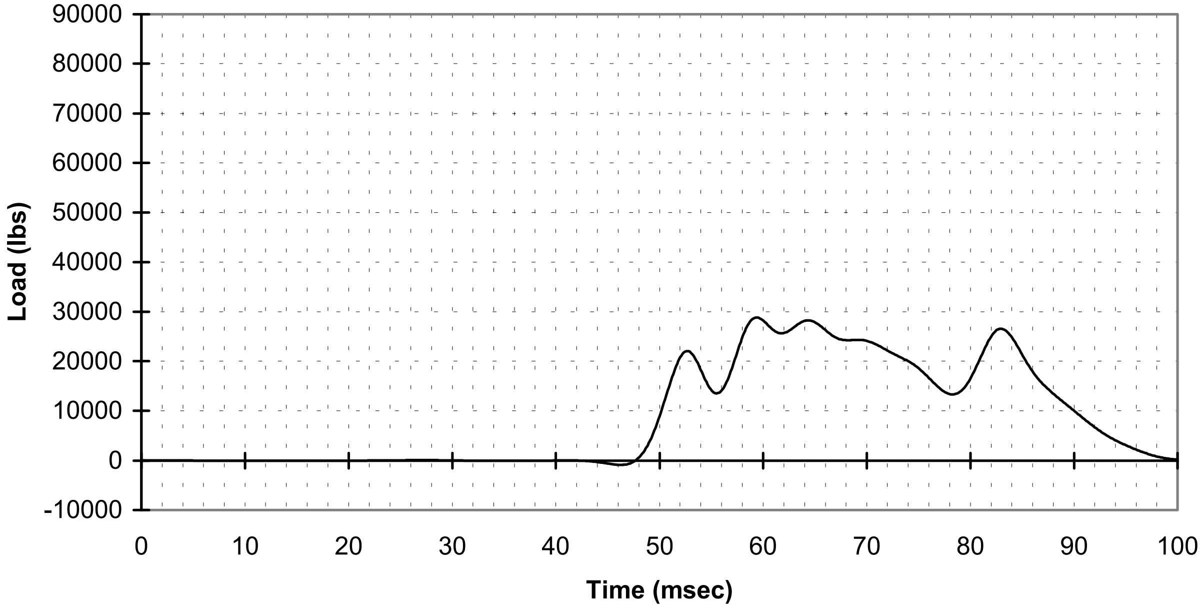

FIGURE A-84. PLATFORM, LOADCELL #1
(channel 113)

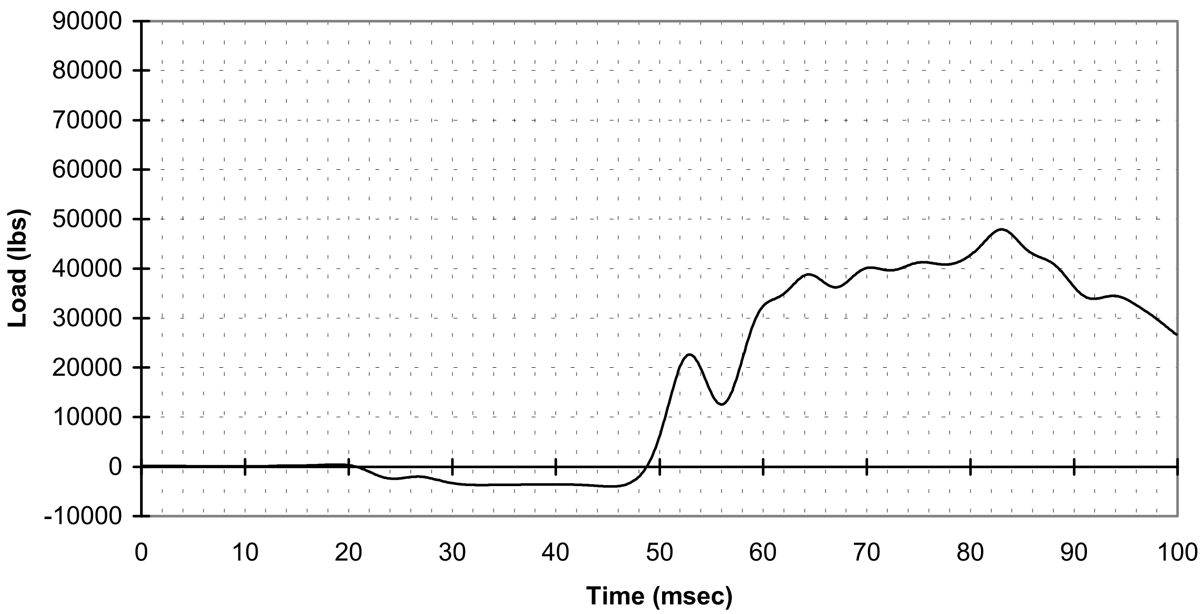

FIGURE A-85. PLATFORM, LOAD CELL #2
(channel 114)

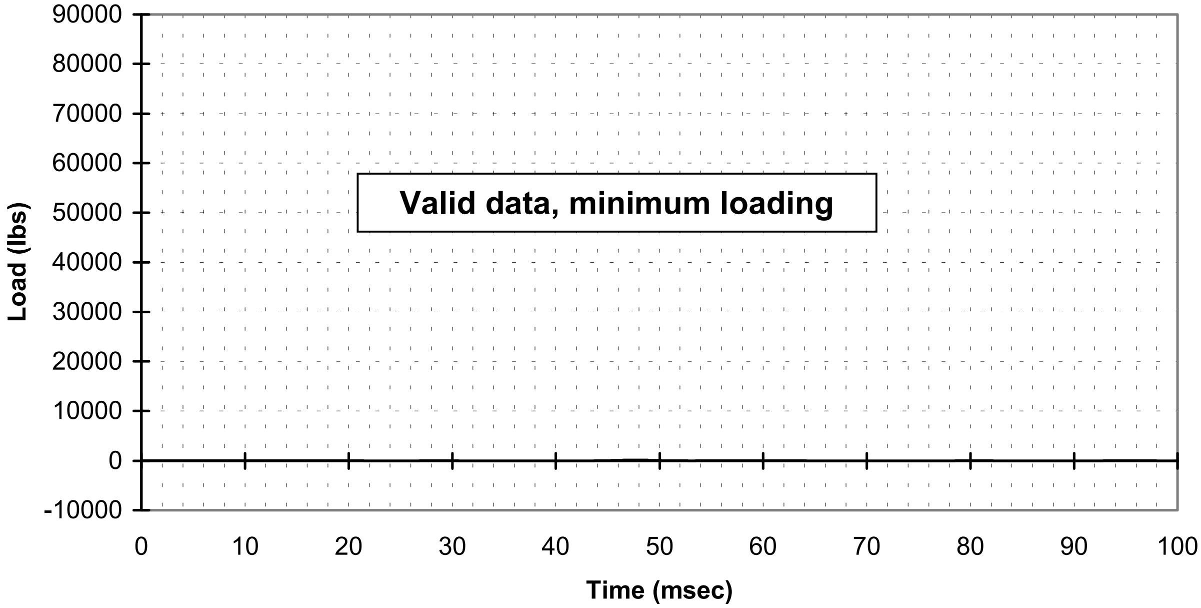

FIGURE A-86. PLATFORM, LOAD CELL#3
(channel 115)

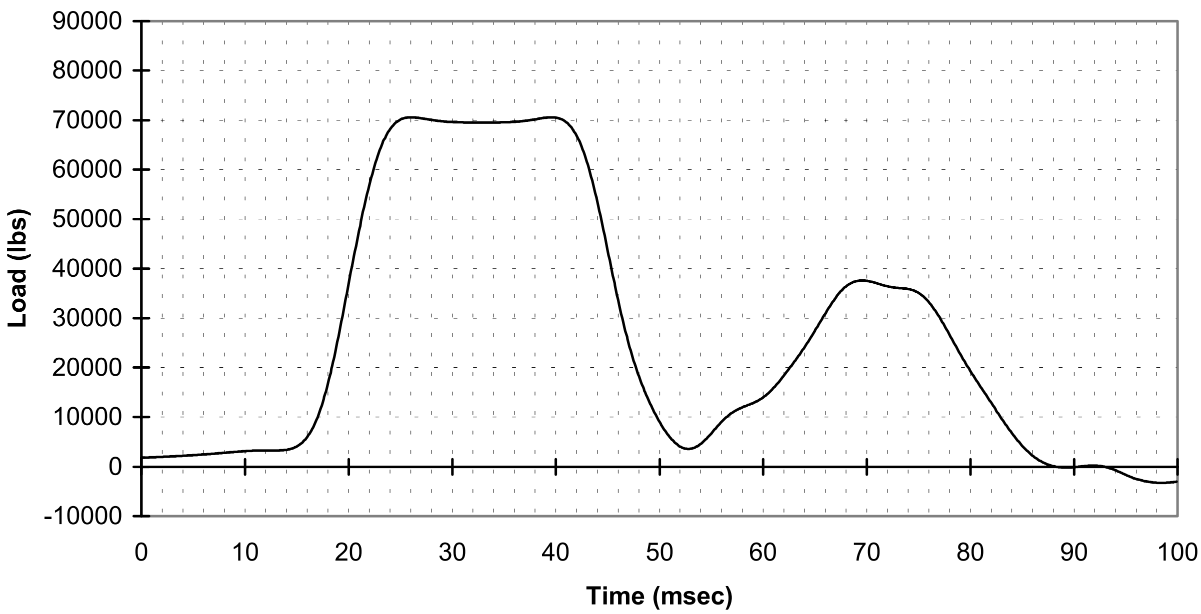

FIGURE A-87. PLATFORM, LOAD CELL #4
(channel 304)

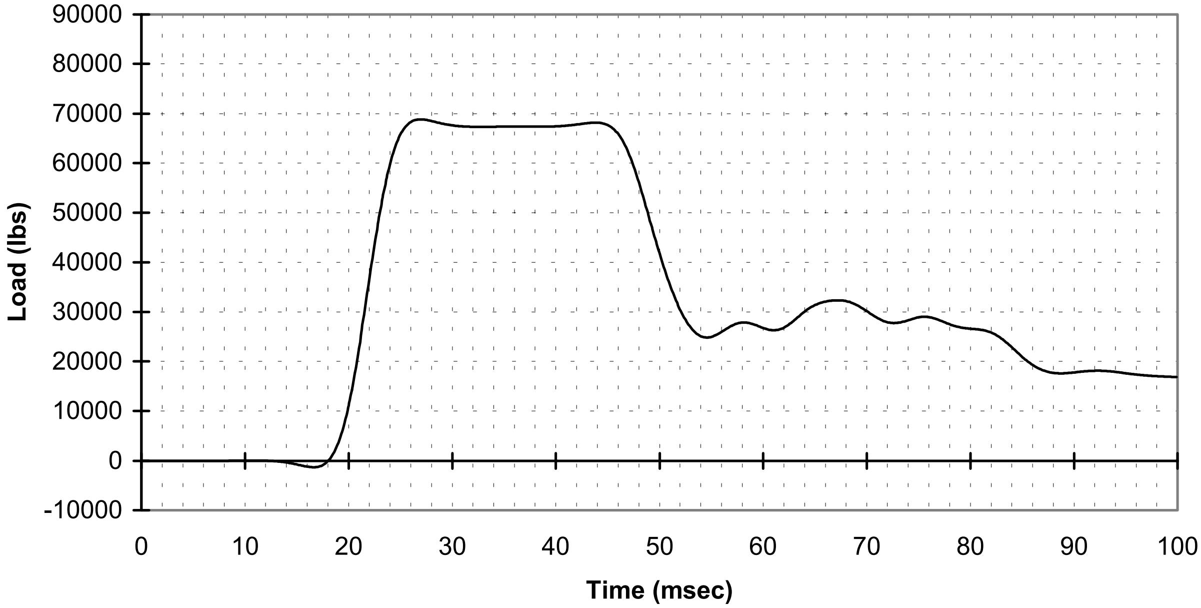

FIGURE A-88. PLATFORM, LOAD CELL #5
(channel 105)

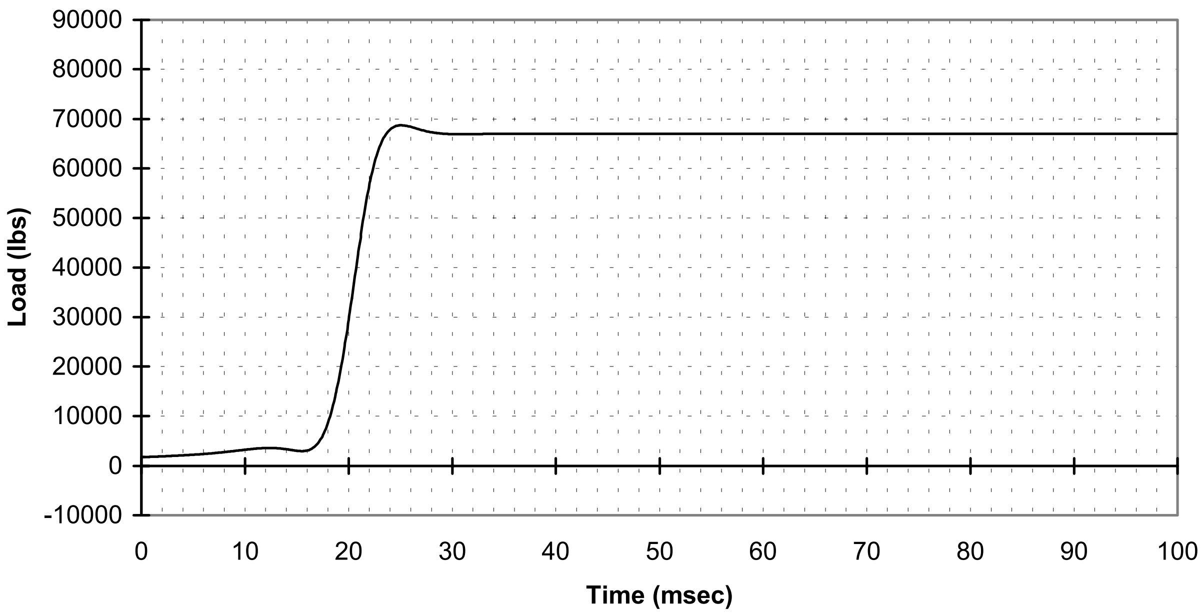

FIGURE A-89. PLATFORM, LOAD CELL #6
(channel 106)

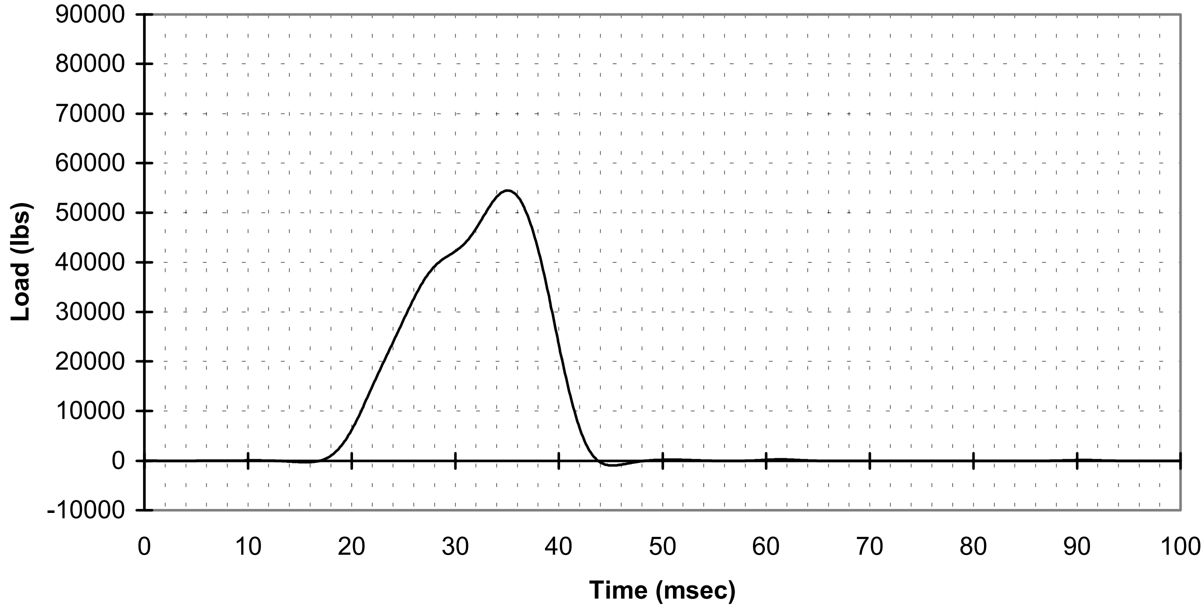

FIGURE A-90. PLATFORM, LOAD CELL #7
(channel 107)

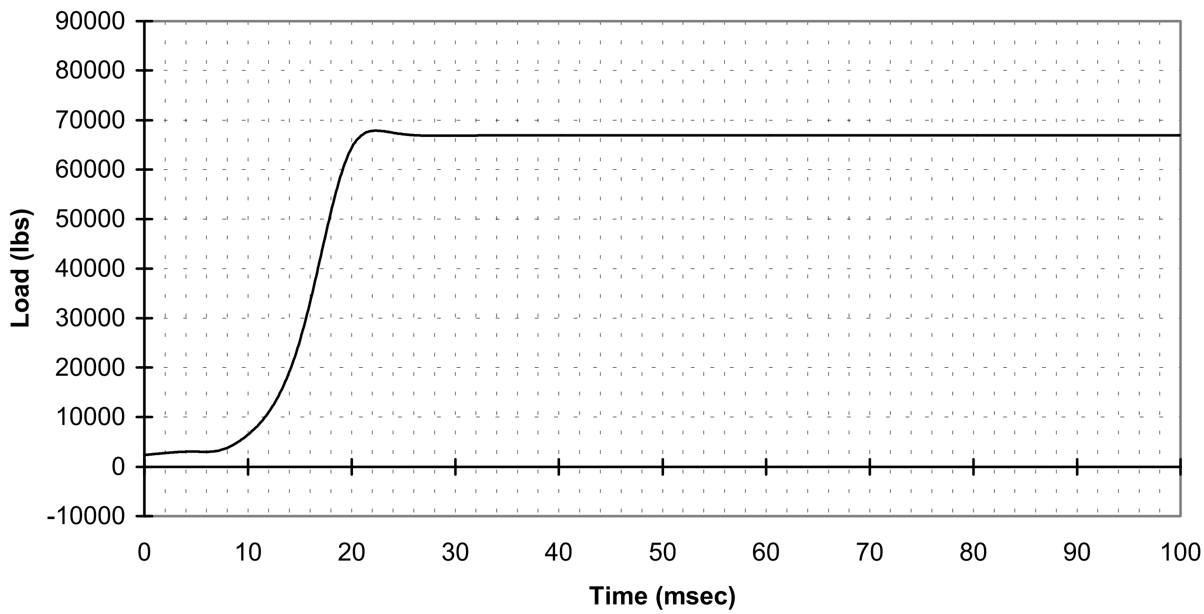

FIGURE A-91. PLATFORM LOAD CELL #8
(channel 108)

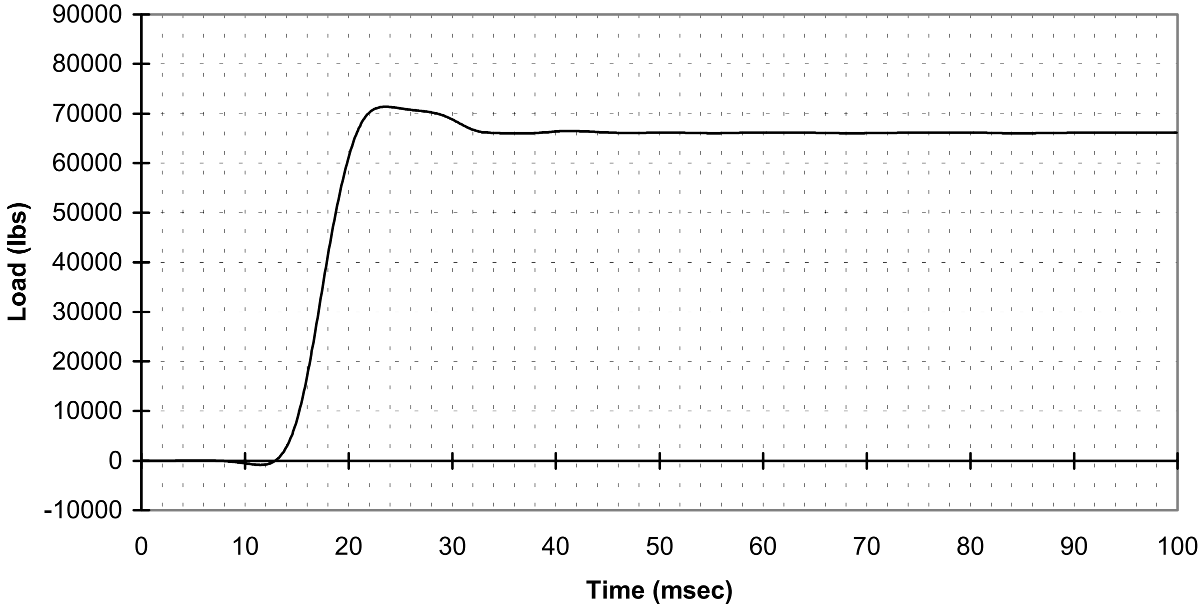

FIGURE A-92. PLATFORM, LOAD CELL #9
(channel 213)

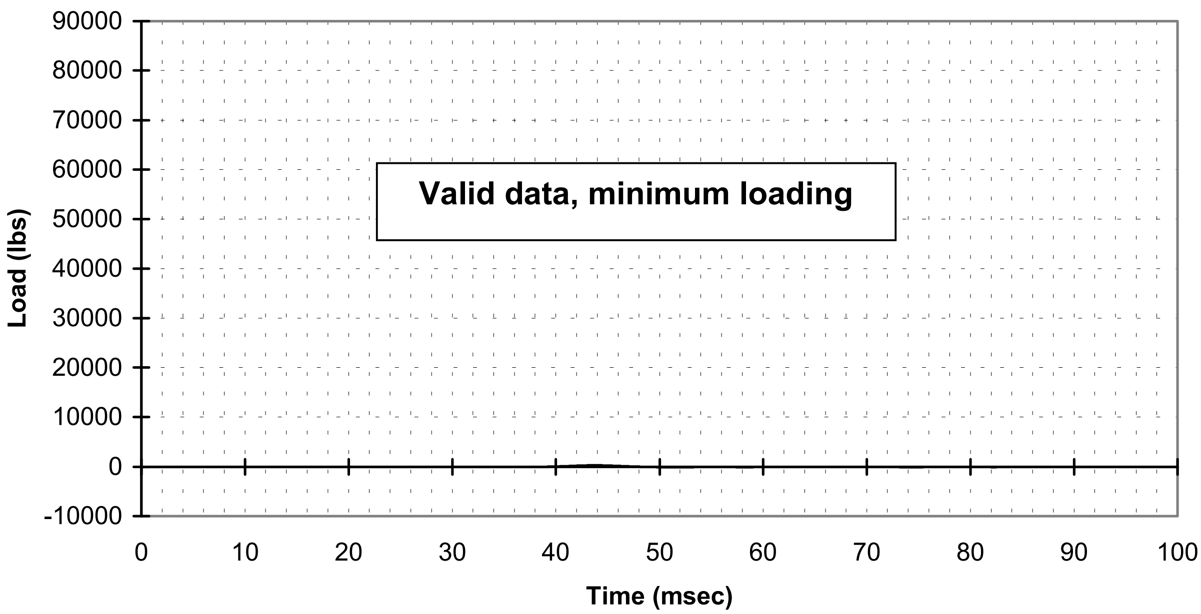

FIGURE A-93. PLATFORM, LOAD CELL #10
(channel 214)

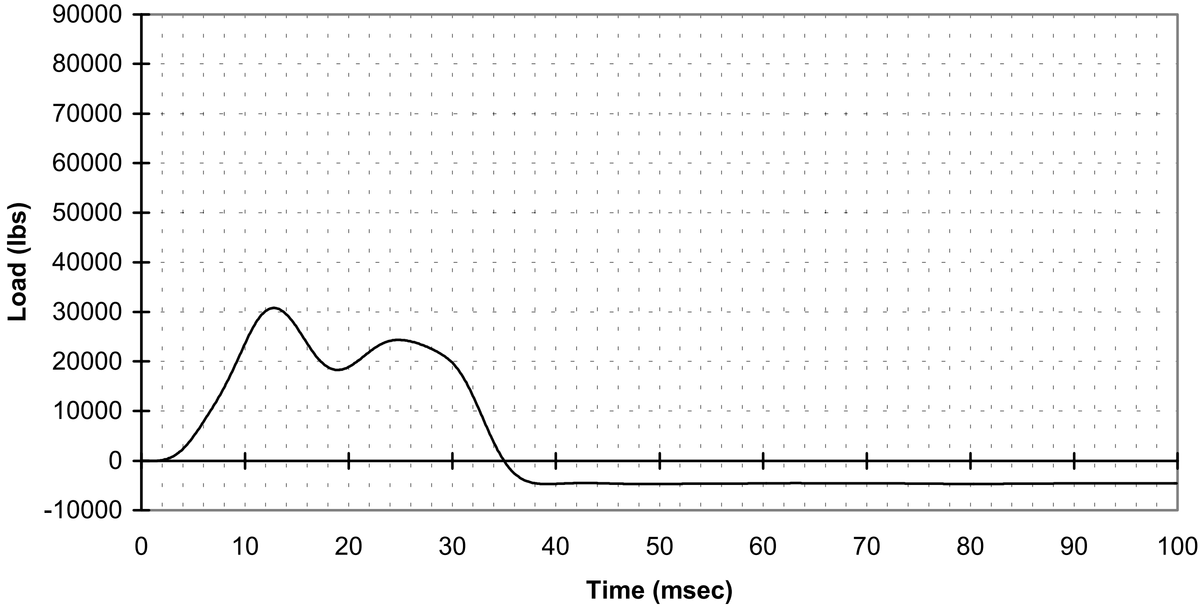

FIGURE A-94. PLATFORM, LOAD CELL #11
(channel 215)

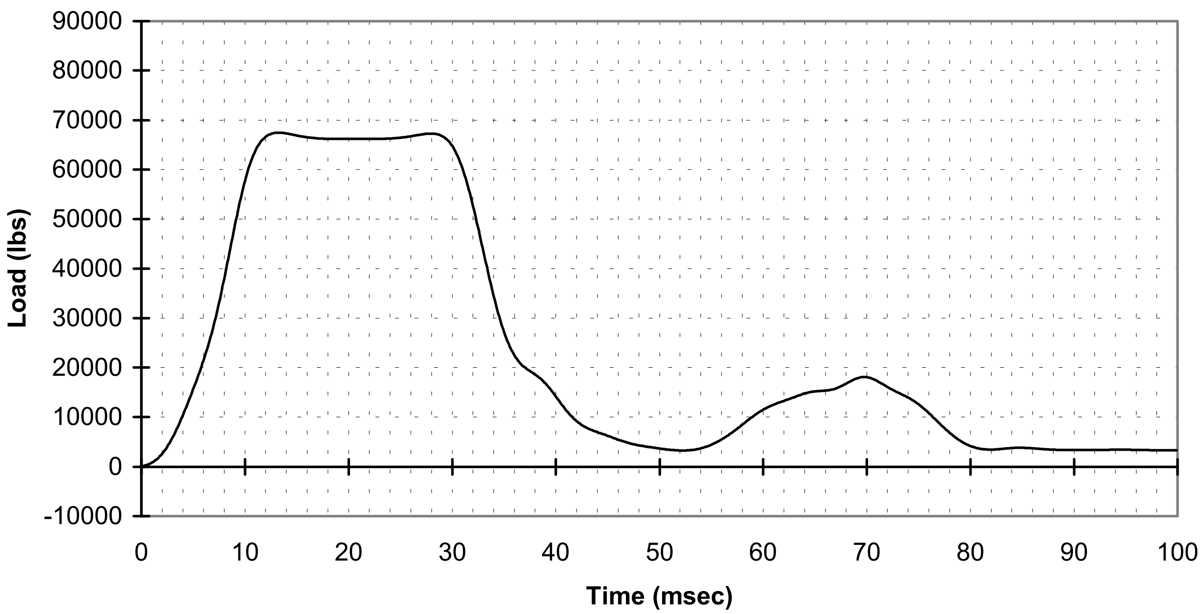

FIGURE A-95. PLATFORM, LOAD CELL #12
(channel 312)

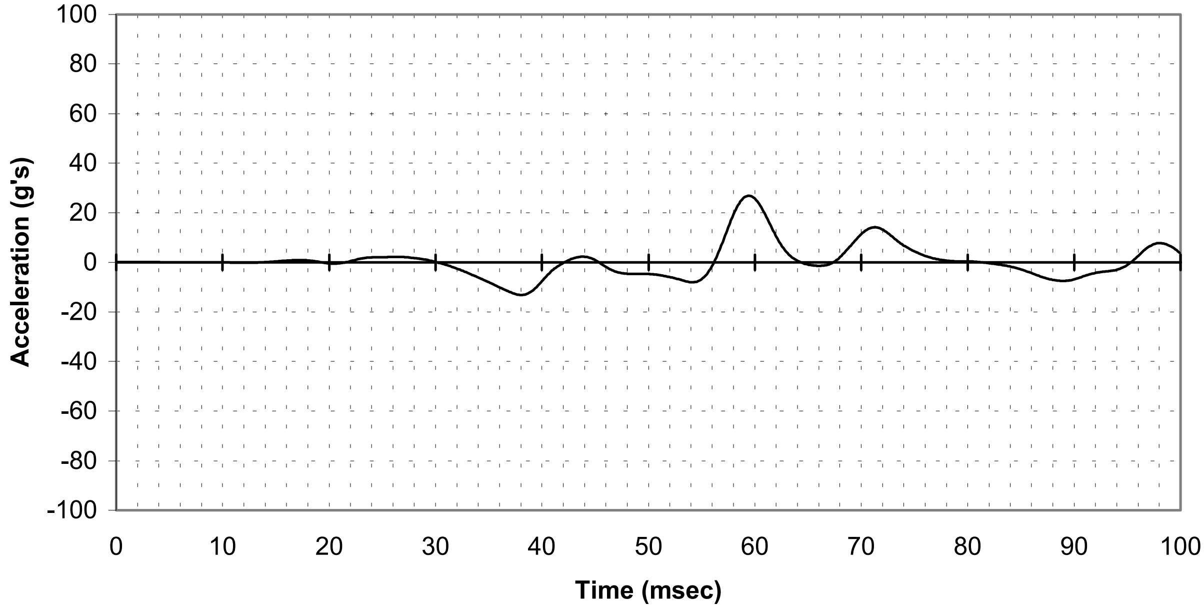

FIGURE A-96. PLATFORM, ACCELEROMETER #1 Z DIRECTION
(channel 201)

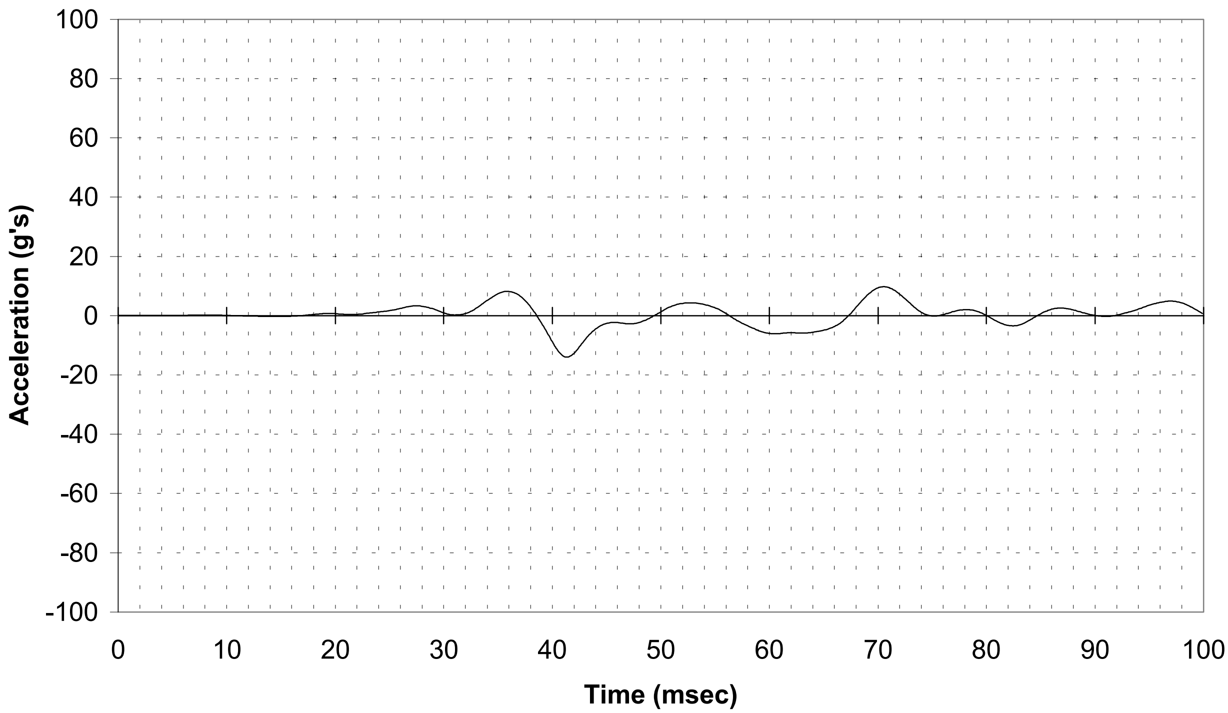

FIGURE A-97. PLATFORM, ACCELEROMETER #2 Z DIRECTION
(channel 202)

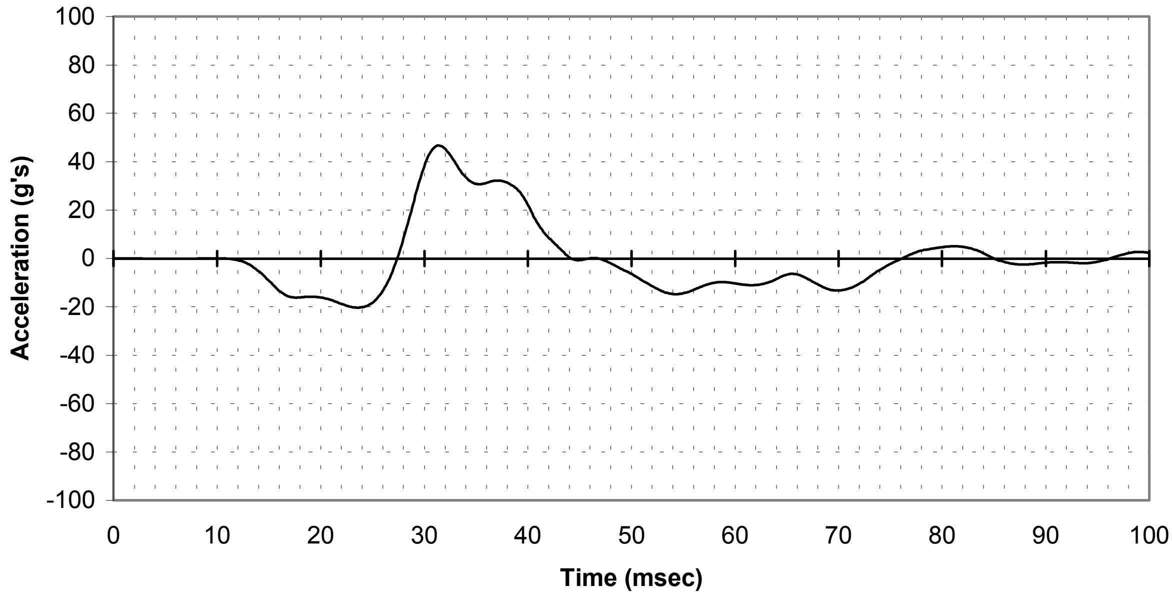

FIGURE A-98. PLATFORM, ACCELEROMETER #3 Z DIRECTION
(channel 203)

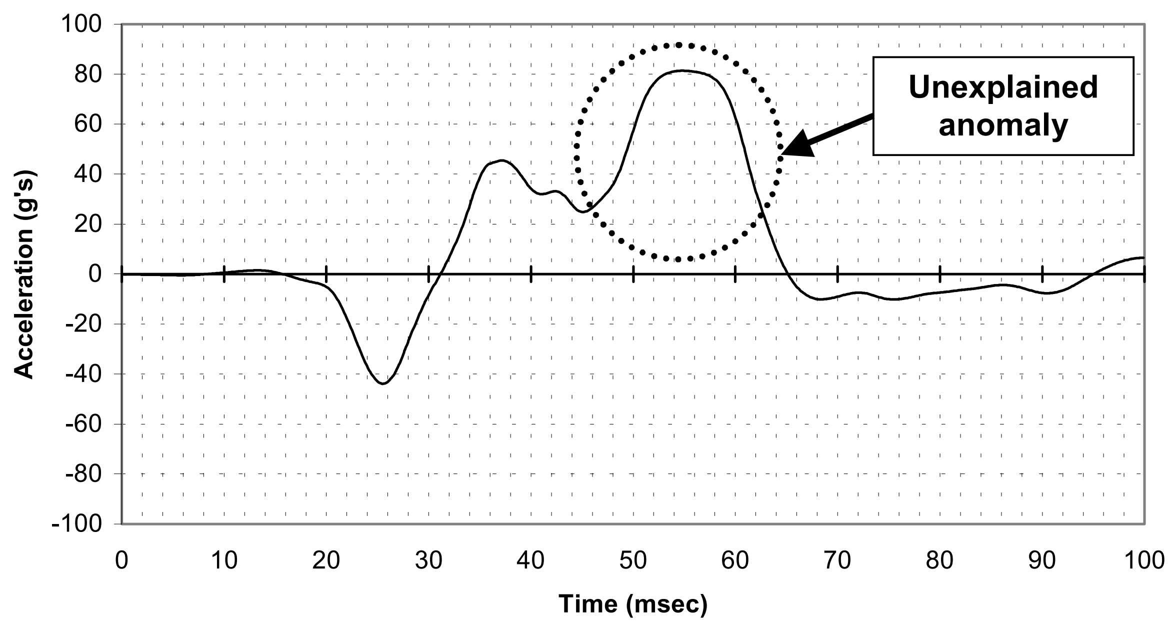

FIGURE A-99. PLATFORM, ACCELEROMETER #4 Z DIRECTION
(channel 204)

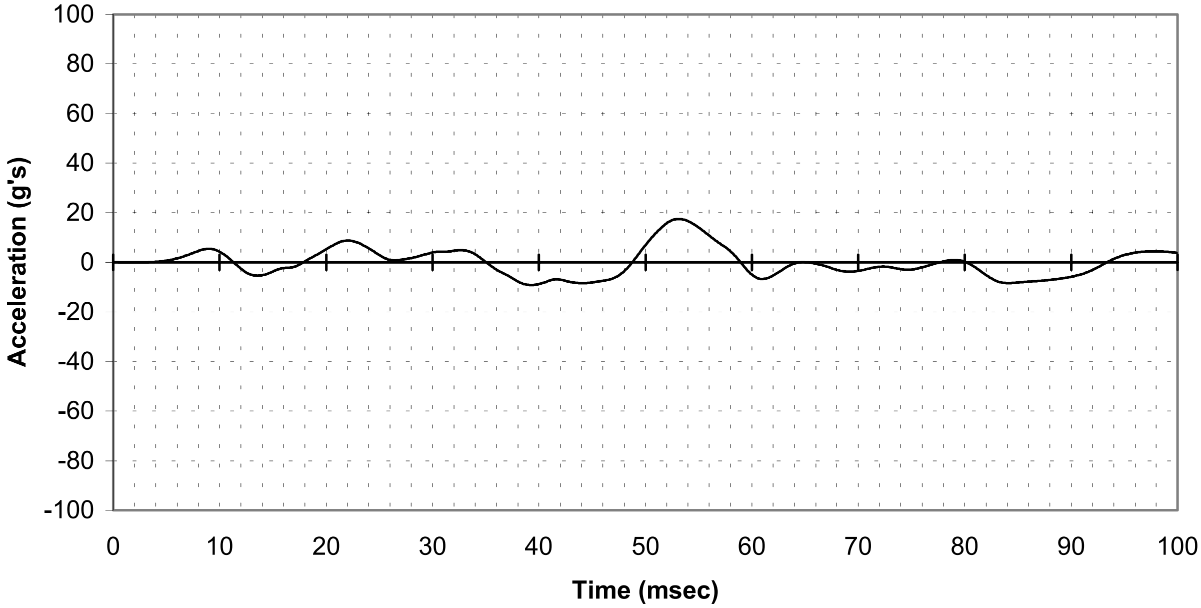

FIGURE A-100. PLATFORM, ACCELEROMETER #5 Z DIRECTION
(channel 205)

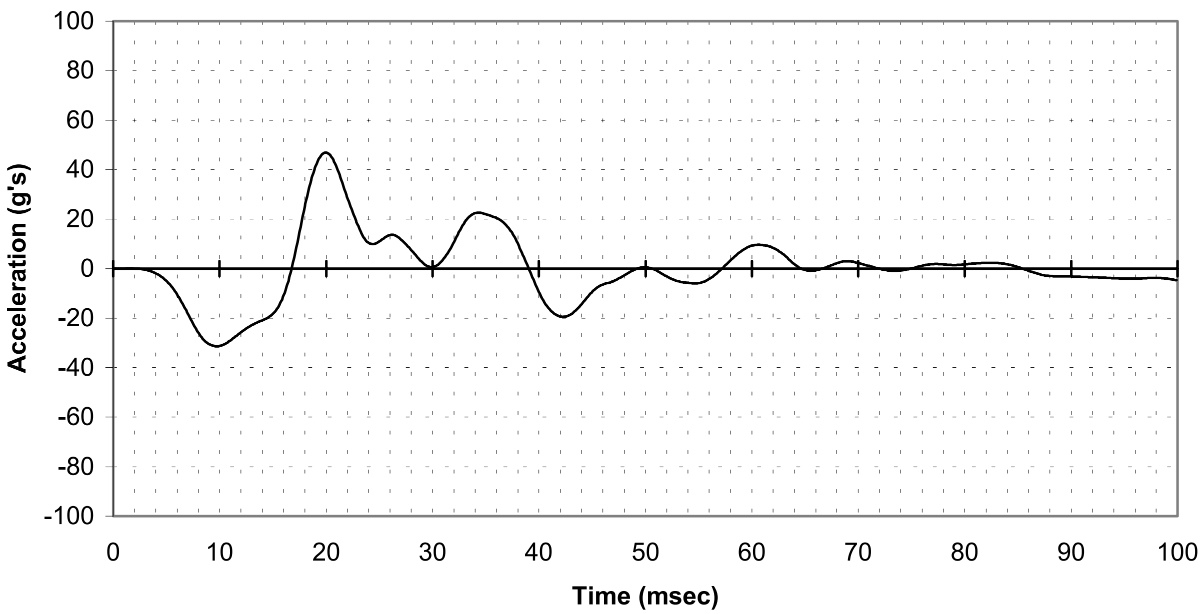

FIGURE A-101. PLATFORM, ACCELEROMETER #6 Z DIRECTION
(channel 206)

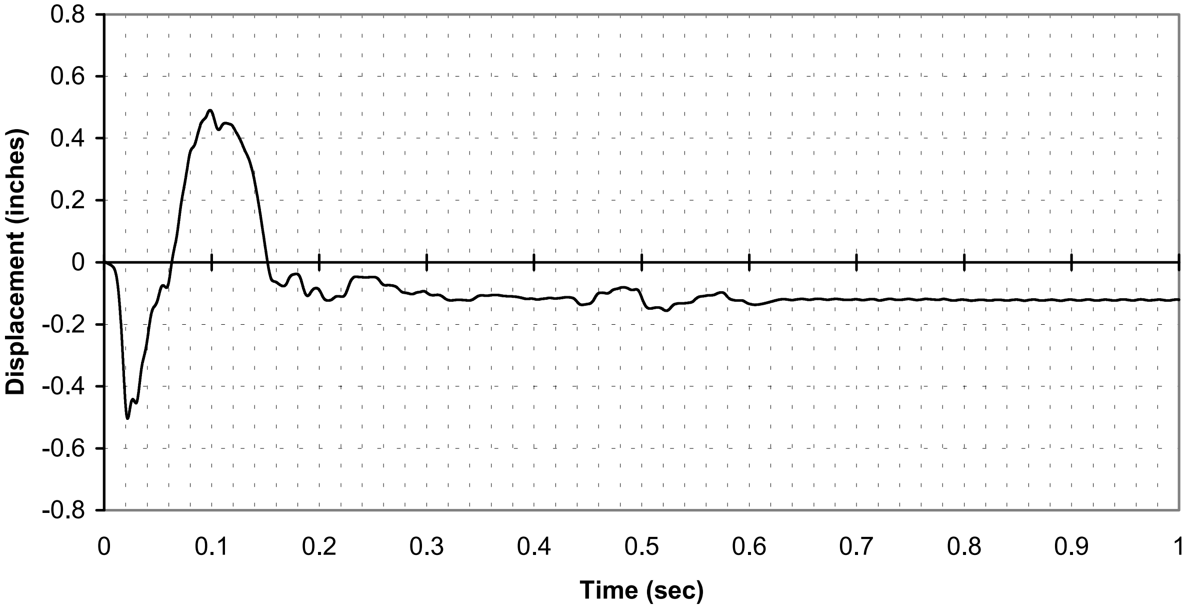

FIGURE A-102. FORWARD PLATFORM, STRING POTENTIOMETER
(channel 25)

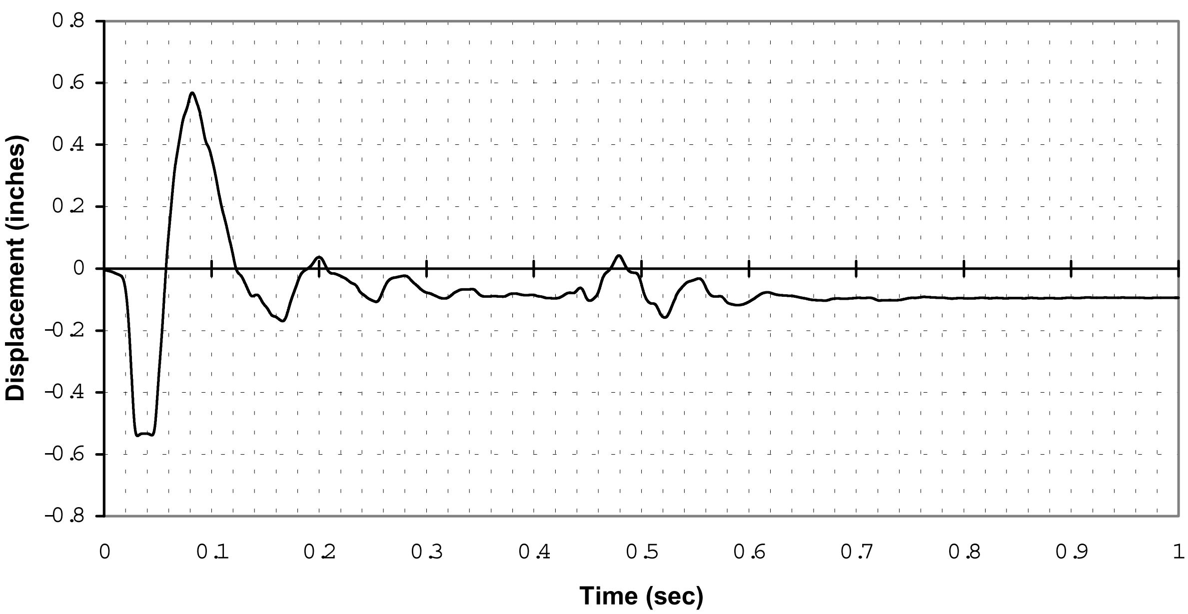

FIGURE A-103. CENTER PLATFORM, STRING POTENTIOMETER
(channel 26)